GNB3$^{-/-}$ RAT: A MODEL FOR Gβ_3-ASSOCIATED RETINOPATHY

By

Marianna Bacellar Teodoro da Silva Galdino

A DISSERTATION

Submitted to
Michigan State University
in partial fulfillment of the requirements
for the degree of

Comparative Medicine and Integrative Biology- Doctor of Philosophy

2017

ABSTRACT

GNB3$^{-/-}$ RAT: A MODEL FOR Gβ_3-ASSOCIATED RETINOPATHY

By

Marianna Bacellar Teodoro da Silva Galdino

The G protein β subunit 3 (Gβ_3) is part of the G-protein signaling cascade in retinal ON bipolar cells (BCs), and cone photoreceptors. Knockout of the encoding gene (*Gnb3*) in mice results in reduced cone photoreceptor sensitivity and marked impairment of both rod and cone ON BC signaling. The latter is revealed as a severe reduction in both the dark- and light-adapted b-wave of the electroretinogram (ERG). Mutations in *GNB3* have been recently reported as an apparently stationary condition associated with a variable degree of loss of rod ERG b-wave and the ON BC component of the light-adapted ERG. *Gnb3*$^{-/-}$ rats were developed and similar to *Gnb3* $^{-/-}$ mice had a severe reduction in rod ON bipolar cell signaling. However, in contrast to the mouse model, cone ON BC signaling was relatively well preserved. Application of L-AP4, a blocker of photoreceptor to ON BC signaling, removed the remaining b-wave from the cone ERG confirming it originated from cone ON BCs. Single cell recording from *Gnb3*$^{-/-}$ retinal slices showed some cone ON BC were functional while rod ON BCs were not functional.

Retinal gene therapy are being extensively used as novel treatments to genetic diseases in the retina. Here we used adeno- associated viral (AAV) vectors developed to target retinal bipolar cells. Intravitreal delivery at early ages (P2) showed to be a promising method targeting bipolar cells in rats. *Gnb3*$^{-/-}$ rats were treated with an AAV containing a copy of the mouse *GNB3*. cDNA in one eye and a human GFP construct as a procedural control in the other eye. No functional rescue was observed on the time course of the

study (3 months) but presence of mRNA was noticed in all the eyes analyzed by qRT-PCR. The *Gnb3*$^{-/-}$ rat is a useful additional model for the study of retinal ON bipolar cell signaling, and as a model for human $G\beta_3$-associated retinopathy.

This dissertation is dedicated to my family in special my Grandmother who was and will be always my example.

ACKNOWLEDGMENTS

I would like to acknowledge many people that contributed to my personal and professional development. First of all to my advisor, Dr. Simon Petersen-Jones, for all the guidance, friendship being a role model during these 6 years of my life. Thank you for the opportunity, and mostly important, the confidence deposited on me during this time. I also would like to thank my committee members, Dr. András Komáromy, Dr. Arthur Weber and Dr. Joshua Bartoe for all the inputs on this work and for being such amazing mentors and inspiration.

Furthermore, many people that were important in this work and in my life:

- Dr. Vilma Yuzbasiyan-Gurkan, Director of the Comparative Medicine and Integrative Biology program (CMIB), for all the support and encouragement words;
- Dr. Kwoon Wong, Dr. Andrew Chervenak and Dr. Aaron Reifler (University of Michigan), for all the work and patience showing and teaching me more about single cell recordings in retina;
- Dr. Naheed Khan (University of Michigan), for the friendship and help with rodent electroretinography;
- Dr. Shannon Boye and Sanford Boye (University of Florida), for the collaboration on the adeno-associated viral (AAV) vectors work;
- Dr. Gregory Fink and Hannah Garver, for the help with the rat model;
- Dr. Laurence Occelli, Dr. Andrea Minella, Dr. Paige Winkler and Ethan Dawson-Baglien, labmates and friends;

- Janice Querubin, for the friendship, and for being an always-available help.
- Brenda Paschke and Cathy Tyler, for taking good care and breeding my rats;
- Kristin Koehl and Christine Harman; for sharing the lab so many times;
- Dr. Gloriani Rosario and Julie Moore, who spend many hours in the lab helping me;
- All the CMIB faculty and students;
- My MSU friends, whom I call my family in Michigan, specially to Dr. Marilia Takada, Dr. Paulo Vilar, Dr. Clarissa Barboza, Dr. Oscar Benitez, Dr. Cynthia Lucidi, Dr. Carine Holz, Dr. Puja Baju and Dr. Luis Carlos Penha Cortes, for being always there cheering me up and encouraging me when sometimes I didn't believe in myself;
- For my friends in Brazil;
- Dr. Fabiano Montiani-Ferreira, my Master's co-adviser, who introduced me to ophthalmology and electrophysiology and became a lifelong friend.
- Dr. Jeffrey Jamison, for the opportunities on continuing working with what I love and being an inspiration;
- The Myers-Dunlap Endowment Fund and CAPES Brazil, for the funding;
- My parents, Regina and Alcebiades. For the love, monetary and emotional support always, I love you!;
- My family, in special, my brothers Arthur Bacellar and Samuel Teodoro da Silva; stepmother Eneleia; in-laws, Edna e Gustavo, sister in-laws Alana

and Brisa, husband's sister in-law Everton, for the innumerous conversations and emotional support throughout these years;

- My Grandmother Terezinha, who I dedicate this work and miss every day, for her emotional support, words and for always being my best friend. For her example which I promise to follow always. I miss you forever,
- For my dogs, Brad, George and Stella, for their company and unstoppable love;
- And lastly, the person who is always on my side, helping, loving and cheering me up the most, my husband Vinicius Rodrigues Galdino. For your patience and love always, even when I was too grumpy. Thanks for always say that I can do it.

TABLE OF CONTENTS

LIST OF TABLES

LIST OF FIGURES

KEY TO ABBREVIATIONS

AAV- adeno associated virus

ARVO – Association for Research in Vision and Ophthalmology

AVMA – American Veterinary Medical Association

Actb- beta actin

BC- bipolar cell

cSLO – Confocal scanning laser ophthalmoscopy

CSNB- congenital stationary night blindness

DAPI – 4’,6-diamino-2-phenylindole

ERG- electroretinography

GC – ganglion cell

G-protein – guanine nucleotide binding protein

GDP- guanosine diphosphate

GFP- green fluorescent protein

GPCR – G-protein coupled receptor

GRK- rhodopsin kinase

GTP- guanosine triphosphate

GNB3- G-protein subunit 3

INL – inner nuclear layer

IPL – inner plexiform layer

IS- inner segment

ISCEV- International Society of Clinical Electrophysiology of Vision

ITR- inverted terminal repeat

IVT – intravitreal

L-AP4 – 2-amino-4-phosphonobutyrate

mGluR6- metabotropic glutamate receptor 6

Nyx- nictalopin

ONL- outer nuclear layer

OPL- outer plexiform layer

OPs- oscillatory potentials

ORF- open reading frame

OS- outer segment

PBS – phosphate buffer saline

PCP2-L7 - Purkinje cell protein 2

PDA- cis-2,3- piperidine dicarboxylic acid

PDE- phosphodiesterase

R* - metarhodopsin II

RGE- retinopathy globe enlarged

RGS- G-protein signaling proteins

RHO - rhodopsin

RPE – retinal pigment epithelium

SD-OCT - spectral-domain optical coherence tomography

SR – subretinal

TRPM1- transient receptor potential cation channel subfamily M member 1

WT- wildtype

CHAPTER 1

INTRODUCTION

1.1 Heterotrimeric G-protein

Multicellular organisms have developed complex systems in order to sense the external world without compromising the internal cellular environment. Guanine nucleotide binding proteins (G-proteins) are one of the many systems found across a multitude of organisms which help to transfer various physiological responses from the external environment to the internal cellular space. G-proteins play an important role in several molecular signaling cascades which are critical for systems such as vision, olfaction, taste, heart rate and other neuronal activities (Offermanns, 2003).

G-proteins are composed of three distinct subunits: alpha (α), beta (β) and gamma (γ). In general, G-proteins are located on the inner membrane surface of the cell coupled to environmental receptors. When the receptor is inactive, G-protein α subunit is bound to GDP (guanosine diphosphate) and is also inactive. When the receptor is activated, GDP is released and GTP (guanosine triphosphate) binds to the α subunit, which causes the complex Gα-GTP to dissociate from the receptor and Gβγ dimer (Cabrera-Vera et al., 2003) (Fig.1.1), resulting in the transference of the external signal to the internal cellular environment.

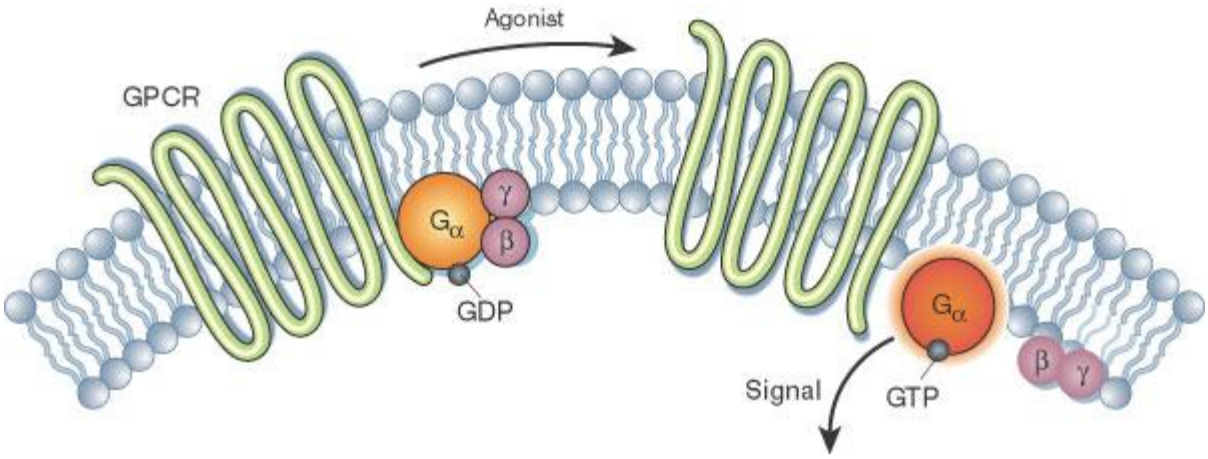

Figure 1.1. Activation of the Gα subunit of a G-protein coupled receptor. http://www.nature.com/scitable/topicpage/gpcr-14047471

G-proteins are the intracellular partners of a G-protein coupled receptor (GPCR) which are the largest class of transmembrane receptors. GPCRs consist of seven transmembrane spanning-helices, a N terminus (extracellular), a C terminus (intracellular) and three interhelical loops on each side of the cellular membrane (Offermanns, 2003, Oldham and Hamm, 2008). There are 16 Gα, 5 Gβ and 13 Gγ subunits already discovered in mammals alone. Combinations of these subunits form different heterotrimeric complexes according to the cellular need (McCudden et al., 2005).

1.2 Retina

In vertebrate organisms, the retina is the neural tissue at the back of the eye responsible for converting photons into a signal recognizable by the brain. The three main neurons in this process are photoreceptors, bipolar cells (BCs) and ganglion cells. Phototransduction is initiated by photons being absorbed by rhodopsin (the G-protein coupled receptor) in rod photoreceptors and cone opsin in cone photoreceptors, resulting in hyperpolarization of the cell. This electrical signal from photoreceptors is transferred to the second order neurons, BCs and horizontal cells (Kolb, 1995c). BCs typically connect to multiple photoreceptors and in addition to transferring the light induced signal from photoreceptors, they also help to accentuate features in the environment such as movement, contrast, and edges. In a simplistic way, BCs tranfer vertically the signal to ganglion cells, and a voltage-graded potential is converted into a spiking potential, which is transmitted to the brain. The retina has also Müller, amacrine and horizontal cells contributing to the vision process. Müller cells provide structural and metabolical support to all retinal neurons, while horizontal cells and amacrine cells contribute to visual processing, and act laterally between the layers of the retina (lateral transmission) (Kolb, 1995a, Maggs, 2008, Grossniklaus et al., 2015). These various cell types form a “layer cake” organization of the retina.

The retinal pigment epithelium (RPE) consists of a monolayer of cells that form a barrier between the neuronal retina and the choroid. It is important in the retinoid cycle providing 11-cis retinal to photoreceptors for formation of the visual pigments and recycling retinoid following phototransduction. It is also important in the phagocytosis and processing of the distal tips of photoreceptor outer segments. When pigmented it helps

to reduce scattery of light and protects against photo oxidation (Kolb, 1995c, Strauss, 2005). Working from the outer retina to the inner retina (Fig. 1.2), the light absorbing portion of the photoreceptors are the outer segments (OS), followed by the inner segments (IS). The outer nuclear layer (ONL) is where nuclei of the photoreceptor are located. The synaptic region between photoreceptors and bipolar cells and horizontal cells is the outer plexiform layer (OPL), and the inner nuclear layer (INL) composes the bipolar cell, horizontal cell and Müller cell nuclei. The inner plexiform layer (IPL) is the synaptic layer between bipolar cells, amacrine cells and ganglion cells. Finally, the ganglion cell layer comprises the cell bodies of ganglion and amacrine cells. The axons of ganglion cells form the retinal nerve fiber layer. The most vitread layer is the inner limiting membrane.

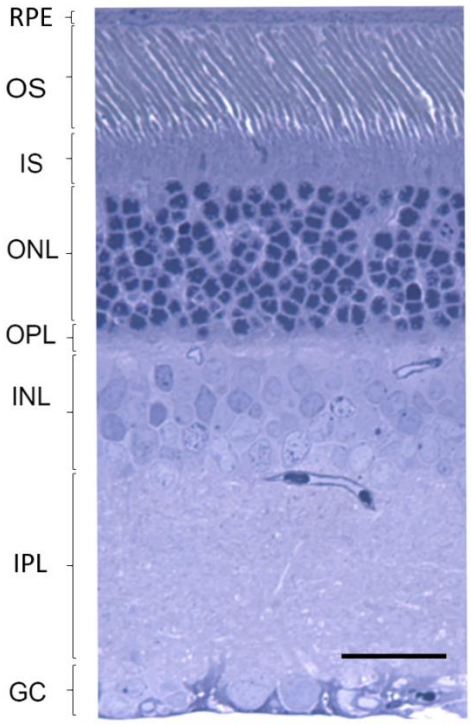

Figure.1.2. **Plastic- embedded retinal section of a Wildtype rat at 6 months of age.** Stain: epoxy tissue stain; Calibration bar: 50µm; Key: RPE- retinal pigmented epithelium; OS- outer segment of photoreceptors; IS- inner segment of photoreceptors; ONL- outer nuclear layer; OPL- outer plexiform Layer; INL- inner nuclear layer; IPL- inner plexiform layer; GC- ganglion cell.

The phototransduction cascade in rod photoreceptors is one of the most studied G-protein pathways. Different isoforms of G-proteins are active in rod and cone photoreceptors. Rods are responsible for lowlight vision requiring significant signal amplification. The G proteins involved in rod phototransduction are $G\alpha_{t1}$, $G\beta_{1}$ and $G\gamma_{1.}$ Cones are responsible for daylight vision and require responsiveness over a broad dynamic range. The G proteins for cone phototransduction are $G\alpha_{t2}$, $G\beta_{3}$ and $G\gamma_{8}$ (Fu and Yau, 2007). Signaling with ON BC also involves a G-protein cascade and this consists of $G\alpha_{o}\beta_{3}\gamma_{13}$ (Dhingra et al., 2012, Ramakrishnan et al., 2015).

1.3 Phototransduction

Phototransduction is the process where light is converted from photons to a graded change in photoreceptor membrane potential. This process has been studied in detail in rod photoreceptors and it is believed that a very similar process occurs in cone photoreceptors (Larhammar et al., 2009).

First a photon of light is absorbed by the photoreceptor photopigment, which contains the protein opsin and the chromophore 11-*cis* retinal (Palczewski, 2012, Tang et al., 2013). Rods utilize the photopigment/opsin known as rhodopsin (RHO). Different types of cones are sensitive to different wavelengths of light; therefore utilize wavelength specific-opsins.

Once the light interacts with the photopigment a series of conformational changes occur. The molecule 11-*cis*-retinal is isomerized into all-*trans*-retinal, which leads to the activation of rhodopsin to Metarhodopsin II (R*). R* binds to the G-protein transducin causing the exchange of GDP to GTP. The G protein α subunit is bound to GTP and is released from the βγ complex. The α-GTP signaling subunit binds to the γ subunit of phosphodiesterase (PDE). PDE is a heterotrimeric enzyme made all of an α and β subunit (PDE-αβ) and two inhibitory γ subunits (PDE-γ). Once α-GTP molecules bind to the two PDE-γ, the active PDE-αβ subunits hydrolyze cGMP to 5'-GMP. This lowers the concentration of cGMP inside the cell and causes the closure of cGMP-gated channels preventing the influx of Na^+ and Ca^{2+} causing hyperpolarization. As a result, glutamate release decreases at the synaptic terminal (Fu and Yau, 2007).

The inactivation of R* occurs through phosphorylation by rhodopsin kinase (GRK) and capping by arrestin. G* inactivation occurs when GTP is hydrolyzed to GDP by GTPase activity (Wang and Kefalov, 2011). Others proteins responsible for the rapid deactivation of transducin include the regulator of G protein signaling proteins (RGS9), a long form of Gβ5 subunit (Gβ5L) and an anchor protein (R9AP), they are also known as the GAP or RGS9 complex. GAP complex facilitates the hydrolysis of the bound GTP to GDP resulting in the inactivation of the G-protein and its subunits (Fu and Yau, 2007, Wang and Kefalov, 2011, Arshavsky and Burns, 2012).

1.4 Bipolar Cells

Bipolar cells (BC) are second order neurons present in the retina which typically connect to multiple photoreceptors. In rare cases, a single BC may associate with a single photoreceptor. Although this typically only occurs in the cone system, BCs are responsible for the transmission and amplification of the light signal from photoreceptors to ganglion cells. There are two broad functional categories of BCs: those that depolarize with the onset of light (ON bipolar cells- ON BC), and those that depolarize with the cessation of light (OFF bipolar cells- OFF BC). This differentiation is due in part of the glutamate receptor expressed in each BC type (Snellman et al., 2008, Strettoi et al., 2010, Euler et al., 2014). The dendritic tips of ON BCs contain mGluR6, a G-protein coupled receptor, which binds glutamate, released from photoreceptors in the dark. Stimulation of mGluR6 is signaled by the G-protein cascade and results in closure of the cation channel TRPM1 (transient receptor potential cation channel subfamily M member 1) and hyperpolarization of the ON BC (Morgans et al., 2010, Shen et al., 2012). OFF BCs express an ionotropic glutamate receptor, which when stimulated by glutamate opens a channel depolarizing the cell membrane. On light-induced reduction of glutamate release the channel closes leading to hyperpolarization of the cell. In the rod system ON BCs are predominantly responsible for transmission of the photoreceptor signal while the cone system uses both ON and OFF BCs (Hartveit, 1997).

Bipolar cells can be further subdivided based on the size of their synaptic and dendritic fields (how many photoreceptors and ganglion cells they connect to) and functional specificities (preferences in directional sensitivity, center/surround, …) (Hartveit, 1997, Euler et al., 2014). Recent molecular studies in mice identified 15 BC types based on their

transcriptomes, in which 8 are ON-BC (Shekhar et al., 2016). Early morphological studies in rats have showed 9 types of cone BCs – 4 OFF BCs, 5 ON BCs - and one rod BC (Hartveit, 1997) (Fig.1.3).

The BCs axon terminals normally stratify in different levels of the IPL, which is subdivided in 5 equal layers. In the rat, the axon terminals of OFF BCs are localized in the first and second layer of the IPL (outer sublamina). Whereas, the axon terminals of ON BCs synapse in the third, fourth and fifth layers (inner sublamina) (Hartveit, 1997).

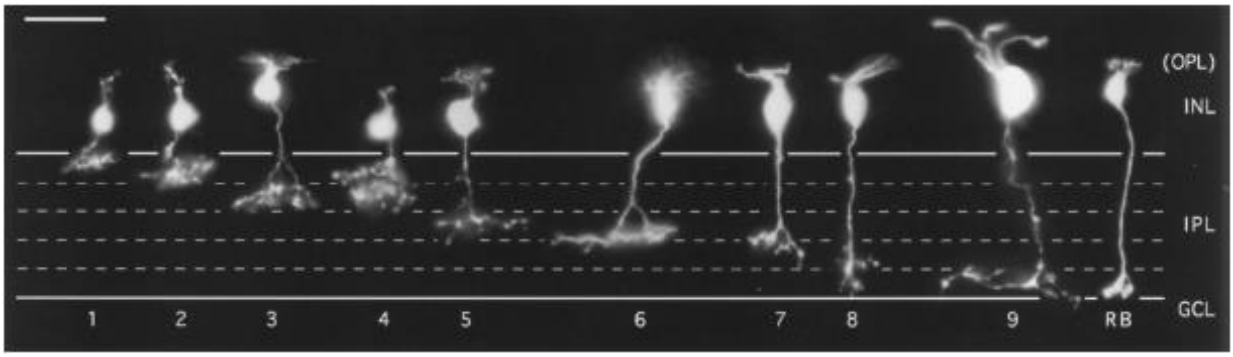

Figure. 1.3. Montage of bipolar cells filled with Lucifer yellow in lightly fixed slices of rat retina from Hartveit, 1997. From left to right, different types of cone bipolar cells (1–9) and a rod bipolar cell (RB). The inner plexiform layer (IPL) has been divided into 5 strata of equal width. OPL, outer plexiform layer; INL, inner nuclear layer; IPL, inner plexiform layer; GCL, ganglion cell layer. Scale bar: 30 mm.

The synaptic architecture between photoreceptors and BCs differs between ON and OFF BCs. The photoreceptor synaptic terminal of cones is called a pedicle and that of rods a spherule. There are synaptic ribbons pointing to the postsynaptic processes. The cone pedicle form “triads” with one invaginating ON BC and two lateral horizontal cells and also has basal junctions (flat contact) with OFF BC. Rod spherules make

invaginating contacts with dendrites of rod BCs and a horizontal cell (Kolb, 1995b, Kolb, 1995a, Haverkamp et al., 2000).

1.4.1 ON Bipolar Cells

In the dark, glutamate released by the photoreceptor stimulates the metabotropic receptor (mGluR6) on ON BCs, which signal through the heterotrimeric G-protein cascade, called G_o (Dhingra et al., 2012, Ramakrishnan et al., 2015). G_o is composed of $G\alpha_o\beta_3\gamma_{13}$. As the G-protein becomes activated, GDP is released and GTP binds to the $G\alpha_o$ subunit. Gαo-GTP dissociates from the receptor and the $G\beta_3\gamma_{13}$ dimer, closing the TRPM1 cation channel, resulting in cell hyperpolarization. There is some debate whether the G-protein component $G\alpha_o$-GTP subunit or $G\beta_3\gamma_{13}$ dimer is the active molecule that closes the TRPM1 cation channel and hyperpolarizes ON-BCs in the dark (Koike et al., 2010, Morgans et al., 2010). Recent studies in mice suggest that in fact both $G\alpha_o$ and $G\beta_3\gamma_{13}$ play a role in the closure of the TRPM1 channel (Xu et al., 2016).

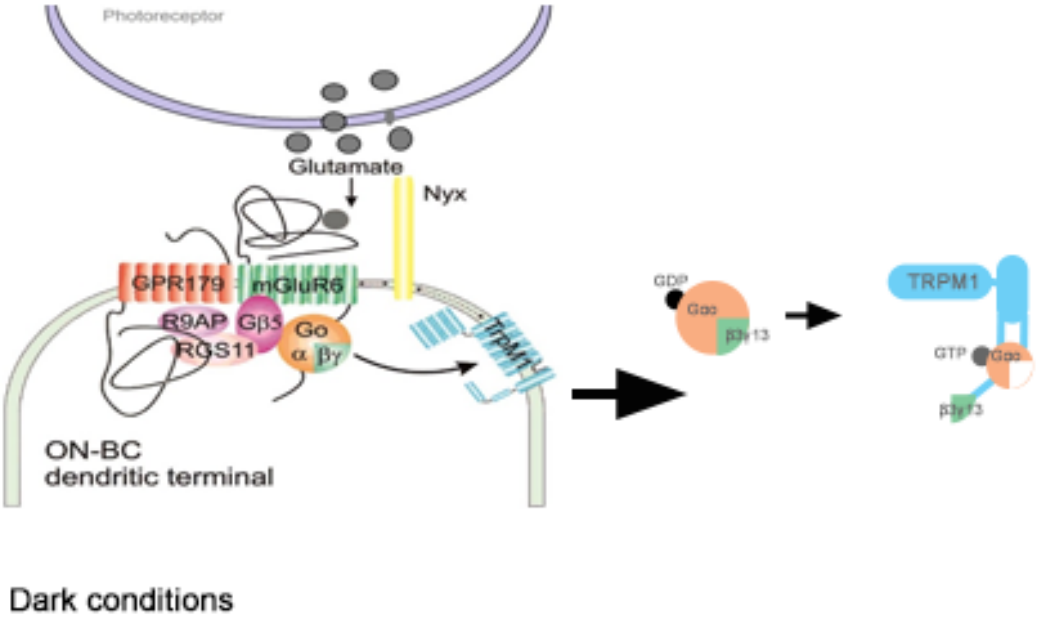

Figure. 1.4. Modified schematic of the ON bipolar cell cascade. In dark conditions, glutamate released by the photoreceptor stimulates the metabotropic receptor (mGluR6), which activate the heterotrimeric G-protein cascade, $G\alpha_o\beta_3\gamma_{13}$. Its inactive state becomes active as GDP is released, and GTP binds to the $G\alpha_o$ subunit, dissociating from the $\beta_3\gamma_{13}$ dimer and both act to cause closure of the TRPM1 channel. Modified from : http://www.nin.knaw.nl/research_groups/kamermans_group/research_line_3.

The depolarization of the ON BC occurs due to the reduced glutamate release from photoreceptors and colocalized RGS (regulators of G-protein signaling) proteins are responsible for inactivation of the ON BC G-protein cascade. Two complexes have been identified that act on this cascade, $G\beta_5$-RGS7 and $G\beta_5$-RGS11, and act as GTPases (Morgans et al., 2007). Their role is similar to the $G\beta_5$L-RGS9 complex role in deactivation of photoreceptors (Fu and Yau, 2007, Morgans et al., 2007). They stimulate GTP hydrolysis, accelerating it to a rapid deactivation on light response. A delay in the ERG b-

wave can be detected in mice lacking RGS7 or RGS11, affecting sensitivity and the time course of ON BC responses (Cao et al., 2012, Shim et al., 2012).

1.5 Functional assessment of the retina

One of the most important tools for the assessment of the retinal function is electroretinography (ERG), which is used for the diagnosis and evaluation of retinal diseases. ERG measures the change in retinal activity due to specific types of light stimulus under dark or light adapted lighting conditions. The change in activity results in a change in current flow around the eye which can be measured at the surface of the cornea using electrodes designed for this purpose (Marmor et al., 2009).

The electric potentials generated by the eye after light stimulation were first described in the late 1800s. Einthoven and Jolly (1908) were the first to observe three different portions of the waveform which they classified as the a-, b- and c-wave: a-wave, the initial negative deflection following a brief flash; b-wave, the subsequent positive peak; and c-wave a later and smaller positive deflection of the ERG.

Even though Einthoven and Jolly had a significant role in this discovery, Ragnar Granit was the first to show the different components of the ERG and origins from different cell types. His discoveries in ocular electrophysiology resulted in a Nobel prize in Medicine in 1967. Granit observed three potentials (PI, PII and PIII) which disappeared during increasingly longer exposure to anesthesia with ether in cats (Fig. 1.5). PI is a slow positive component, first to disappear under anesthesia, and somewhat correlates to the c-wave. PII is a positive peak that decreases as the light goes off, and correlates to the b-wave. PIII, the fast negative peak which is maintained with the light exposure, correlates to the a-wave. Additional work using more specific pharmaceutical agents as well as intra-retinal and intracellular recordings established that the a-wave is generated mostly by

photoreceptor activity: the b-wave by ON-BCs and the c-wave by retinal pigmented epithelium (Noell, 1953, Steinberg et al., 1970, Pepperberg et al., 1978) (Fig. 1.5).

Pharmacological dissection of the ERG has proven to be helpful in understanding the retinal components and determining their contribution to the ERG waveform (Sieving et al., 1994, Xu et al., 2003, Sharma et al., 2005). There are many drugs used to block different types of cells in the retina. The most common ones are 2-amino-4-phosphonobutyrate (L-AP4) and cis-2,3-piperidine dicarboxylic acid (PDA) (Sieving et al., 1994, Robson and Frishman, 1996, Xu et al., 2003, Sharma et al., 2005). L-AP4 is a glutamatergic receptor agonist which selectively blocks the transmission from photoreceptors to ON-BCs, leaving the OFF-BCs responses intact. In rats and other animals, the use of this drug removes the b-wave of the ERG, since the ON pathway is a major contribution to this waveform. PDA, a glutamatergic receptor antagonist, is a less selective drug that blocks the transmission from photoreceptors to OFF-BCs and horizontal cells (Sharma et al., 2005). The use of PDA in monkeys resulted in a reduction in a-wave amplitude and an increase of b-wave amplitude in the photopic ERG. These results suggest that OFF BC activity contributes to the a-wave and that the b-wave is shaped by an interaction between opposing field potentials generated by ON and OFF pathways (Sieving et al., 1994).

Oscillatory potentials (OPs) are imposed on the leading edge of the b-wave. They result from the activity of inner retinal cells. Studies suggested that the primary origin of OPs is the amacrine and ganglion cells (Lachapelle et al., 1998, Wachtmeister, 1998, Sandmeyer et al., 2007). The earlier wavelets (OP1-OP3) are related to the on-pathway

and the later wavelets (OP4-OP6) related to the off-pathway, as they are sensitive to GABA and glycine, respectively (Wachtmeister, 1998).

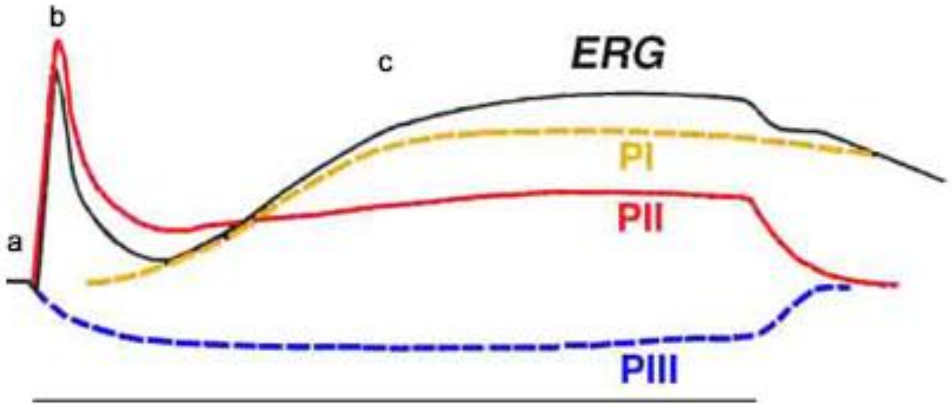

Figure 1.5. Diagrammatic representation of the Granit waveforms (PI, PII and PIII) overlapped to an ERG. Horizontal line represents the light stimulus. Modified from: http://webvision.med.utah.edu/book/electrophysiology/the-electroretinogram-erg/

Currently, there are standard ERG protocols for clinicians for assessment of retinal activity set by the International Society of Clinical Electrophysiology of Vision (ISCEV) (McCulloch et al., 2015). This standard screening protocol could not have been established without the prior efforts to understand the origin of the ERG potentials. The standard protocol includes a mix of dark and light-adapted ERGs which give an initial indication of rod, rod bipolar, cone, cone bipolar functions. Many factors that can affect

ERG recordings such as background light, light or dark adaption time, light exposure history, diet, depth of anesthesia and of course proper positioning of the electrodes (Ofri, 2002, Mentzer et al., 2005, Tuntivanich et al., 2005, McCulloch et al., 2015). In addition to the ISCEV standard protocol, one can probe further aspects of the retinal function using different colored light flashes and a broader range of flash intensities. Analysis of the ERG waveform and time measurements can provide information to identify sites and mechanisms of retinal dysfunction (Ekesten et al., 2013).

1.6 $G\beta_3$ mutation in animal models

A spontaneous null mutation in *Gnb3* resulting in the absence of $G\beta_3$, occurs in chickens (Tummala et al., 2006). Roger Curtis first described the phenotype in commercial egg laying chickens and the phenotype was named retinopathy globe enlarged (RGE) (Curtis et al., 1987, Curtis et al., 1988, Montiani-Ferreira et al., 2003). As the name suggests, affected chickens develop progressive globe enlargement associated with retinal thinning. Most likely, the increase in globe enlargement is a secondary effect of reduced visual function (Ritchey et al., 2010; Petersen-Jones personal communications). Affected birds have markedly reduced vision and abnormal electroretinograms (ERG) (Montiani-Ferreira et al., 2003, Montiani-Ferreira et al., 2007). Pharmacologic agents were used to selectively block activity of different retinal neurons and isolate the origin of the abnormal ERG findings. These studies showed that the mutant birds had reduced photoreceptor sensitivity and a marked reduction in ON BC activity (Petersen-Jones et al., 2007). Behavioral vision testing using an optokinetic reflex device showed diminished vision in both dim and normal room lighting conditions, suggesting that both the rod and cone pathways are affected by this mutation (Montiani-Ferreira et al., 2003). Histology demonstrated a progressive retinal thinning as the globe enlarged and disorganization of the synapse between photoreceptors and BCs (Montiani-Ferreira et al., 2005).

A Gnb3 knockout mouse (*Gnb3* $^{-/-}$ mice) was generated and demonstrated impairment of both rod and cone ON BC signaling (Dhingra et al., 2012) but without a secondary globe enlargement. The lack of ON BC function in *Gnb3*$^{-/-}$ mice was demonstrated by a marked reduction in both the dark- and light-adapted ERG b-wave. A lack of ERG b-

wave has also been reported as a result of mutations of other ON BC expressed genes. Collectively this presentation is known as a “no b-wave” or “nob” phenotype (Pardue and Peachey, 2014)(Fig.1.6).

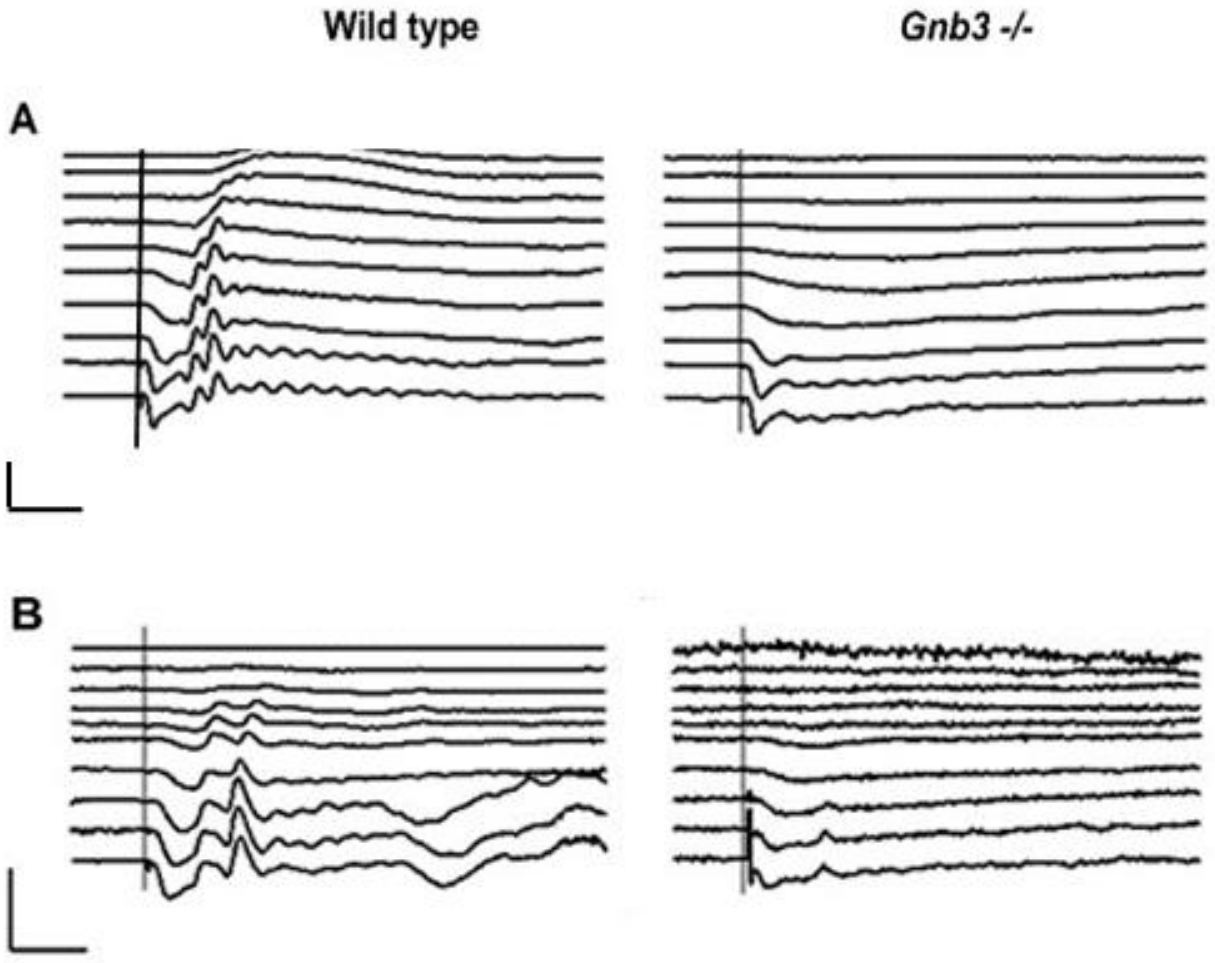

Figure. 1.6. **Electroretinographic responses from *Gnb3*$^{-/-}$ mice. A**. Averaged dark adapted series in WildType and *Gnb3*$^{-/-}$ mice. **B**. Averaged light adapted series in WildType and *Gnb3*$^{-/-}$ mice (n=3). Size bars: 100µV/ 50 mSec.

Comparison between *Gnb3*$^{-/-}$ and other “no b-wave” mouse models suggested that a small ON BC component was still present in both the dark- and light-adapted ERGs of *Gnb3*$^{-/-}$ mice (Dhingra et al., 2012). The lack of $G\beta_3$, which is also involved in cone phototransduction (cone beta transducin), in *Gnb3*$^{-/-}$ mice resulted in reduced cone sensitivity, but surprisingly, normal kinetics and saturating responses (Nikonov et al., 2013), suggesting that $G\beta_3$ is not necessary for signal transduction in cones. *Gnb3*$^{-/-}$ mice also showed abnormalities in the rod to rod BC synapses with a lack of invagination at the rod spherule (Dhingra et al., 2012). This physical disassociation is likely to contribute to the loss of ERG b-wave in these animals.

1.7 Congenital Stationary Night Blindness

The class of human non-progressive disorders known as congenital stationary night blindness (CSNB) result from a lack of communication between photoreceptor and ON BC cells. (Bech-Hansen et al., 2000; Dryja et al., 2005; Audo et al., 2009; Peachey et al., 2012; Zeitz et al., 2013).. CSNB can be divided according to the degree of function into incomplete (iCSNB) and complete CSNB (cCSNB) (Miyake et al., 1986). The former is associated with mutations in pre-synaptic proteins and the latter with mutations in ON BC dendritic tips. cCSNB is characterized by normal fundus appearance and night blindness (Schubert and Bornschein, 1952, Riggs, 1954). In cCSNB the ERG phenotype has a normal dark adapted a-wave but lacks a b-wave in the light adapted ERG and has a delay in the b-wave (Bech-Hansen et al., 2000, Dryja et al., 2005, Audo et al., 2009, Peachey et al., 2012, Zeitz et al., 2013).

Recently, mutations in GNB3 were identified in human patients by two separate groups. One report of 4 patients described the phenotype as a form of CSNB with a variable degree of ON-BC dysfunction and reduced cone sensitivity (Vincent et al., 2016). While the second report was of a single individual homozygous for a presumed null mutation who showed some macular abnormalities including shortened cone outer segments and disruption of the ellipsoid zone. The ellipsoid zone is detected on optical coherence tomography and is thought to represent reflection of the laser light from mitochondria in cone inner segments. The patient had difficulties with near vision and although night blindness was not reported, the rod ERG had a very reduced b-wave and there were also abnormalities of the light-adapted ERG (Arno et al., 2016).

1.8 Gene Therapy

The method of introducing therapeutic genes into an organism is called gene therapy. The objective of this therapy is to reduce or abate the symptoms of a specific disease. The primary method of gene delivery utilizes a viral vector to deliver a genetic payload into the target cell. Non-viral delivery methods have been investigated but viral vector based methods show the greater promise. Recombinant adeno-associated viral vectors (AAV) have been shown to be effective in targeting photoreceptors and retinal pigment epithelium in animal models (Acland et al., 2001, Komaromy et al., 2010, Annear et al., 2013, Boyd et al., 2016). The lack of pathogenicity and availability of several serotypes of AAV makes it a good delivery tool for gene therapy (Daya and Berns, 2008). These small (25nm) viruses can hold about 4.7 kb of DNA, and can only replicate with a helper virus, either adenovirus or herpesvirus (Daya and Berns, 2008). The WildType AAV structure comprises the inverted terminal repeats (ITRs) on both ends, two open reading frames (ORFs) and three promoters (Fig. 1.7). Moreover, the AAV capsid consists of 60 polypeptides and holds the single-stranded DNA. ITRs are mainly responsible for replication, additionally they have been shown to be required for transcription and site-specific integration of wildtype AAV into the host cell (Daya and Berns, 2008). In the case of gene therapy, the ORFs are replaced by the gene of interest and the vector capsids can be modified to increase efficacy.

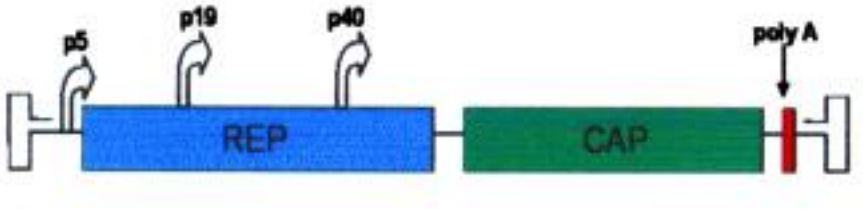

Figure. 1.7. **Basic genome organization of the WildType adeno-associated viral vector with three promoters (p5, p19 and p40), two open reading frames (REP and CAP) and a polyA tail**. Modified from Daya and Berns, 2008.

After being introduced to the target cell, the AAV binds to a receptor on the cell surface. It is endocytosed by a clathrin-coated pit and goes through endosomal processing steps for its integration (Schultz and Chamberlain, 2008). Cytoplasmic AAV traffic is different for each serotype. A parcel of the AAV2 virions accumulates in the Golgi apparatus before its release to the cytoplasm, while other virions traffic through late (Rab7) and recycling endosomes (Rab11) (Nonnenmacher and Weber, 2012). This process leads to conformational changes to the capsid proteins exposing the phospholipase domain located on the capsid. Upon entering the nucleus the capsid is removed (viral uncoating) and the vector genome is released (Daya and Berns, 2008) (Fig.1.8). Subsequently, the genome becomes double-stranded by annealing of a complimentary single stranded vector genome or by DNA repair mechanisms of the host cell. The double stranded DNA form episomes (circular structures) that are positioned in the nucleus and enable long lasting transduction (Schultz and Chamberlain, 2008).

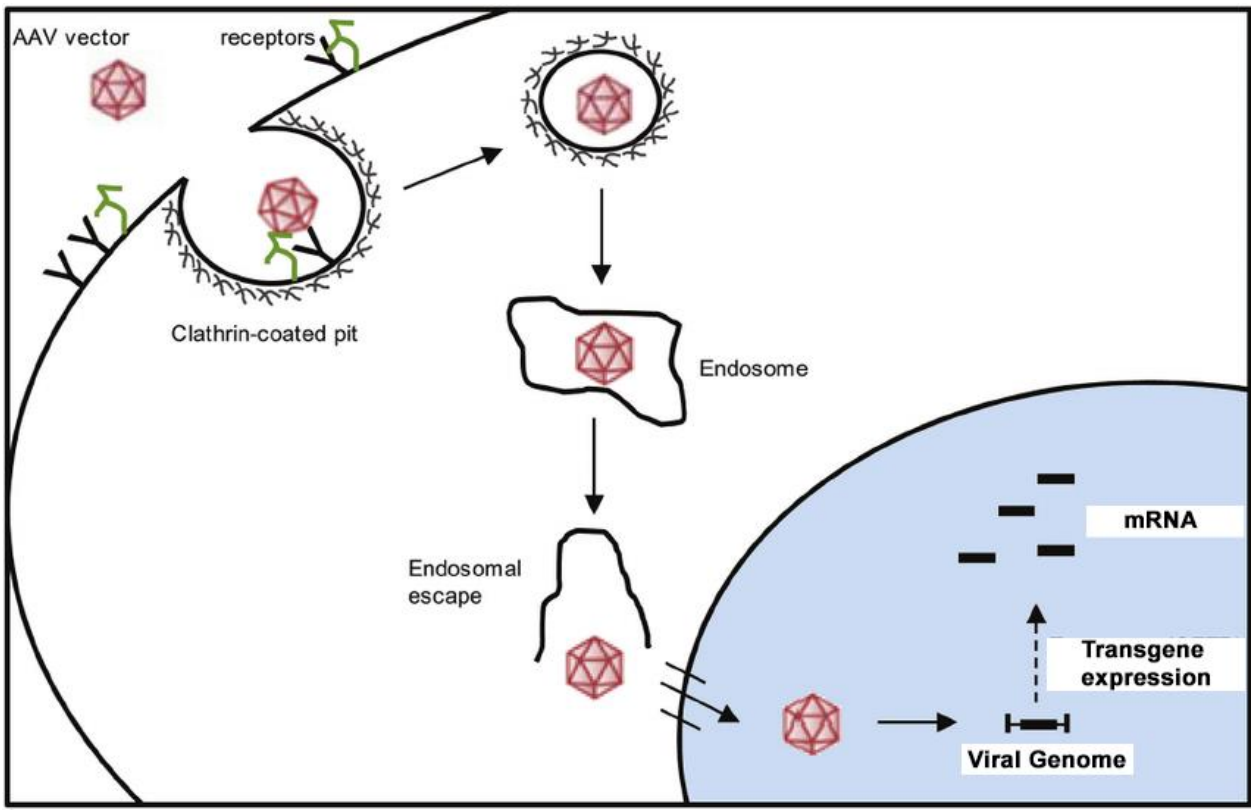

Figure.1.8. Viral entry into the cell. Modified from Martini et al. (2011). Adeno-associated viral (AAV) vector is endocytosed into the cell by clathrin-coated pits, passing through endosomal processing and migration to the nucleus. Into the nuclei, the viral genome transgene is expressed.

The main considerations for selecting a viral vector delivery method are the ability to attach and enter the target cell, effectively transfer to the nucleus with expression of the transgene, and the absence of any secondary adverse events or toxicity. The AAV2 serotype is commonly used for gene therapy but different serotypes can be more efficient in some tissues (Kay et al., 2013, Minella et al., 2014). The binding of the receptor to the AAV is dependent on the capsid sequences, which are different in each serotype. The tropism of AAV can be increased by using the pseudotyping approach, which uses the

genome from one serotype packaged within the capsid of another (Daya and Berns, 2008).

As mentioned before, in a therapeutic AAV the ORFs are replaced with the expression cassete consisting of a promoter, transgene of interest and polyadenylation signal. The promoter can be specific to a particular cell type or ubiquitous across many cell types. Specific cell type promoters can decrease the off target effect and potential toxicity (Schultz and Chamberlain, 2008) but may have a lower transduction efficiency. Modification of the AAV capsid sequences is commonly used to improve and modify transduction. Replacement of tyrosine residues with phenylalanine residues has been used for this purpose and to also decrease immune responses (Schultz and Chamberlain, 2008, Kay et al., 2013). Different approaches are being continuously developed to enhance the transgene expression.

The eye is one of the most studied organ for gene therapy purposes due its small size, easy visualization and examination of target tissues *in vivo*, the availability of unique promoters to target specific cell types, as well as it's immune privilege (Lipinski et al., 2013). Many studies to treat diseases of the photoreceptors and RPE have been carried out, but only recently a study demonstrated a successful delivery of an AAV2 gene therapy to bipolar cells in a CSNB mice model (Scalabrino et al., 2015). This was the first time that gene therapy targeting ON BCs was capable of partially restoring the ON BC signaling pathway.

New Optogenetic therapies aiming the inner retina have been studied (Cronin et al., 2014, Mace et al., 2015, De Silva et al., 2016, van Wyk et al., 2017). The use of AAV

targeting ganglion cells using a photo switch channelrhodopsin-2 is on phase I clinical trials in human patients (NCT02556736). A synthetic AAV capsid (AAV8BP2) with a modified GRM6 promoter showed to be a good option for delivery of light-sensing molecules to bipolar cells (Cronin et al., 2014). Another AAV with modified capsid residues (AAV27m8) encoding channelrhodopsin using a specific BC promoter (GRM6 modified promoter fragment) showed ON and OFF responses and locomotory behavior in treated rd1 mouse (Mace et al., 2015). A recent study using optogenetic targeting BCs compared four AAV capsid variants showing that all of them had a good transgene expression in wildtype BCs but not in degenerated mouse retinas (van Wyk et al., 2017).

There is a large unmet need for therapy for patients with CSNB and this disease is caused by many different genes. This recent demonstration of gene therapy to target bipolar cells opens up the opportunity for future gene therapy studies for ON BC disorders.

1.9 Dissertation aims and hypotheses

BCs are responsible for connecting photoreceptors to ganglion cells in the retina. Knockout of *Gnb3*, the gene that encodes the $G\beta_3$ protein, in mice results in a severe reduction in ON BC signaling. However, preliminary studies in *Gnb3*$^{-/-}$ rat show a similar lack of b-wave response in the dark-adapted ERG and a modest reduction of b-wave in the light adapted ERG.

The contributions of this research was firstly to elucidate the process of cone ON BC signaling in *Gnb3*$^{-/-}$ rats. Our central hypotheses was that cone ON BC signaling in rats is not dependent on $G\beta_3$, and secondly, to develop a treatment protocol for $G\beta_3$-associated retinopathy.

Our two specific aims were:

- To identify the signal transduction process in cone ON BCs in rats lacking $G\beta_3$; and
- Develop an AAV-mediated gene therapy for $G\beta_3$-associated retinopathy.

REFERENCES

REFERENCES

Acland GM, Aguirre GD, Ray J, Zhang Q, Aleman TS, Cideciyan AV, Pearce-Kelling SE, Anand V, Zeng Y, Maguire AM, Jacobson SG, Hauswirth WW, Bennett J (2001) Gene therapy restores vision in a canine model of childhood blindness. Nature genetics 28:92-95.

Annear MJ, Mowat FM, Bartoe JT, Querubin J, Azam SA, Basche M, Curran PG, Smith AJ, Bainbridge JW, Ali RR, Petersen-Jones SM (2013) Successful gene therapy in older Rpe65-deficient dogs following subretinal injection of an adeno-associated vector expressing RPE65. Human gene therapy 24:883-893.

Arno G, Holder GE, Chakarova C, Kohl S, Pontikos N, Fiorentino A, Plagnol V, Cheetham ME, Hardcastle AJ, Webster AR, Michaelides M, Consortium UKIRD (2016) Recessive Retinopathy Consequent on Mutant G-Protein beta Subunit 3 (GNB3). JAMA ophthalmology 134:924-927.

Arshavsky VY, Burns ME (2012) Photoreceptor signaling: supporting vision across a wide range of light intensities. Journal of Biological Chemistry 287:1620-1626.

Audo I, Kohl S, Leroy BP, Munier FL, Guillonneau X, Mohand-Said S, Bujakowska K, Nandrot EF, Lorenz B, Preising M, Kellner U, Renner AB, Bernd A, Antonio A, Moskova-Doumanova V, Lancelot ME, Poloschek CM, Drumare I, Defoort-Dhellemmes S, Wissinger B, Leveillard T, Hamel CP, Schorderet DF, De Baere E, Berger W, Jacobson SG, Zrenner E, Sahel JA, Bhattacharya SS, Zeitz C (2009) TRPM1 is mutated in patients with autosomal-recessive complete congenital stationary night blindness. American journal of human genetics 85:720-729.

Bech-Hansen NT, Naylor MJ, Maybaum TA, Sparkes RL, Koop B, Birch DG, Bergen AA, Prinsen CF, Polomeno RC, Gal A, Drack AV, Musarella MA, Jacobson SG, Young RS, Weleber RG (2000) Mutations in NYX, encoding the leucine-rich proteoglycan nyctalopin, cause X-linked complete congenital stationary night blindness. Nature genetics 26:319-323.

Boyd RF, Sledge DG, Boye SL, Boye SE, Hauswirth WW, Komaromy AM, Petersen-Jones SM, Bartoe JT (2016) Photoreceptor-targeted gene delivery using intravitreally administered AAV vectors in dogs. Gene therapy 23:400.

Cabrera-Vera TM, Vanhauwe J, Thomas TO, Medkova M, Preininger A, Mazzoni MR, Hamm HE (2003) Insights into G protein structure, function, and regulation. Endocrine reviews 24:765-781.

Cao Y, Pahlberg J, Sarria I, Kamasawa N, Sampath AP, Martemyanov KA (2012) Regulators of G protein signaling RGS7 and RGS11 determine the onset of the light response in ON bipolar neurons. Proceedings of the National Academy of Sciences of the United States of America 109:7905-7910.

Cronin T, Vandenberghe LH, Hantz P, Juttner J, Reimann A, Kacso AE, Huckfeldt RM, Busskamp V, Kohler H, Lagali PS, Roska B, Bennett J (2014) Efficient transduction and optogenetic stimulation of retinal bipolar cells by a synthetic adeno-associated virus capsid and promoter. EMBO molecular medicine 6:1175-1190.

Curtis PE, Baker JR, Curtis R, Johnston A (1987) Impaired vision in chickens associated with retinal defects. The Veterinary record 120:113-114.

Curtis R, Baker JR, Curtis PE, Johnston A (1988) An inherited retinopathy in commercial breeding chickens. Avian pathology : journal of the WVPA 17:87-99.\

Daya S, Berns KI (2008) Gene therapy using adeno-associated virus vectors. Clinical microbiology reviews 21:583-593.

De Silva SR, Charbel Issa P, Singh MS, Lipinski DM, Barnea-Cramer AO, Walker NJ, Barnard AR, Hankins MW, MacLaren RE (2016) Single residue AAV capsid mutation improves transduction of photoreceptors in the Abca4-/- mouse and bipolar cells in the rd1 mouse and human retina ex vivo. Gene therapy 23:767-774.

Dhingra A, Ramakrishnan H, Neinstein A, Fina ME, Xu Y, Li J, Chung DC, Lyubarsky A, Vardi N (2012) Gbeta3 is required for normal light ON responses and synaptic maintenance. The Journal of neuroscience : the official journal of the Society for Neuroscience 32:11343-11355.

Dryja TP, McGee TL, Berson EL, Fishman GA, Sandberg MA, Alexander KR, Derlacki DJ, Rajagopalan AS (2005) Night blindness and abnormal cone electroretinogram ON responses in patients with mutations in the GRM6 gene encoding mGluR6. Proceedings of the National Academy of Sciences of the United States of America 102:4884-4889.

Ekesten B, Komaromy AM, Ofri R, Petersen-Jones SM, Narfstrom K (2013) Guidelines for clinical electroretinography in the dog: 2012 update. Documenta ophthalmologica Advances in ophthalmology 127:79-87.

Euler T, Haverkamp S, Schubert T, Baden T (2014) Retinal bipolar cells: elementary building blocks of vision. Nature reviews Neuroscience 15:507-519.

Fu Y, Yau K-W (2007) Phototransduction in mouse rods and cones. Pflügers Archiv-European Journal of Physiology 454:805-819.

Grossniklaus HE, Geisert EE, Nickerson JM (2015) Introduction to the Retina. Progress in molecular biology and translational science 134:383-396.

Hartveit E (1997) Functional organization of cone bipolar cells in the rat retina. Journal of neurophysiology 77:1716-1730.

Haverkamp S, Grunert U, Wassle H (2000) The cone pedicle, a complex synapse in the retina. Neuron 27:85-95.

Kay CN, Ryals RC, Aslanidi GV, Min SH, Ruan Q, Sun J, Dyka FM, Kasuga D, Ayala AE, Van Vliet K, Agbandje-McKenna M, Hauswirth WW, Boye SL, Boye SE (2013) Targeting photoreceptors via intravitreal delivery using novel, capsid-mutated AAV vectors. PloS one 8:e62097.

Koike C, Obara T, Uriu Y, Numata T, Sanuki R, Miyata K, Koyasu T, Ueno S, Funabiki K, Tani A, Ueda H, Kondo M, Mori Y, Tachibana M, Furukawa T (2010) TRPM1 is a component of the retinal ON bipolar cell transduction channel in the mGluR6 cascade. Proceedings of the National Academy of Sciences of the United States of America 107:332-337.

Kolb H (1995a) Outer plexiform layer. In: Webvision: The organization of the retina and visual system (Kolb H, F. E., Nelson R, ed) Salt Lake City UT.

Kolb H (1995b) Photoreceptors. In: Webvision: organization of the retina and visual system (Kolb, H., Fernandez, E., Nelson, R., ed) Salt Lake City UT.

Kolb H (1995c) Simple anatomy of the retina. In: Webvision: The organization of the retina and visual system (Kolb, H., Fernandez, E., Nelson, R., ed) Salt Lake City UT.

Komaromy AM, Alexander JJ, Rowlan JS, Garcia MM, Chiodo VA, Kaya A, Tanaka JC, Acland GM, Hauswirth WW, Aguirre GD (2010) Gene therapy rescues cone function in congenital achromatopsia. Human molecular genetics 19:2581-2593.

Lachapelle P, Rousseau S, McKerral M, Benoit J, Polomeno RC, Koenekoop RK, Little JM (1998) Evidence supportive of a functional discrimination between photopic oscillatory potentials as revealed with cone and rod mediated retinopathies. Documenta ophthalmologica Advances in ophthalmology 95:35-54.

Larhammar D, Nordstrom K, Larsson TA (2009) Evolution of vertebrate rod and cone phototransduction genes. Philosophical transactions of the Royal Society of London Series B, Biological sciences 364:2867-2880.

Lipinski DM, Thake M, MacLaren RE (2013) Clinical applications of retinal gene therapy. Progress in retinal and eye research 32:22-47.

Mace E, Caplette R, Marre O, Sengupta A, Chaffiol A, Barbe P, Desrosiers M, Bamberg E, Sahel JA, Picaud S, Duebel J, Dalkara D (2015) Targeting channelrhodopsin-2 to ON-bipolar cells with vitreally administered AAV Restores ON and OFF visual responses in blind mice. Molecular therapy : the journal of the American Society of Gene Therapy 23:7-16.

Maggs DJ, Miller, P.E., Ofri, R., Slatter, D.H. (2008) Slatter's fundamentals of veterinary ophthalmology. Philadelphia PA: Saunders Elsevier.

Marmor MF, Fulton AB, Holder GE, Miyake Y, Brigell M, Bach M, International Society for Clinical Electrophysiology of V (2009) ISCEV Standard for full-field clinical electroretinography (2008 update). Documenta ophthalmologica Advances in ophthalmology 118:69-77.

McCudden CR, Hains MD, Kimple RJ, Siderovski DP, Willard FS (2005) G-protein signaling: back to the future. Cellular and molecular life sciences : CMLS 62:551-577.

McCulloch DL, Marmor MF, Brigell MG, Hamilton R, Holder GE, Tzekov R, Bach M (2015) ISCEV Standard for full-field clinical electroretinography (2015 update). Documenta ophthalmologica Advances in ophthalmology 130:1-12.

Mentzer AE, Eifler DM, Montiani-Ferreira F, Tuntivanich N, Forcier JQ, Petersen-Jones SM (2005) Influence of recording electrode type and reference electrode position on the canine electroretinogram. Documenta ophthalmologica Advances in ophthalmology 111:95-106.

Minella AL, Mowat FM, Willett KL, Sledge D, Bartoe JT, Bennett J, Petersen-Jones SM (2014) Differential targeting of feline photoreceptors by recombinant adeno-associated viral vectors: implications for preclinical gene therapy trials. Gene therapy 21:913-920.

Miyake Y, Yagasaki K, Horiguchi M, Kawase Y, Kanda T (1986) Congenital stationary night blindness with negative electroretinogram. A new classification. Archives of ophthalmology 104:1013-1020.

Montiani-Ferreira F, Fischer A, Cernuda-Cernuda R, Kiupel M, DeGrip WJ, Sherry D, Cho SS, Shaw GC, Evans MG, Hocking PM, Petersen-Jones SM (2005) Detailed histopathologic characterization of the retinopathy, globe enlarged (rge) chick phenotype. Molecular vision 11:11-27.

Montiani-Ferreira F, Li T, Kiupel M, Howland H, Hocking P, Curtis R, Petersen-Jones S (2003) Clinical features of the retinopathy, globe enlarged (rge) chick phenotype. Vision research 43:2009-2018.

Montiani-Ferreira F, Shaw GC, Geller AM, Petersen-Jones SM (2007) Electroretinographic features of the retinopathy, globe enlarged (rge) chick phenotype. Molecular vision 13:553-565.

Morgans CW, Brown RL, Duvoisin RM (2010) TRPM1: the endpoint of the mGluR6 signal transduction cascade in retinal ON-bipolar cells. BioEssays : news and reviews in molecular, cellular and developmental biology 32:609-614.

Morgans CW, Weiwei L, Wensel TG, Brown RL, Perez-Leon JA, Bearnot B, Duvoisin RM (2007) Gbeta5-RGS complexes co-localize with mGluR6 in retinal ON-bipolar cells. The European journal of neuroscience 26:2899-2905.

Nikonov SS, Lyubarsky A, Fina ME, Nikonova ES, Sengupta A, Chinniah C, Ding XQ, Smith RG, Pugh EN, Jr., Vardi N, Dhingra A (2013) Cones respond to light in the absence of transducin beta subunit. The Journal of neuroscience : the official journal of the Society for Neuroscience 33:5182-5194.

Noell WK (1953) Experimentally induced toxic effects on structure and function of visual cells and pigment epithelium. American journal of ophthalmology 36:103-116.

Nonnenmacher M, Weber T (2012) Intracellular transport of recombinant adeno-associated virus vectors. Gene therapy 19:649-658.

Offermanns S (2003) G-proteins as transducers in transmembrane signalling. Progress in biophysics and molecular biology 83:101-130.

Ofri R (2002) Clinical electrophysiology in veterinary ophthalmology--the past, present and future. Documenta ophthalmologica Advances in ophthalmology 104:5-16.

Oldham WM, Hamm HE (2008) Heterotrimeric G protein activation by G-protein-coupled receptors. Nature Reviews Molecular Cell Biology 9:60-71.

Palczewski K (2012) Chemistry and biology of vision. Journal of Biological Chemistry 287:1612-1619.

Pardue MT, Peachey NS (2014) Mouse b-wave mutants. Documenta ophthalmologica Advances in ophthalmology 128:77-89.

Peachey NS, Ray TA, Florijn R, Rowe LB, Sjoerdsma T, Contreras-Alcantara S, Baba K, Tosini G, Pozdeyev N, Iuvone PM, Bojang P, Jr., Pearring JN, Simonsz HJ, van Genderen M, Birch DG, Traboulsi EI, Dorfman A, Lopez I, Ren H, Goldberg AF, Nishina PM, Lachapelle P, McCall MA, Koenekoop RK, Bergen AA, Kamermans M, Gregg RG (2012) GPR179 is required for depolarizing bipolar cell function and is mutated in autosomal-recessive complete congenital stationary night blindness. American journal of human genetics 90:331-339.

Pepperberg DR, Brown PK, Lurie M, Dowling JE (1978) Visual pigment and photoreceptor sensitivity in the isolated skate retina. The Journal of general physiology 71:369-396.

Ramakrishnan H, Dhingra A, Tummala SR, Fina ME, Li JJ, Lyubarsky A, Vardi N (2015) Differential function of Ggamma13 in rod bipolar and ON cone bipolar cells. The Journal of physiology 593:1531-1550.

Riggs LA (1954) Electroretinography in cases of night blindness. American journal of ophthalmology 38:70-78.

Robson JG, Frishman LJ (1996) Photoreceptor and bipolar cell contributions to the cat electroretinogram: a kinetic model for the early part of the flash response. Journal of the Optical Society of America A, Optics, image science, and vision 13:613-622.

Sandmeyer LS, Breaux CB, Archer S, Grahn BH (2007) Clinical and electroretinographic characteristics of congenital stationary night blindness in the Appaloosa and the association with the leopard complex. Veterinary ophthalmology 10:368-375.

Scalabrino ML, Boye SL, Fransen KM, Noel JM, Dyka FM, Min SH, Ruan Q, De Leeuw CN, Simpson EM, Gregg RG, McCall MA, Peachey NS, Boye SE (2015) Intravitreal delivery of a novel AAV vector targets ON bipolar cells and restores visual function in a mouse model of complete congenital stationary night blindness. Human molecular genetics 24:6229-6239.

Schubert G, Bornschein H (1952) [Analysis of the human electroretinogram]. Ophthalmologica Journal international d'ophtalmologie International journal of ophthalmology Zeitschrift fur Augenheilkunde 123:396-413.

Schultz BR, Chamberlain JS (2008) Recombinant adeno-associated virus transduction and integration. Molecular therapy : the journal of the American Society of Gene Therapy 16:1189-1199.

Sharma S, Ball SL, Peachey NS (2005) Pharmacological studies of the mouse cone electroretinogram. Visual neuroscience 22:631-636.

Shekhar K, Lapan SW, Whitney IE, Tran NM, Macosko EZ, Kowalczyk M, Adiconis X, Levin JZ, Nemesh J, Goldman M, McCarroll SA, Cepko CL, Regev A, Sanes JR (2016) Comprehensive Classification of Retinal Bipolar Neurons by Single-Cell Transcriptomics. Cell 166:1308-1323 e1330.

Shen Y, Rampino MA, Carroll RC, Nawy S (2012) G-protein-mediated inhibition of the Trp channel TRPM1 requires the Gbetagamma dimer. Proceedings of the National Academy of Sciences of the United States of America 109:8752-8757.

Shim H, Wang CT, Chen YL, Chau VQ, Fu KG, Yang J, McQuiston AR, Fisher RA, Chen CK (2012) Defective retinal depolarizing bipolar cells in regulators of G protein signaling (RGS) 7 and 11 double null mice. The Journal of biological chemistry 287:14873-14879.

Sieving PA, Murayama K, Naarendorp F (1994) Push–pull model of the primate photopic electroretinogram: a role for hyperpolarizing neurons in shaping the b-wave. Visual neuroscience 11:519-532.

Snellman J, Kaur T, Shen Y, Nawy S (2008) Regulation of ON bipolar cell activity. Progress in retinal and eye research 27:450-463.

Steinberg RH, Schmidt R, Brown KT (1970) Intracellular responses to light from cat pigment epithelium: origin of the electroretinogram c-wave. Nature 227:728-730.

Strauss O (2005) The retinal pigment epithelium in visual function. Physiological reviews 85:845-881.

Strettoi E, Novelli E, Mazzoni F, Barone I, Damiani D (2010) Complexity of retinal cone bipolar cells. Progress in retinal and eye research 29:272-283.

Tang PH, Kono M, Koutalos Y, Ablonczy Z, Crouch RK (2013) New insights into retinoid metabolism and cycling within the retina. Progress in retinal and eye research 32:48-63.

Tummala H, Ali M, Getty P, Hocking PM, Burt DW, Inglehearn CF, Lester DH (2006) Mutation in the guanine nucleotide-binding protein beta-3 causes retinal degeneration and embryonic mortality in chickens. Investigative ophthalmology & visual science 47:4714-4718.

Tuntivanich N, Mentzer AL, Eifler DM, Montiani-Ferreira F, Forcier JQ, Johnson CA, Petersen-Jones SM (2005) Assessment of the dark-adaptation time required for recovery of electroretinographic responses in dogs after fundus photography and indirect ophthalmoscopy. American journal of veterinary research 66:1798-1804.

van Wyk M, Hulliger EC, Girod L, Ebneter A, Kleinlogel S (2017) Present Molecular Limitations of ON-Bipolar Cell Targeted Gene Therapy. Frontiers in neuroscience 11:161.

Vincent A, Audo I, Tavares E, Maynes JT, Tumber A, Wright T, Li S, Michiels C, Consortium GNB, Condroyer C, MacDonald H, Verdet R, Sahel JA, Hamel CP, Zeitz C, Heon E (2016) Biallelic Mutations in GNB3 Cause a Unique Form of Autosomal-Recessive Congenital Stationary Night Blindness. American journal of human genetics 98:1011-1019.

Wachtmeister L (1998) Oscillatory potentials in the retina: what do they reveal. Progress in retinal and eye research 17:485-521.

Wang J-S, Kefalov VJ (2011) The cone-specific visual cycle. Progress in retinal and eye research 30:115-128.

Xu L, Ball SL, Alexander KR, Peachey NS (2003) Pharmacological analysis of the rat cone electroretinogram. Visual neuroscience 20:297-306.

Xu Y, Orlandi C, Cao Y, Yang S, Choi CI, Pagadala V, Birnbaumer L, Martemyanov KA, Vardi N (2016) The TRPM1 channel in ON-bipolar cells is gated by both the alpha and the betagamma subunits of the G-protein Go. Scientific reports 6:20940.

Zeitz C, Jacobson SG, Hamel CP, Bujakowska K, Neuille M, Orhan E, Zanlonghi X, Lancelot ME, Michiels C, Schwartz SB, Bocquet B, Congenital Stationary Night Blindness C, Antonio A, Audier C, Letexier M, Saraiva JP, Luu TD, Sennlaub F, Nguyen H, Poch O, Dollfus H, Lecompte O, Kohl S, Sahel JA, Bhattacharya SS, Audo I (2013) Whole-exome sequencing identifies LRIT3 mutations as a cause of autosomal-recessive complete congenital stationary night blindness. American journal of human genetics 92:67-75.

CHAPTER 2

A FACEMASK FOR GASEOUS ANESTHESIA IN LABORATORY RODENTS AND CHICKS THAT ALLOWS EASY ACCESS TO THE EYES FOR OPHTHALMIC PROCEDURES

Bacellar M, Querubin J, Petersen-Jones SM (2013) A facemask for gaseous anesthesia in laboratory rodents and chicks that allows easy access to the eyes for ophthalmic procedures. Vet Ophthalmol. 16(4):316-7. Epub 2012 Oct 15. PMID:23066660

2.1 Abstract

Purpose. The purpose of this paper is to report a method for making a cheap and effective anesthesia facemask for laboratory rodents and chicks that allows access to the eyes for ophthalmic procedures such as electroretinography (ERG) and optical coherence tomography (OCT). *Methods.* The facemask is fabricated from a bulb syringe and a medicine dropper (Luvs®, Jamaica, NY) both intended for use in infants. The tip of the bulb syringe is removed to make a plastic cone (1.5 cm in length) to fit over the animal's nose. The bulb is removed from the medicine dropper and a small hole on the side of bulb near the closed end made into which the narrow end of the plastic cone is fitted and the joint glued with a hot glue gun. The facemask is then attached over the anesthetic tubing. *Results.* Following induction of anesthesia the facemask and a non-rebreathing circuit (Baines system) is suitable to maintain anesthesia in laboratory rodents and chicks while allowing ready access to the eyes for ERG and OCT. The mask fits snuggly, reducing leakage of anesthetic gasses and it has a minimum of deadspace. *Conclusions.* The materials required for making the facemask are cheap and readily available and it is easy to fabricate. We found it excellent for use with mice and chicks and it allows easy access to the eyes for techniques such as ERG and OCT.

Keywords: facemask, inhalation anesthesia, ERG, OCT, mouse, chicken

2.2 Introduction

Laboratory rodents are commonly used in ophthalmic research. Techniques such as electroretinography (ERG) and optical coherence tomography (OCT) are used to assess retinal function and morphology, respectively. General anesthesia is required and anesthesia with inhaled agents such as isofluorane is useful for such studies because they are easy to administer, allow for close control of the depth of anesthesia, and have a low rate of complications allowing animals to remain hemodynamic stable over long anesthesia protocols (Chaves et al., 2001, Szczesny et al., 2004).

We have designed an effective anesthesia facemask that is easy to fabricate from readily available material and is suitable for delivering gaseous anesthesia for ophthalmic procedures such as electroretinography (ERG) and optical coherence tomography (OCT) thus providing a cost-effective alternative to commercially available facemasks.

2.3 Methods

The facemask is made from a bulb syringe and a medicine dropper (Luvs®, Jamaica, NY) intended for use in babies (Figure 2.1a) to make a simple facemask for anesthesia of laboratory rodents. Using a scalpel the tip of the bulb syringe is removed to create a plastic cone (1.5 cm in length) that will fit over the animal's nose. The wider end of the resulting cone is trimmed so the opening to fit over the nose measures approximately 1cm in diameter (Figure 2.1b). The remaining bulb portion of the syringe is discarded. The bulb is removed from the medicine dropper (shown in green in Figure 2.1) and a small hole in the side of the bulb near the closed end is made (Figure 2.1b), into which the narrow end of the plastic cone created from the bulb syringe fits (Figure 2.1c and d). The two pieces are glued together using a hot glue gun and then coupled outside the anesthetic tubing (Figure 2.1d and 2.2). A plastic clip was used to hold the facemask to the anesthetic tube (figure 2.1d).

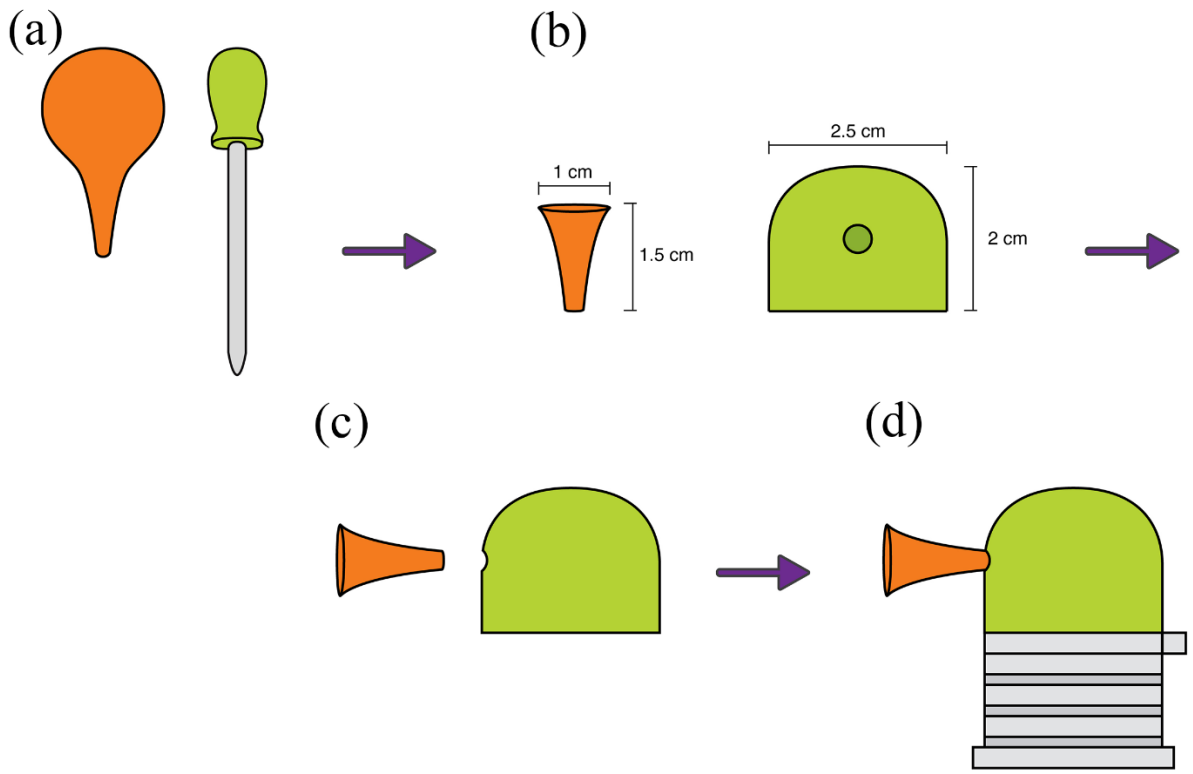

Figure 2.1. **Fabrication of the facemask**. **a.** A bulb syringe (colored brown in this diagram) and an infant dropper syringe (with a bulb colored green in this diagram). **b.** The 1.5 cm end of the bulb syringe has been removed and is used to create a cone with an opening of approximately 1cm that will fit over the nose or beak. The bulb (green) is removed from the dropper syringe and a small opening cut in the side near the closed end to receive the cone. **c**. The narrow end of the cone will fit into the hole made in the bulb from the dropper syringe. **d**. Once the facemask is assembled it fits over the end of the anesthesia tubing (shown in grey).

2.4 Results

The facemask effectively delivers gaseous anesthesia to both mice and chickens while allowing ready access to the eyes for procedures such as ERG and OCT. The mask fits snuggly round the nose or beak minimizing leakage of anesthetic gasses and has a minimum amount of deadspace.

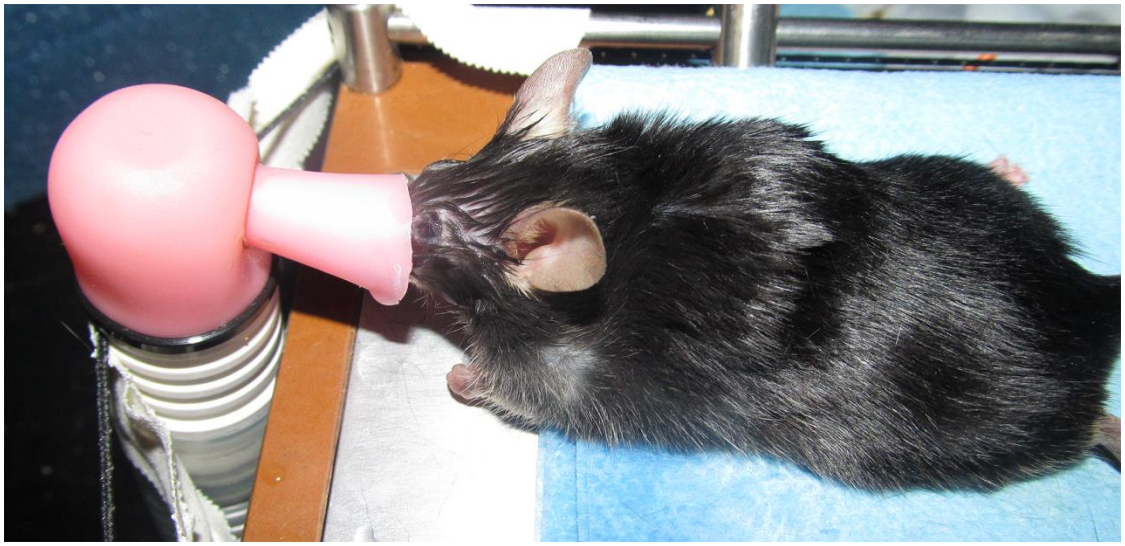

Figure 2.2. A photograph of a mouse being maintained under isoflurane anesthesia using the facemask (pink in color) coupled to a Baines system.

2.5 Conclusion and Summary

The materials required for making the facemask are cheap and readily available and it is quick and easy to fabricate. We found it excellent for use in both mice and chicks and it allows easy access to the eyes for techniques such as ERG and OCT.

2.6 Acknowledgement

To Bruna M. Fraga for the great job on the schematic drawing.

REFERENCES

REFERENCES

Chaves AA, Weinstein DM, Bauer JA (2001) Non-invasive echocardiographic studies in mice: influence of anesthetic regimen. Life sciences 69:213-222.

Szczesny G, Veihelmann A, Massberg S, Nolte D, Messmer K (2004) Long-term anaesthesia using inhalatory isoflurane in different strains of mice-the haemodynamic effects. Laboratory animals 38:64-69.

CHAPTER 3

$G\beta_3$ IS NOT ESSENTIAL FOR CONE ON-BIPOLAR SIGNALING IN RATS

Author Contributions

Conceived and designed the experiments: Marianna Bacellar-Galdino, Simon Petersen-Jones, Kwoon Y. Wong. Performed the experiments: MBG, Andrew P. Chervenak, Aaron N. Reifler. Analyzed the data: MBG, APC, ANR. Wrote the paper: MBG, SMP-J. Provided input for writing the manuscript: KYW, APC, ANR.

3.1 Introduction

G-protein signaling in the retina is important both in photoreceptors, as part of phototransduction, and in the second order neurons, ON-center or depolarizing bipolar cells (ON BC). Bipolar cells (BCs) synapse with photoreceptors and transmit the light response from photoreceptors directly or indirectly to ganglion cells. There are two types of bipolar cells, ON BCs and OFF-center or hyperpolarizing bipolar cells (OFF-BCs). The dendritic tips of ON BCs contain a metabotropic receptor (mGluR6), a G-coupled receptor, which is activated by the neurotransmitter glutamate, released from photoreceptors in the dark. The activated metabotropic receptor signals through a heterotrimeric G-protein, now known to consist of $G\alpha_o$ combined with a dimer of $G\beta_3$ and $G\gamma_{13}$ (Dhingra et al., 2012). G-protein signaling, leads to closure of a cation channel, Trpm1, and hyperpolarization of the ON BCs (Morgans et al., 2010, Shen et al., 2012). There is some debate whether the alpha or beta/gamma subunit is the active G-protein in ON BC (Koike et al., 2010, Morgans et al., 2010). Upon light stimulation, photoreceptors glutamate release decreases, reducing activation of mGluR6 and ON BC G-protein signaling, andTrpm1 ion channels opening, depolarizing the cell.

A spontaneous null mutation in *Gnb3,* which encodes $G\beta_3$, was reported in chickens (Tummala et al., 2006). Affected birds have markedly reduced vision, and an abnormal electroretinogram (ERG) (Montiani-Ferreira et al., 2003, Montiani-Ferreira et al., 2007). The use of selective drugs to block activity of specific retinal neurons were used to interrogate this abnormal ERG suggesting the birds had a marked reduction in ON BC function (Petersen-Jones, 2007). The affected chickens develop a progressive globe enlargement associated with retinal thinning; most likely as a secondary effect of reduced

visual function (Petersen-Jones unpublished observations; Ritchey et al, 2010). *Gnb3*$^{-/-}$ mice (which lack Gβ_3), have a marked impairment of both rod and cone ON-BC signaling (Dhingra et al., 2012). This finding confirmed Gβ_3 as the G protein beta subunit involved in ON BC signaling. The lack of ON BC function in *Gnb3* $^{-/-}$ mice results in a marked reduction in both dark- and light-adapted ERG b-wave. A similar no b-wave (nob) ERG phenotype can result from mutations of any one of several ON-BC expressed genes (Pardue and Peachey, 2014). A comparison of *Gnb3* $^{-/-}$ mice with another no b-wave mouse model suggested that a very small ON BC component was present in both dark- and light-adapted ERGs of *Gnb3* $^{-/-}$ mice (Dhingra et al., 2012). The lack of Gβ_3 (also known as cone beta transducin) in cones of *Gnb3*$^{-/-}$ mice resulted in reduced cone sensitivity, but surprisingly, normal kinetics and saturating response (Nikonov et al., 2013).

A lack of ON-BC function (e.g. due to mutations in *NYX, GRM6, TRPM1* and other ON-BC genes), causes congenital stationary night blindness (CSNB) in human patients (Bech-Hansen et al., 2000, Dryja et al., 2005, Audo et al., 2009, Peachey et al., 2012, Zeitz et al., 2013). Recently, mutations in *GNB3* were identified in humans by two separate groups. One report of 4 patients described the phenotype as a form of CSNB with a variable degree of ON BC dysfunction and reduced cone sensitivity (Vincent et al., 2016). While the second publication reported a single individual homozygous for a presumed null mutation in *GNB3* who showed some macular abnormalities including shortened cone outer segments and disruption of the ellipsoid zone on spectral domain optical coherence tomography. The patient had difficulties with near vision and although

night blindness was not reported the rod ERG had a very reduced b-wave and there were also abnormalities of the light-adapted ERG (Arno et al., 2016).

In this study, we show that similarly to the mouse model, *Gnb3* $^{-/-}$ rats have a lack of rod ON BC function. But in contrast to the mouse model, cone ON BC can still signal sufficiently to generate a light-adapted ERG b-wave, although somewhat reduced in amplitude. Single cell recordings from, retinal slices confirmed some cone ON BCs retain a degree of function.

3.2 Materials and Methods

3.2.1 Ethics Statement

All procedures were performed in accordance with the ARVO statement for the Use of Animals in Ophthalmic and Vision Research and approved by the Michigan and Michigan State University Institutional Animal Care and Use Committees.

3.2.2 Animals

Gnb3 $^{-/-}$ rats were supplied by The Medical College of Wisconsin. They had been generated on a Dahl/Salt sensitive background using a ZNK finger strategy to delete 15 base pairs from the 3' end of exon 7, intron 7 and 5 base pairs from the 5' end of exon 8. This causes a frameshift at codon 161 and a premature stop codon after 20 altered codons. We confirmed the lack of $G\beta_3$ in the retina of the *Gnb3$^{-/-}$ rats* by immunohistochemistry and Western blot (Fig. 3.1).

Rats were housed at Michigan State University under 12L:12D cycles and fed a commercial low salt diet. Heterozygous animals were maintained and breeding performed to produce wild type controls and homozygous *Gnb3* knockouts (*Gnb3$^{-/-}$*). A standard PCR genotyping assay was used on DNA samples extracted from rail tail (Reverse primer: CTGAAGGGCACTCACACAGA; Forward primer: TTATCTCTCCTGTTGCCGCT). The product size for the wild-type allele is 375 bp, and from the *Gnb3$^{-/-}$* allele 264bp.

3.2.3 Collection of retinal samples

Rats were euthanized following the AVMA guidelines for rodent euthanasia. Animals received a higher dose of CO_2 (8%) until loss of consciousness followed by an

intraperitoneal injection of pentobarbitone (100mg/kg – Fatal Plus, Vortech Pharmaceuticals, Dearborn MI) and creation of a pneumothorax. Following euthanasia the globes were enucleated.

3.2.4 Immunohistochemistry (IHC)

After enucleation, the globes were fixed in 4% paraformaldehyde in buffer for 10 minutes, then the posterior segment eyecup was dissected and placed back in the same fixation solution for 10 minutes. Eyecups were rinsed 3 times in phosphate buffer saline for 5 minutes, placed in 30% buffered sucrose for 30 minutes then embedded in OCT medium (Tissue-Tek® O.C.T. Compound, Sakura Finetek USA Inc, Torrance CA). 14µm thick sagittal cryosections were cut (Leica CM3050-S, Leica Microsystems, Buffalo Grove IL), placed on slides and frozen at -20C until use. Slides were defrosted at room temperature and sections were hydrated in phosphate buffer for 10 minutes, blocked with 10% normal horse serum, 0.5% Triton X-100 in phosphate buffer for 2 hours, then incubated in primary antibody ($G\beta_3$ antibody 1:400, Sigma Aldrich, St Louis, MO) at 4^0C overnight. They were then washed and incubated for 1 ½ hours in secondary antibody (AlexaFluor 488 goat anti rabbit, Thermo Fisher, Waltham, MA) conjugated to a fluorescent marker, washed, counterstained with DAPI (4',6-diamidino-2-phenylindole; Invitrogen) for 5 minutes and coverslipped and imaged with a confocal microscope (Olympus FluoView 1000 confocal, Center Valley, PA).

3.2.5 Western blot (WB)

Retinas were dissected from freshly enucleated eyes, flash frozen in liquid nitrogen and stored at −80˚C until used. Frozen retina was homogenized in lysis buffer containing (1M

Tris, Triton X-100) centrifuged at 14,000 x *g* for 20 minutes and the supernatant collected. Proteins were run on Mini-Protean Gel TGX 4-20% (BioRad Laboratories Inc., Hercules, CA) and transferred to a polyvinylidene difluoride membrane. Membranes were blocked (0.5% dry milk in Tris-buffered saline (TBS) with 0.01% Tween-20), washed 3 times with TBS and incubated overnight with $G\beta_3$ antibody (C-16) (1:1000, sc-381, Santa Cruz Biotechnology), then washed 3 times with TBS. They were then incubated with the correspondent anti-host IgG secondary antibody labeled with horseradish peroxidase (HRP; 1:10,000 diluted in 0.5% dry milk; Pierce Biotechnology Inc.) for 1 hour, washed 3 times with TBS, exposed to substrate (WBLUR0100, Luminata Crescendo Western, Millipore) for 5 minutes and visualized by chemiluminescence using the ChemiDoc XRS (Bio-Rad Laboratories Inc.) and analyzed using Quantity One software (Bio-Rad Laboratories Inc.). Anti-human β tubulin (1:10,000; #2146, Cell Signaling Tecnology, Danvers MA) served as the loading control.

3.2.6 Quantification of mRNA by real-time PCR

Eyes from 3 months old wildtype, heterozygote and *Gnb3*$^{-/-}$ animals were enucleated. Retinas were dissected, flash frozen in liquid nitrogen and stored at -80°C until used. Retinas (n = 2 per genotype) were homogenized in lysis buffer (Buffer RLT; RNeasy Protect Mini Kit; Qiagen, Inc., Hilden, Germany). RNA extraction was performed with a stabilization and purification kit (RNeasy Protect Mini Kit; Qiagen, Inc.), adding the DNase step to remove contaminating DNA (RNase-Free DNase set, Qiagen, Inc.). One microgram of DNase-treated RNA was reverse transcribed (Transcriptor First Strand cDNA Synthesis Kit, Roche Molecular Systems, Inc., Basel, Switzerland) and used in real-time PCR (Prime-Time® Gene Expression Master Mix, Integrated DNA Technologies

(IDT), Coralville, IA; and 7500 Fast Real-Time PCR System, ThermoFischer Scientific Inc., Waltham, MA) to measure Gnb3 and β-actin transcripts. PrimeTime mixes containing primer pairs and probe (Integrated DNA Technologies) for each transcript are included in Table 3.1. PrimeTime mixes were validated according to Bustin et al (2009) guidelines. Results are the average of three technical replicates for each sample. Relative gene expression was calculated using the $2^{-\Delta\Delta CT}$ method (Livak and Schmittgen, 2001).

Table 3.1. qRT-PCR primers/probe

Primer Name	Sequence 5' to 3'
actb FWD	GGCATAGAGGTCTTTACGGATG
actb REV	TCACTATCGGCAATGAGCG
actb probe	56-FAM/TCCTGGGTA/ZEN/TGGAATCCTGTGGC/3IABkFQ/
GNB3 FWD	CAGGTTATCTCTCCTGTTGCC
GNB3 REV	ACGAACACTGTCTTCTGCTG
GNB3 probe	56-FAM/ACGTGGTGT/ZEN/CCCCAGAGCTAGTC/3IABkFQ

Probes are double-quenched using a 5′ 6-FAM fluorophore, 3′ IBFQ quencher and inner ZEN quencher, all trademark Integrated DNA Technologies

3.2.7 Plastic embedded sections

Eyes from 6 month old *Gnb3*$^{-/-}$ rats and an age-matched wildtype (WT) rat were fixed in 3% glutaraldehyde and 2% paraformaldehyde in 0.2 M sodium cacodylate buffer (Electron Microscopy Sciences, Hatfield, PA, USA) for 30 minutes, the anterior segment of the eye removed and the eyecup placed back into the fixative overnight at 4°C. The samples were washed and stored in 0.2 M sodium cacodylate buffer at 4°C until dissected. A 3.0 mm portion of the retina was dissected about 1-2 mm lateral to the optic nerve and then embedded in 1-2% agarose in 0.1 M sodium cacodylate buffer to facilitate handling of the tissue samples without detachment of the retina during processing. Tissue samples were post-fixed in 2% osmium tetroxide for 15 mins before dehydration in

acetone and infusion of Spurr resin (Spurr, 1969). Samples were sectioned with an RMC MTX ultramicrotome (Boeckeler Instruments, Tucson, AZ, USA). Thick sections (500 nm) were stained with epoxy tissue stain (Electron Microscopy Sciences, Hatfield, PA, USA) and imaged with a light microscope (Nikon Eclipse 80i, Nikon Instruments Inc., Melville NY).

3.2.8 Electroretinography (ERG)

Prior to ERGs the animals were dark adapted for 12 hours. Manipulations were then performed under a dim red light. Anesthesia was induced and maintained by isoflurane 2% (IsoFlo; Abbott Laboratories, North Chicago IL) in oxygen. Body temperature was maintained with a heating table. Pupils were dilated with 1 % topical tropicamide (Falcon Pharmaceuticals, Ltd., Fort Worth TX). Corneal electrodes (Mayo, Japan) were placed against the cornea coupled with 2.5% Hypromellose Ophthalmic demulcent solution (Akorn Pharmaceuticals, Lake Forest, IL). A clip reference electrode was placed on the tongue and as a ground a skin needle electrode (Grass Technologies, Warwick RI) placed subcutaneously over the dorsum. ERGs were recorded with an Espion E^2 electrophysiology system with ColorDome Ganzfeld (Diagnosys LLC, Lowell, MA, USA). A dark-adapted luminance-response series (-2.3 to 2.8 log cd.s/m^2), followed by light adaptation (10 minutes exposure to a 30 cd/m^2 white light), and a light-adapted series (−0.9 to 2.8 log cd.s/m^2) were recorded. Longflash ERG using a 500mSec, 1250 cd/m^2 stimulus and a cone flicker (33Hz flicker) were also recorded. ERG a- and b-wave amplitudes and implicit time were measured in a standard fashion. The oscillatory potentials (OPs) were isolated from the photopic full field ERG using an equiripple passband filter with half passbands of 22.5 to 55 Hz. They were normalized by

subtracting the mean amplitude between 10 and 120 mSec. The OP signal was zeroed, 0<t<120 mSec to reduce the influence of the a-wave and negate the potential of artefacts (Matlab^{TM}, Mathworks Inc.). They were numbered OP1 through OP3, starting at the first positive peak (Wachtmeister, 1998). Their amplitude and time were measured. Statistical comparisons for ERG measures were made using a Two-way ANOVA (p< 0.05).

3.2.9 Drug dissection ERG

Injection of different drugs into the vitreous were used to block the responses from different retinal neurons. Pre-injection ERGs as described above were recorded. Animals were then re-dark adapted overnight, briefly anesthetized under dim red light and given an intravitreal injection using a 34G needle attached to a Hamilton syringe (Hamilton Company, Reno NV) and then allowed to recover. They were reanesthetized and the ERG was recorded one hour post injection. Intravitreal drugs utilized were L-AP4 (2-amino-4-phosphonobutyrate) and PDA (cis-2,3-piperidine dicarboxylic acid) (Sigma Aldrich, St Louis MO)(Xu et al., 2003) in a volume of 5µl to give a final vitreal concentration of 4mM and 15Mm, respectively. Five rats aged 3 months from each genotype (WT and *Gnb3*$^{-/-}$) were used for each drug dissection. All rats received a saline intravitreal injection in the contralateral eye as control. ERG waveforms (a- and b-wave) amplitudes and implicit times were measured. To allow for easier analysis of the portion of the ERG waveform removed by the drug action the post injection waveforms were digitally subtracted from the pre injection waveforms. All analyzes were performed using Two-way ANOVA (Prism 7.01, GraphPad®) (P<0.05).

3.2.10 Retinal Slice Preparation

Wild-type or *Gnb3*$^{-/-}$ rats were dark-adapted in a ventilated light-proof box overnight prior to each experiment. On the morning of the experiment, animals were euthanized under dim red light using carbon dioxide, followed by cervical dislocation. Both eyes were collected and hemisected, placed into a dish with Ames' medium gassed with 95% O_2 / 5% CO_2 at room temperature. The sclera was removed and the retinas were halved. Each retina half was mounted on a filter paper (0.45µm HA; EMD Millipore, Billerica, MA) with the ganglion cell layer down and then cut into 400µm thick slices using Feather blades (Ted Pella Inc., Redding, CA) mounted on a manual tissue slicer (Stoelting Co., Wood Dale, IL). Slices were kept in the dark in Ames' medium gassed with 95% O_2 / 5% CO_2 at room temperature for up to 8 hours before being used for whole-cell recording.

3.2.11 Whole Cell Recording, Light Stimulation

A single retinal slice was mounted perpendicular to the surface of the recording chamber, which was placed on a fixed-stage upright microscope (Eclipse FN1; Nikon Instruments, Melville, NY). The chamber was continuously superfused with Ames' medium gassed with 95% O_2 / 5% CO_2 and fresh media at 32°C was delivered to the dish at 2–3 mL/min via a peristaltic pump. The superfused slice was kept in the dark until stimulus presentation.

The slice was visualized using infrared transillumination and NIS Elements D imaging software (Nikon Instruments Inc., Melville, NY). A glass pipette (5 – 10 µm tip diameter) was positioned near the surface of the inner nuclear layer and suction gently applied to remove the top 2 – 3 layers of cells and debris in a small area, exposing a layer of bipolar cells. Whole-cell recordings were obtained from randomly selected bipolar cells located

in the distal half of the inner nuclear layer using either a MultiClamp 700A or 700B amplifier (Molecular Devices, Sunnyvale, CA). Glass micropipettes with tip resistances 10–15 MΩ were pulled from thick-walled borosilicate tubing on a Narishige PC-10 puller (East Meadow, NY), and were filled with a K^+-based internal solution containing (in mM): 120 K-gluconate; 5 NaCl; 4 KCl; 10 HEPES; 2 EGTA; 4 Mg-ATP; 0.3 Na-GTP; 7 Tris-phosphocreatine; 0.1% Lucifer Yellow; and KOH to adjust pH to 7.3. The liquid junction potential was calculated to be ~13mV using CLAMPEX software (Molecular Devices) and was taken into account in all recordings. PCLAMP 9 or 10 software (Molecular Devices) was used for data acquisition, with signals low-pass filtered at 2.4 kHz and sampled at 5kHz.

One-second, uniform, full-field light stimuli were presented from below the recording chamber's transparent bottom. The wavelength of the light was set at 500nm using a narrow-band filter and the light intensity was varied using neutral density (ND) filters. Stimulus timing was regulated by a CLAMPEX-driven electromechanical shutter. Since experiments were carried out on two different rigs using different filter sets, stimulus intensities varied slightly between the rigs. Therefore, when pooling data from the two rigs at a certain intensity (e.g. ND8), the light intensities shown in Figures 3.8 and 3.9 represent the midpoint of the intensity range ± half of that range. For example, "8.4 ± 0.3 log photons cm^{-2} s^{-1}" denotes 8.1 log photons cm^{-2} s^{-1} to 8.7 log photons cm^{-2} s^{-1}. Light intensities were measured using a UDT S370 radiometer (Gamma Scientific, San Diego, CA).

3.2.12 Morphology and Data Analysis

For comparison of bipolar cell morphology between wild-type and *Gnb3*$^{-/-}$ retinas, Lucifer Yellow fills were visualized using FITC epifluorescence after whole-cell recordings were completed. Movies were recorded as the cells were imaged at different focal planes, starting when the soma just came into view and ending when the last dendrites were visible. Single frames from the movies were then combined to create a z-projection using ImageJ software (National Institutes of Health, Bethesda, MD). These Lucifer yellow fills enabled identification of the specific bipolar cell types based on morphology (Hartveit, 1997).

The recordings shown in Figures 3.8B and 3.9A were notch-filtered (60Hz center frequency, -3dB width of 3Hz) offline, and the analyses shown in Figures 3.8C and 3.9B,C were based on the notch-filtered recordings. The resting membrane potential of each cell was measured during the 1-sec interval prior to the first light presentation to that cell. In the averaged light response traces (Figure 3.9A), the dark line indicates the average and the gray area above and below the average represents the S.E.M. Photoresponse peak amplitude (Figure 3.9B) was calculated by subtracting the baseline membrane potential during the 1-sec pre-stimulus interval from the most positive membrane potential recorded during the 1-sec stimulus. Photoresponse peak amplitude and latency to peak were both reported as the average for all cells for a given genotype and bipolar cell type. All data averaging and statistical analysis was performed using Origin 6.0 software (Microcal, Northampton, MA). Statistical comparisons were made using the unpaired Student's *t* test with a significance level at a *p*-value of 0.05. Error values and error bars

represent the S.E.M., and *p*-values in the graphs are represented by asterisks: * $p<0.05$; ** $p<0.01$; *** $p<0.005$.

3.3 Results

Gnb3$^{-/-}$ rats lacked detectable Gβ$_3$ immunolabelling of retinal sections and Gβ$_3$ was not detected by Western blot (Fig 3.1 A & B). Relative gene expression of GNB3 from Heterozygote animals (n=2) was lower when compared to WildType animals and it were not detectable from Gnb3-/- animals using the qRT-PCR assay (Fig 3.1C).

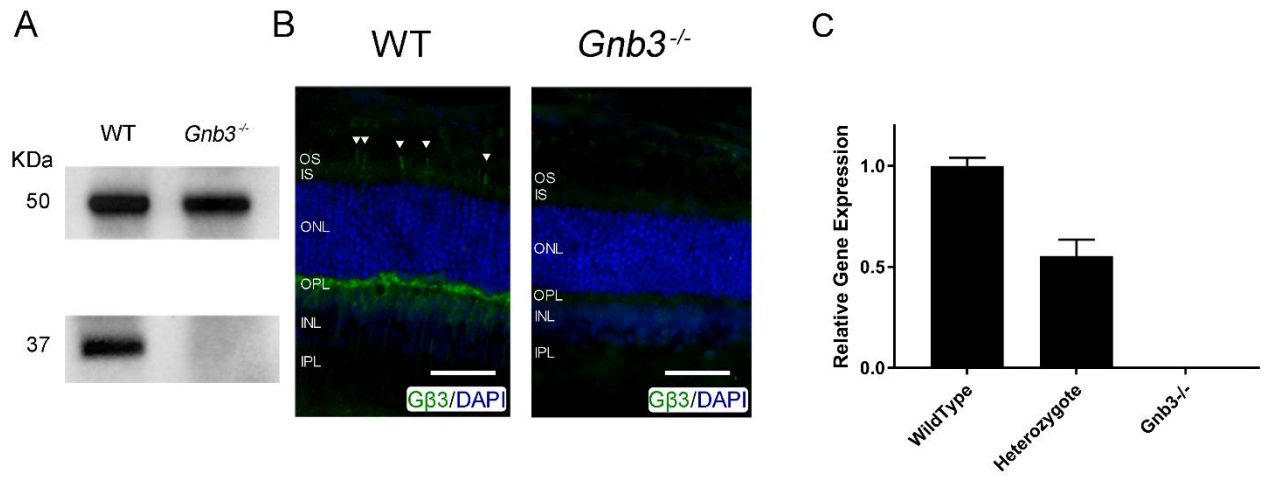

Figure 3.1. Confirmation of Gnb3 knockout. A. Western blots for *Gβ3* (lower band ~37KDa) with *β-tubulin* (upper band ~50KDa) as a loading control in wild type (WT) and *Gnb3*$^{-/-}$ rat retina showing absence of the *Gβ3* band in *Gnb3*$^{-/-}$ retina. **B.** Immunohistochemistry of retinal cross sections labeled for Gβ3. Wildtype rat has labeling of cone outer segments (arrows) and cell processes in the outer plexiform layer and the cells within the inner nuclear layer. Gβ3 immunostaining is absent in the *Gnb3*$^{-/-}$ rat retina. Blue is DAPI nuclear dye. Key: OS, left eye; PR, photoreceptor layer; ONL, outer nuclear layer; OPL, outer plexiform layer; INL, inner nuclear layer; IPL, inner plexiform layer. **C.** Relative gene expression for *Gβ3* normalized to *β-actin* in WildType, Heterozygote and *Gnb3*$^{-/-}$ rats.

Plastic embedded retinal sections in WildType and *Gnb3*$^{-/-}$ rats show no major morphological change (Fig.3.2).

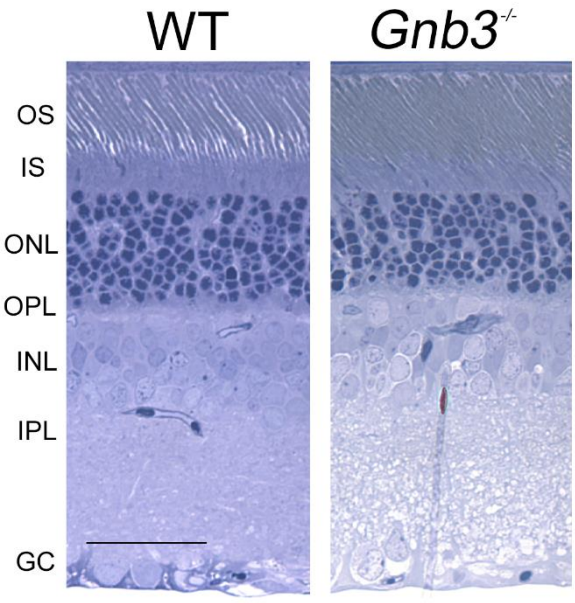

Figure 3.2. Plastic embedded retinal sections of a 6 month old WildType (WT) and *Gnb3*$^{-/-}$ rats stained with epoxy tissue. Calibration bar: 50µm; Key: OS- outer segment of photoreceptors; IS- inner segment of photoreceptors; ONL- outer nuclear layer; OPL- outer plexiform Layer; INL- inner nuclear layer; IPL- inner plexiform layer; GC- ganglion cell.

3.3.1 *Gnb3*$^{-/-}$ rat ERGs show the phenotype is stationary

ERGs of WT and *Gnb3*$^{-/-}$ rats were performed at 3 different ages (50, 90 and 180 days of age). There was no significant change in dark-adapted ERG a-wave amplitude with age of either *Gnb3*$^{-/-}$ or WT rats. Furthermore these was no significant differences between the phenotypes (Fig 3.3 A). The light-adapted ERG a-wave amplitudes of the *Gnb3*$^{-/-}$ and WT rats did not change significantly with age. However at a single luminance the *Gnb3*$^{-/-}$ rats has a higher amplitude than the WT rats at all ages (P<) (Fig. 3.3 B). The light-adapted b-wave of *Gnb3*$^{-/-}$ rats had a significantly lower amplitude than age-matched WT rats (Fig. 3.3 C). There was a significant decrease in b-wave amplitude of WT rats between 50 days of age and 90/180 days of age at a single luminance (Fig. 3.3 C 0.7 log

cds/m^2) (p<0.002). There was no difference in any of the ERG waveform implicit times between ages for either phenotype.

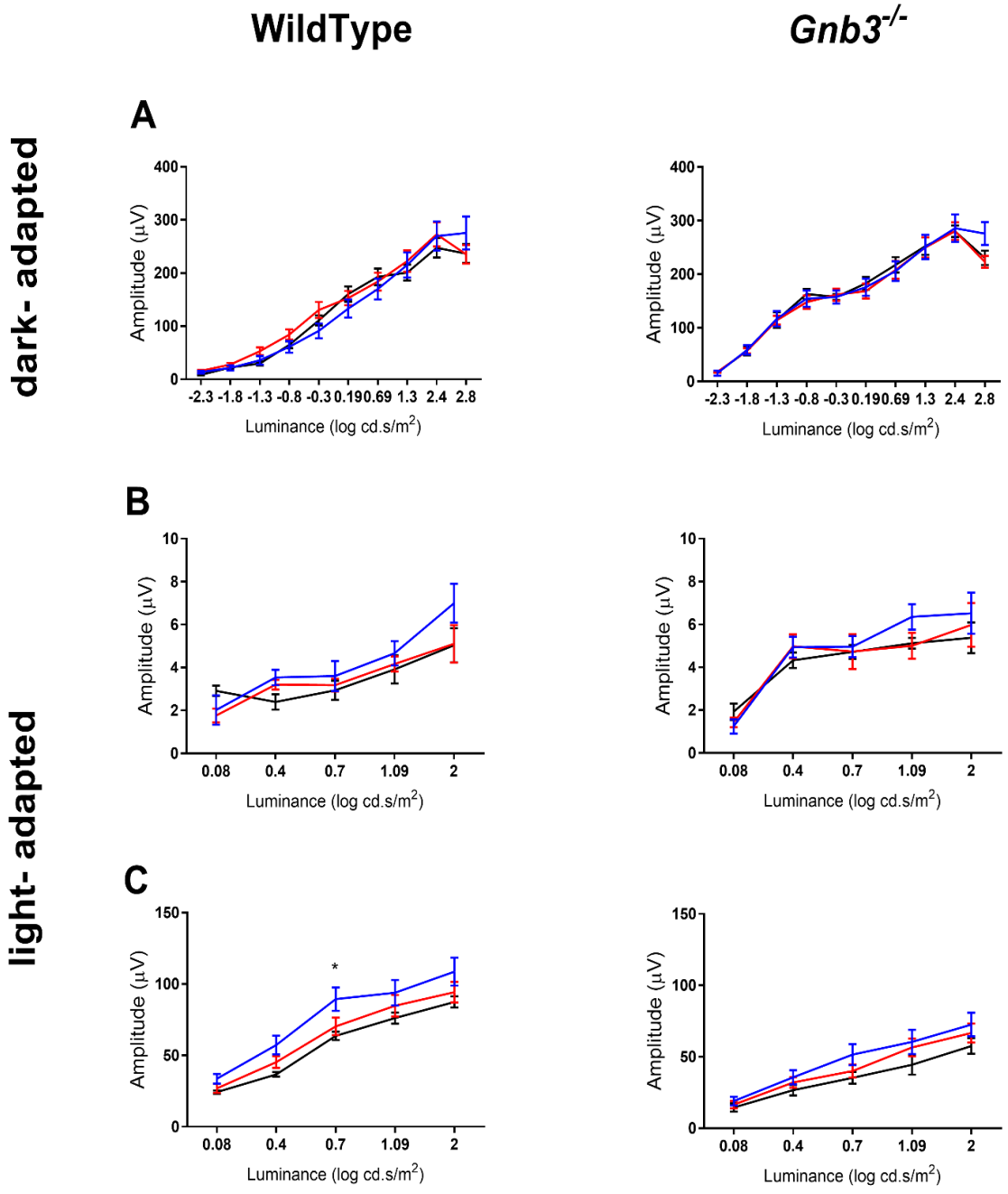

Figure 3.3. Electroretinographic (ERG) responses from Wildtype and *Gnb3*$^{-/-}$ rats at 50, 90 and 180 days of age. A. Mean dark-adapted a-wave amplitude versus stimulus luminance. **B**. Mean light-adapted a-wave amplitude versus stimulus luminance. **C**. Mean light-adapted b-wave amplitude versus stimulus luminance. Error bars indicate standard error. *p< 0.002. Legend: blue – 50 days; red – 90 days; and black – 180 days of age.

3.3.2 ERGs showed lack of rod ON BC responses and reduced cone ON BC responses

Dark-adapted ERGs from *Gnb3*$^{-/-}$ rats lacked a b-wave (Fig. 3.4 A), but had an a-wave of comparable threshold and amplitude to that of WT controls (Fig. 3.4 A & E). The b-wave amplitude of the light-adapted ERG of *Gnb3*$^{-/-}$ rats was significantly smaller than that of WT controls ($p<0.05$), while the a-waves were not significantly different (Fig. 3.4 B & F). The mean of the amplitudes of the long-flash ERG responses were lower in the *Gnb3*$^{-/-}$ rats compared to WT controls, but the difference was not significant (Fig. 3.4 C). The 33Hz (cone) flicker ERG responses of *Gnb3*$^{-/-}$ rats had a short delay in the down phase of the waveform but amplitudes were not significantly different from those of WT controls (Fig. 3.4 D). Oscillatory potentials (OPs) extracted from the light-adapted ERG waveforms showed some difference between phenotypes, with OP2 and OP3 of *Gnb3*$^{-/-}$ rats having significantly smaller amplitudes and increased implicit time ($p<0.02$and $p< 0.03$ data not shown).

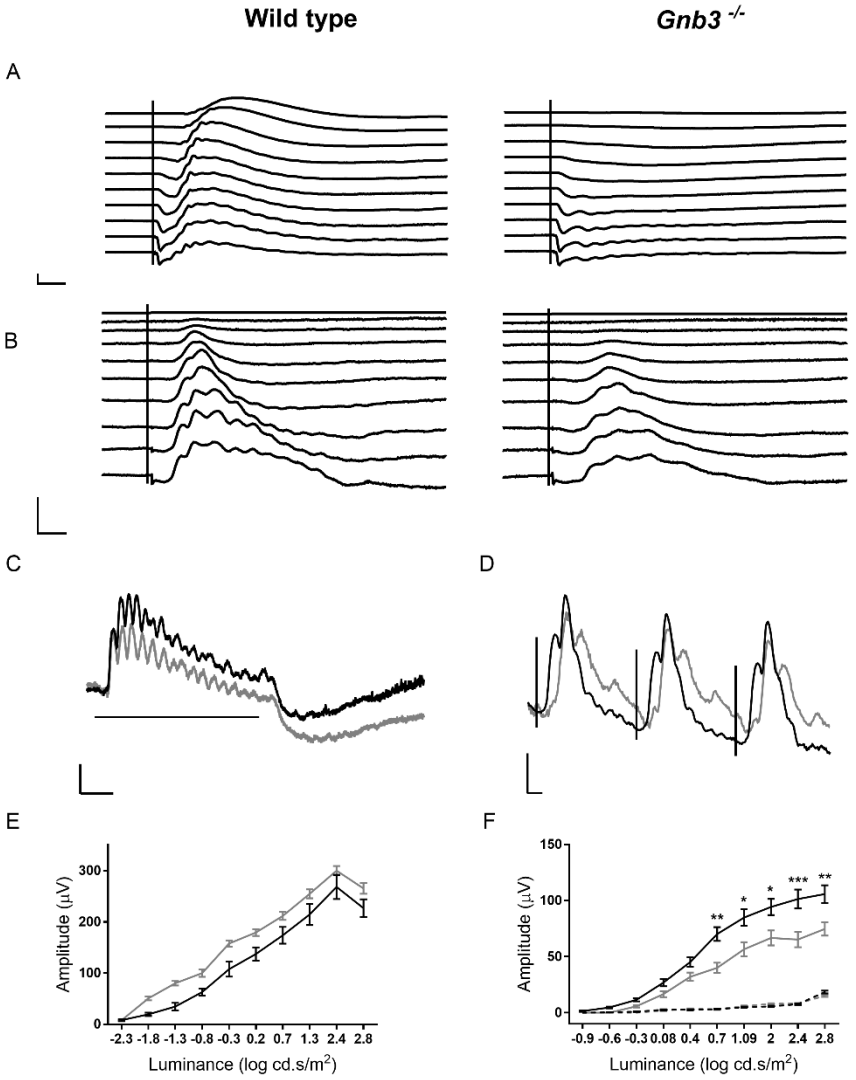

Figure 3.4. Electroretinographic (ERG) responses from *Gnb3*$^{-/-}$ rats. A. Dark-adapted luminance series in wild type and *Gnb3*$^{-/-}$ rats (luminances vary from -2.3 log cd.s/m^2 – top tracing to 2.8 log cd.s/m^2 lower tracing). Tracings are an average of 12 animals. Note that there is a lack of b-wave in the *Gnb3*$^{-/-}$ animals. **B**. Light-adapted luminance series in wild type and *Gnb3*$^{-/-}$ rats (luminances vary from -0.9 log cd.s/m^2 – top tracing to 2.8 log cd.s/m^2 lower tracing). Tracings are an average of 12 animals. Note the clearly discernable b-wave in the *Gnb3*$^{-/-}$ rat. **C**. Long-flash ERG response to a 500 mSec flash of 1250 cd/m^2 imposed on 30 cd/m^2 background light in wild type (black) and *Gnb3*$^{-/-}$ (grey) rats. Horizontal line represent the light stimulus. **D**. 30Hz Flicker response on 30 cd/m^2 background in wild type (black) and *Gnb3*$^{-/-}$ (grey) rats. There was a slight delay in the return to baseline in the tracing from the *Gnb3*$^{-/-}$ rats **E**. Mean scotopic amplitude of a-wave of wild type (black) and *Gnb3*$^{-/-}$ (grey) rats with standard error bars in different light stimulus. **F.** Mean photopic amplitude of a- (dashed) and b-wave (solid) of wild type (black) and *Gnb3*$^{-/-}$ (grey) with standard error bars in different light stimulus. *p=0.02; **p=0.003; ***p<0.0001.(size bars- A: 200µV/ 50 mSec;

B: 50µV/ 50 mSec; C: 20µV /100 mSec; D: 50µV/20 mSec). Vertical lines in A,B,D indicate timing of flash stimulus.

Intravitreal saline injections did not result in any significant differences in ERG amplitudes in either genotype. Intravitreal L-AP4 removed the b-wave from both dark- and light-adapted ERGs of WT control rats (Figs 3.5 & 3.6). Following drug action, an a-wave remained which had a characteristic small positive incursion after the initial trough. This waveform post L-AP4 treatment was very similar to that of the dark-adapted *Gnb3*$^{-/-}$ rats. Subtraction of the post-injection ERG from the pre-injection ERG reveals the ON bipolar cell component of the waveform that is removed by L-AP4 (shown in the right-hand column Figure 3.5 and Fig 3.6 A & B). In the dark-adapted ERG of the WT control rat, the L-AP4 sensitive component of the ERG consisted of an initial small negative waveform followed by a large positive waveform that was the major contributor to the b-wave (Fig.3.5). L-AP4 removed very little of the dark-adapted waveform of the *Gnb3*$^{-/-}$ rats (Fig.3.5), indicating very little ON BC contributions to this waveform.

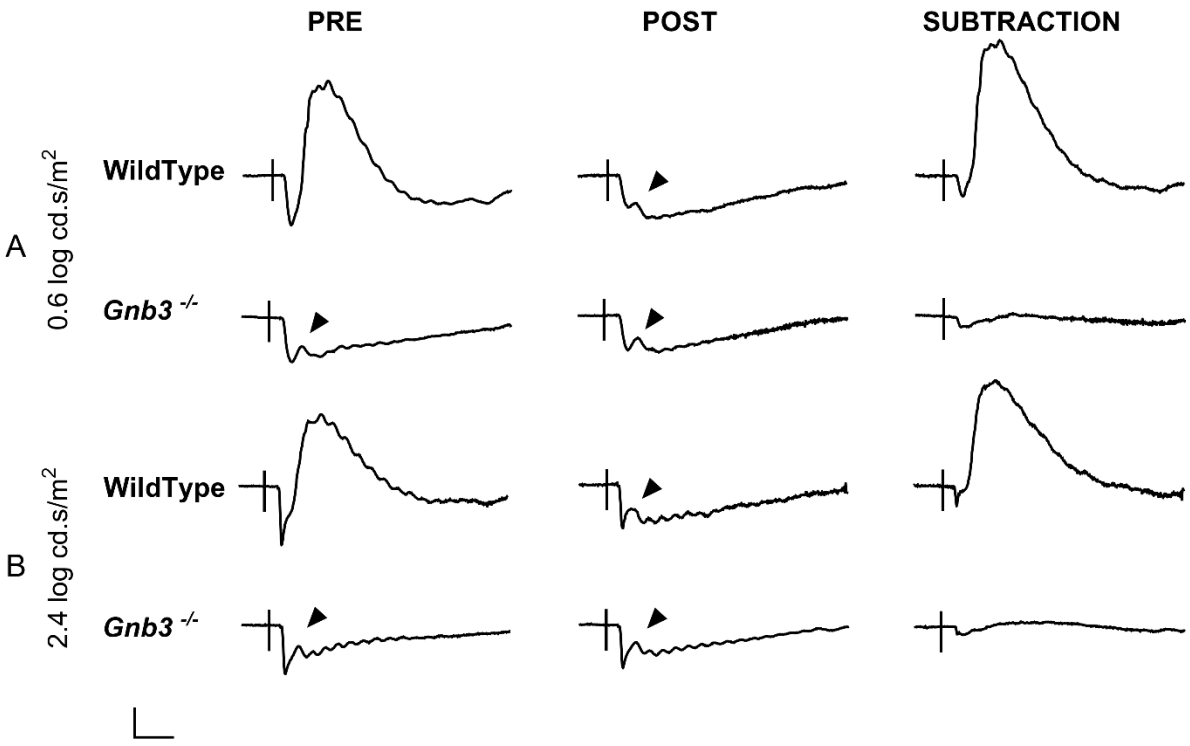

Figure 3.5. Use of L-AP4 to block ON-BC responses in dark-adapted ERGs. A. Stimulus of 0.6 log cd.s/m^2; **B**. Stimulus of 2.4 log cd.s/m^2. Pre L-AP4 ERG is shown in the first column. The second column is following injection of L-AP4 and the final column is the subtraction of post from pre waveforms showing the response removed by L-AP4. Note that in the wild type rat the b-wave is completely removed. The *Gnb3-/-* rats lack a b-wave prior to injection and L-AP4 only removes a very small component of the waveform. Vertical lines on the waveform correspond to light stimulus. Amplitude = 50µV/ time= 50 mSec.

L-AP4 removes the light-adapted b-wave in both WT and *Gnb3*$^{-/-}$ rats (Fig.3.6 A &B). The amplitude of the light-adapted a-wave post L-AP4 was significantly increased in the WT rat (Fig 3.6 C), but not in the *Gnb3*$^{-/-}$ rats (Fig 3.6 D). Amplitude of the light-adapted a-wave post L-AP4 in WT rat was significant increased in 4 out of 5 luminances compared to the a-wave post L-AP4 in *Gnb3*$^{-/-}$ rats (Fig. 3.6 E) ($p<0.04$). Figure 3.6F plots the amplitude of the waveforms removed by L-AP4 against stimulus strength; revealing that the L-AP4 responsive component (primarily representing the cone ON BC response) of the *Gnb3*$^{-/-}$ rat light-adapted ERG were significantly lower than that of WT controls.

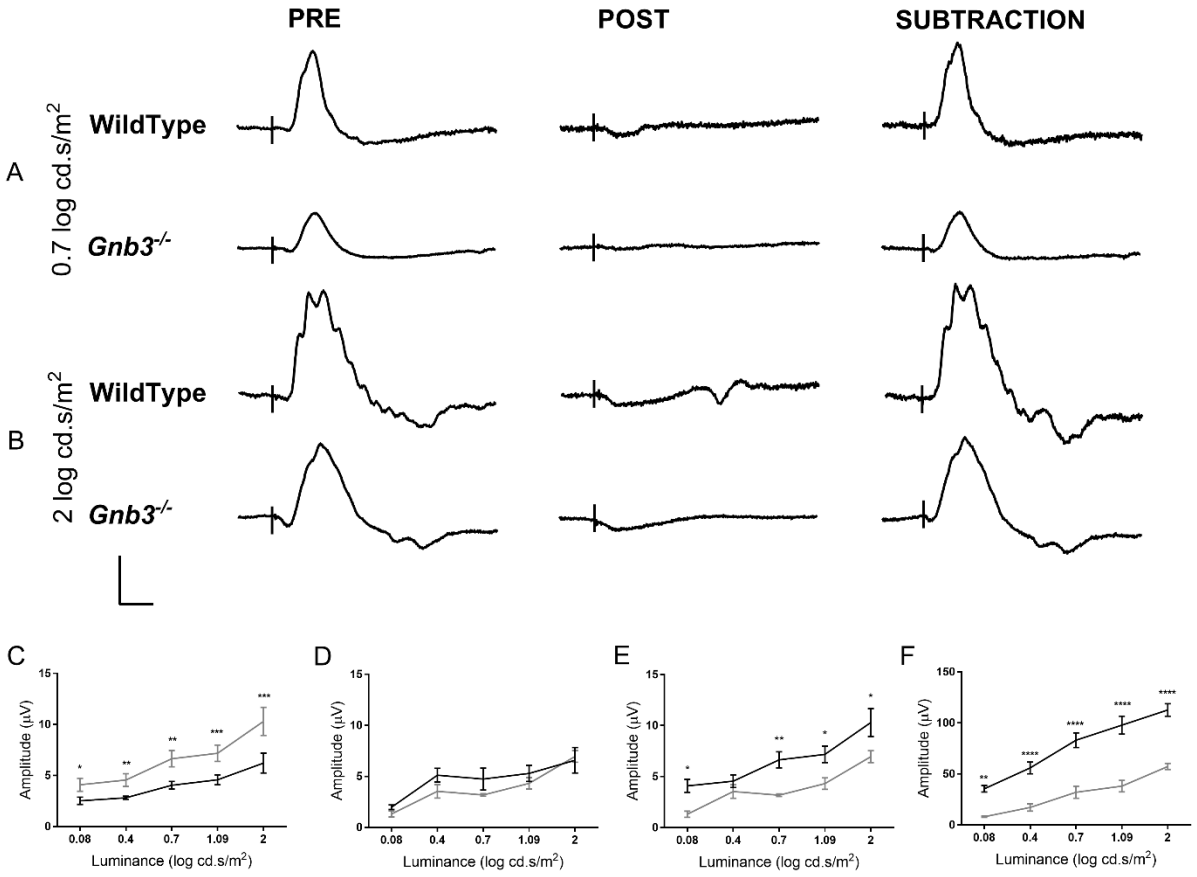

Figure 3.6. Use of L-AP4 to block ON-BC responses in light-adapted ERGs. A. Stimulus of 0.7 log cd.s/m^2; **B**. Stimulus of 2 log cd.s/m^2, on a 30 cd/m2 background light. Pre L-AP4 ERG is shown in the first column. The second column is following injection of L-AP4 and the final column is the subtraction of post from pre waveforms showing the response removed by L-AP4. Note that the b-wave is completely removed in both the wild type and *Gnb3-/-* rat. Vertical lines on the waveform correspond to light stimulus. Amplitude = 50µV/ time= 50 mSec. **C.** Mean a-wave amplitude vs Light luminance pre (black) and post (grey) L-AP4 injection in WildType (WT) rats. *p=0.01; **p<0.03; ***p<0.001. **D**. Mean a-wave amplitude vs Light luminance pre (black) and post (grey) L-AP4 injection in *Gnb3$^{-/-}$* rats. **E**. Mean a-wave amplitude vs Light luminance post L-AP4 injection in WT (black) and *Gnb3$^{-/-}$* (grey) rats. *p<0.04; **p<0.007. **F**. Mean subtracted b-wave amplitude vs Light luminance in WildType (WT) (black) and *Gnb3$^{-/-}$* (grey) rats on photopic ERGs pre and post L-AP4 injection. **p= 0.002; **** p<0.0001.

PDA, a drug that blocks photoreceptor transmission to OFF BC and horizontal cells, had minor effects on the shape of the waveform under dark (Fig. 3.7A) and light adaptation (Fig. 3.7B) in both phenotypes.

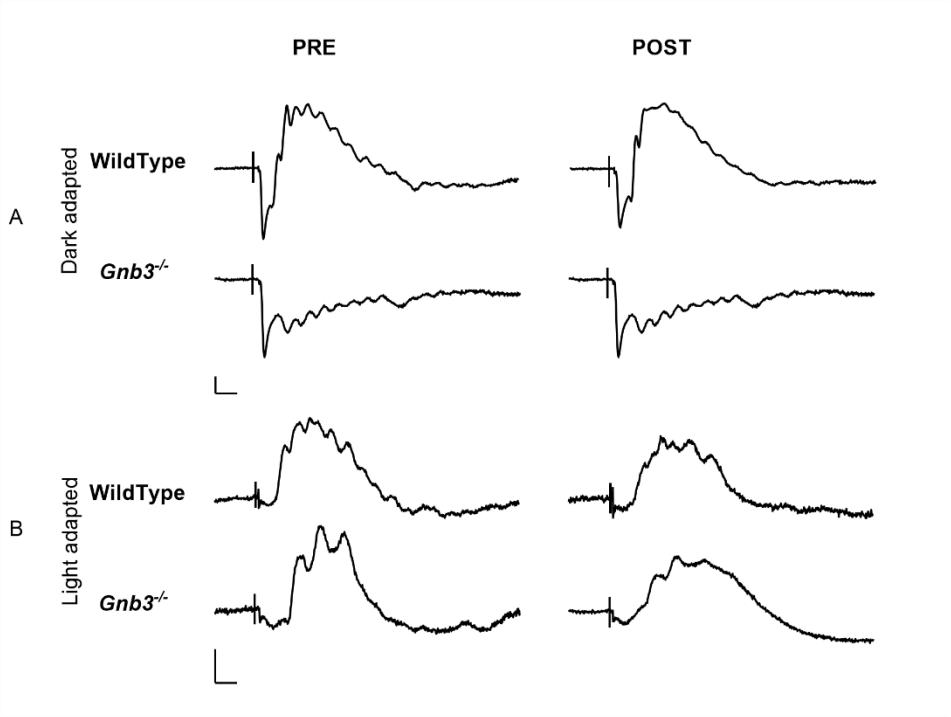

Figure 3.7. Use of PDA to block transmission to OFF-BC and horizontal cells. **A.** Dark-adapted response to a luminance of 2.4 log cd.s/m^2. **B.** Light-adapted responses to a luminance of 2 log cd.s/m^2. Note that PDA has only minor effects of the shape of the waveform. Vertical lines on the waveform correspond to light stimulus. Size bars vertical 50µV in A. and 20µV in B. Horizontal 50 mSec.

3.3.3 Single cell recording shows lack of rod ON BC function and some residual cone ON BC function

We recorded from randomly chosen bipolar cells in retinal slice preparations from wild-type (n=38 cells) and *Gnb3*$^{-/-}$ rats (n=77 cells). In retinas from both wild-type and *Gnb3*$^{-/-}$ rats, the recorded cells included all 3 major classes of bipolar cells—rod bipolar cells (RBC), ON cone bipolar cells (ON-CBC), and OFF cone bipolar cells (OFF-CBC). Bipolar cells in the *Gnb3*$^{-/-}$ retinas showed no noticeable morphological differences when compared to those in wild-type retinas (Figure 3.8A). The resting membrane potentials of the three classes of bipolar cells also did not differ between wild-type and *Gnb3*$^{-/-}$ retinas (Figure 3.8B). However, there were noticeable differences in the light responses between wild-type and *Gnb3*$^{-/-}$ bipolar cells. Not all recorded cells responded to light, even in wild-type retinas (Table 3.2). Fig. 6C shows example recordings from each bipolar cell class in wild-type and *Gnb3*$^{-/-}$ retinas, and Fig. 7A shows averaged recordings. In *Gnb3*$^{-/-}$ retinas, none of the rod bipolar cells responded to light, while a few ON cone bipolar cells and many OFF cone bipolar cells did respond to light (Table 3.2; Figure 3.9A). On average, the responses of the mutant ON cone bipolar cells were much weaker compared to those from wild-type ON cone bipolar cells (Figure 3.9B, middle panel), while responses from mutant OFF cone bipolar cells were only slightly smaller than those from wild-type OFF cone bipolar cells (Figure 3.9B, bottom panel). Not only were the light responses in OFF cone bipolar cells weaker than those of wild-type cells, they were also significantly slower at the lowest light intensity that elicited a response (Figure 3.9C).

Table 3.2. Number cells analyzed on whole cell recording.

	RBC		ON-CBC		OFF-CBC	
	WT	***Gnb3*$^{-/-}$**	**WT**	***Gnb3*$^{-/-}$**	**WT**	***Gnb3*$^{-/-}$**
light response	7	0	9	2	9	9
no response	3	33	6	21	4	12
TOTAL	10	33	15	23	13	21
% responding	70.0	0.0	60.0	8.7	69.2	42.9

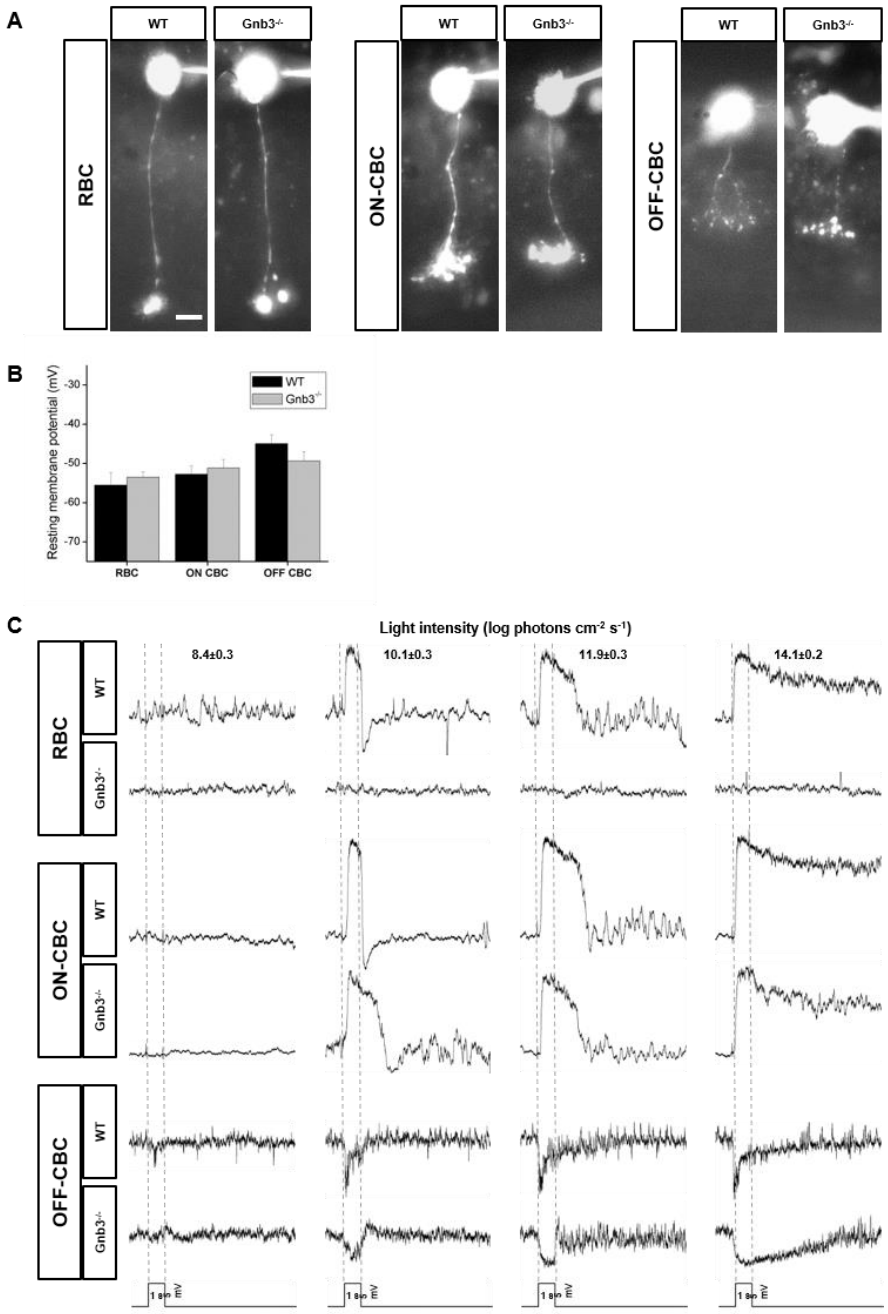

Figure 3.8. Morphologies and whole-cell recordings of bipolar cells from wild-type and *Gnb3*$^{-/-}$ rats. A. Representative images of Lucifer Yellow-filled rod bipolar cells (RBC; left panels), ON cone bipolar cells (ON-CBC; middle panels), and OFF cone bipolar cells (OFF-CBC; right panels) in wild-type and *Gnb3*$^{-/-}$ retinal slices. The attached recording pipette can be seen to the right of the somas. Scale bar = 10µm. **B**. Averaged resting membrane potentials. **C**. Example recordings of single cells in response to 1-sec light steps.

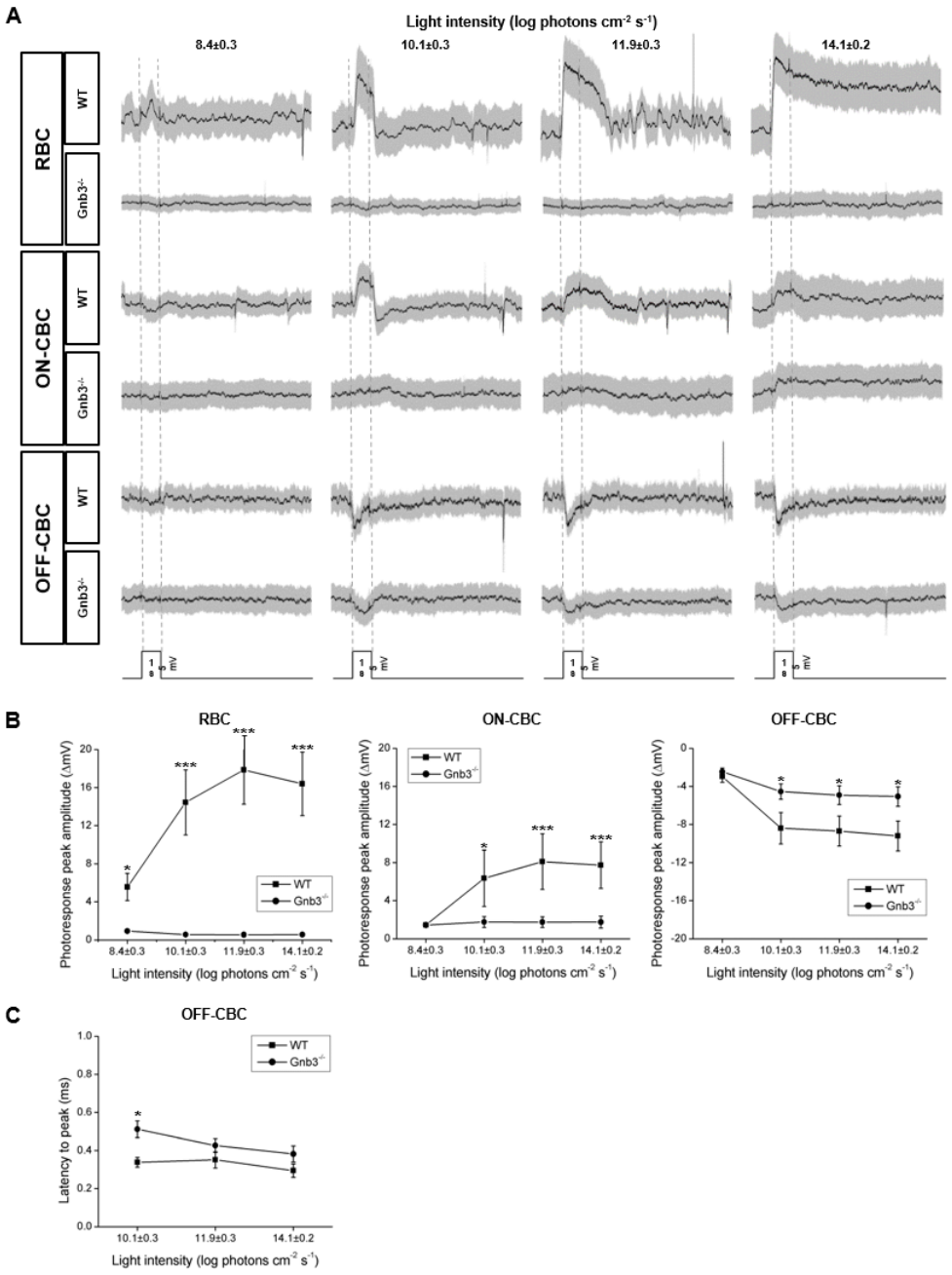

Figure 3.9. Analyses of whole-cell recordings of wild-type and *Gnb3*$^{-/-}$ bipolar cells. A. Averaged recordings from all rod (RBC; top recordings), ON cone (ON-CBC; middle recordings), and OFF cone bipolar cells (OFF-CBC; bottom recordings), with S.E.M. shown in gray. **B.** Averaged peak photoresponse amplitudes. The asterisks denote the light intensities where the wild-type and *Gnb3*$^{-/-}$ peak response amplitudes are significantly different. **C**. Averaged latency to peak for OFF cone bipolar cells. The asterisks denote the light intensities where the wild-type and peak response amplitudes are significantly different. * p<0.05, ** p<0.01, *** p<0.005.

3.4 Discussion

The effects of *GNB3* mutations on visual function are now available for four different species. Analysis of ERG amplitude of *Gnb3*$^{-/-}$ rat at three different ages (up to 180 days) showed no change in age suggesting that the phenotype was stationary. The recent reports in human patients suggest that the resulting phenotype can vary. The single patient reported by Arno et al (2016) and two of the four patients reported by Vincent et al (2016) appeared to completely, or almost completely, lack rod bipolar cell function on ERG, although night blindness was not reported for all of the patients. The ERGs of these patients also suggest they have cone dysfunction; with the patient of Arno et al exhibiting a mild central macular abnormality with a suggestion of cone morphological changes on SD-OCT imaging (Arno et al., 2016) and the two patients of Vincent et al having color vision deficits (Vincent et al., 2016). Two other patients in the study of Vincent et al had a small rod-mediated b-wave and a less severe reduction in the amplitude of the cone b-wave, although the timing was delayed (Vincent et al., 2016). It is conceivable that differences in severity of the mutations in *GNB3* could contribute to these differences between patients with some mutations allowing for some residual function. Chickens with an in-frame single-codon deletion within *Gnb3* that results in a lack of $G\beta_3$, have very reduced vision. This suggests that in this species a lack of $G\beta_3$ has a more profound effect on cone function than is the case in human patients and was found in *Gnb3*$^{-/-}$ mice (based on single cell recording) and is suggested in the current study in *Gnb3*$^{-/-}$ rats (based on cone-mediated ERG responses). A lack of normal $G\beta_3$ in humans, mice and rats markedly reduces rod bipolar cell function. The relatively low contribution of rods to the chicken ERG makes this component difficult to assess in this species. The

effect of the lack of $G\beta_3$ on the cone pathways appears to show the greatest difference between species. *Gnb3*$^{-/-}$ mice had a lack of cone ERG b-wave showing severely reduced cone ON BC signaling. The effect on human patients varied between individuals and could reflect some remaining function in $G\beta_3$ in the patients with missense mutations and in-frame deletion mutations (Vincent et al., 2016). As shown in the current study, rats with a lack of $G\beta_3$ have only a modest reduction in cone ON BC signaling, which is in contrast to *Gnb3*$^{-/-}$ mice where cone ON BC signaling is severely reduced (Dhingra et al., 2012). Using L-AP4, a drug that blocks photoreceptor to ON BC signaling, we were able to confirm that the cone ERG b-wave of *Gnb3*$^{-/-}$ rats does originate from cone ON BC function. The waveform removed by the action of L-AP4 (subtractions shown in Figure 3.6 A & B) most clearly shows the cone ON BC component of the light-adapted ERG. Single cell recording from retinal slices confirmed that some cone ON BC had light-induced responses. The single cell recording also confirmed the lack of rod bipolar cell responses which had been suggested by the lack of b-wave in the dark-adapted ERG and also by the L-AP4 subtraction which made very little difference to the dark-adapted ERG waveform (although in the same animals it removed the light-adapted b-wave).

In *Gnb3* mutant chickens, the light-adapted ERG has a slow and abnormally shaped b-wave that is not removed by L-AP4 suggesting that it does not have a large cone ON-BC contribution, whereas in wild-type chickens L-AP4 completely removes the light-adapted ERG b-wave (Petersen-Jones, 2007). There are several possible reasons for the clear species difference that lack of Gβ3 has on cone ON BC signaling. It is known in mammalian species that there are multiple forms of cone ON BC subtypes, with a recent study in mice identifying 8 ON BC subtypes based on their transcriptomes

(Shekhar et al., 2016). It is conceivable that there may be some difference in signaling between the subtypes and that this may further vary between species. Although cone ON-bipolar cells have been studied in detail in rats the transcriptomes of different subtypes have not been reported so the possibility remains that different signaling proteins may be involved. In *Gnb3*$^{-/-}$ mice the lack of Gβ3 was associated with down regulation of all BC signaling associated genes and with age loss of synaptic connections (Dhingra et al., 2012) and this is likely to be a contributory factor in the markedly reduced signaling. The light-adapted ERG b-wave in *Gnb3*$^{-/-}$ rats was maintained, even in older rats (Fig.3.3 C) suggesting that cone to cone ON-BC synaptic connections are maintained in *Gnb3*$^{-/-}$ rats. Recent studies in mice have suggested that both the α and βγ subunits of Go act to gate the TRPM1 channel (Xu et al., 2016). Presumably if any of the components of Go were absent this would alter the gating of the channel.

Analysis of the ERG and effect of PDA subtraction (a drug that blocks photoreceptor to OFF BC and horizontal cell transmission) suggested that both in the wild-type and *Gnb3*$^{-/-}$ rat, cone OFF BC do not make a major contribution to the ERG waveform. This is in contrast to the situation in retinas where cones have a more dominant effect which includes primates and chickens (Sieving et al., 1994, Petersen-Jones, 2007). The human patients with *GNB3* mutations appeared to have preserved OFF-pathway contributions to their ERGs. OFF BC respond to photoreceptor glutamate release via ionotropic receptors which do not involve G-protein signaling. In this study retinal slice recording from cone OFF BCs showed these cells had significantly lower light-induced responses. This may be simply a reflection of reduced cone sensitivity due to lack of Gβ3 interfering with cone phototransduction. Single cell recording from cones in *Gnb3*$^{-/-}$ mice

showed that there was reduced cone sensitivity, presumably because of reduced efficiency of the cone phototransducation cascade as an result of lack of $G\beta_3$ (Nikonov et al., 2013). Although we have not performed cone single cell recording in the *Gnb3*$^{-/-}$ rats, examination of the remaining light-adapted ERG waveform following L-AP4 subtraction can be used as an indicator of cone photoresponse and this was significantly smaller in the *Gnb3*$^{-/-}$ animals compared to wild-type controls (Figure 3.6E). It should be noted that this component may still contain some inner retinal components from the OFF pathway (Petersen-Jones, 2007), although these are very small in the rat (Xu et al., 2003) but we cannot completely rule out reduced OFF BC signaling in the *Gnb3*$^{-/-}$ rats due to direct changes in the OFF-pathway rather than via reduced cone sensitivity.

The generation of Gnb3$^{-/-}$ rats expands the tools available to study G-protein signaling within the retina and shows that there are potentially species differences in signaling within cone ON BCs.

REFERENCES

REFERENCES

Arno G, Holder GE, Chakarova C, Kohl S, Pontikos N, Fiorentino A, Plagnol V, Cheetham ME, Hardcastle AJ, Webster AR, Michaelides M, Consortium UKIRD (2016) Recessive Retinopathy Consequent on Mutant G-Protein beta Subunit 3 (GNB3). JAMA ophthalmology 134:924-927.

Audo I, Kohl S, Leroy BP, Munier FL, Guillonneau X, Mohand-Said S, Bujakowska K, Nandrot EF, Lorenz B, Preising M, Kellner U, Renner AB, Bernd A, Antonio A, Moskova-Doumanova V, Lancelot ME, Poloschek CM, Drumare I, Defoort-Dhellemmes S, Wissinger B, Leveillard T, Hamel CP, Schorderet DF, De Baere E, Berger W, Jacobson SG, Zrenner E, Sahel JA, Bhattacharya SS, Zeitz C (2009) TRPM1 is mutated in patients with autosomal-recessive complete congenital stationary night blindness. American journal of human genetics 85:720-729.

Bech-Hansen NT, Naylor MJ, Maybaum TA, Sparkes RL, Koop B, Birch DG, Bergen AA, Prinsen CF, Polomeno RC, Gal A, Drack AV, Musarella MA, Jacobson SG, Young RS, Weleber RG (2000) Mutations in NYX, encoding the leucine-rich proteoglycan nyctalopin, cause X-linked complete congenital stationary night blindness. Nature genetics 26:319-323.

Bustin SA, Benes V, Garson JA, Hellemans J, Huggett J, Kubista M, Mueller R, Nolan T, Pfaffl MW, Shipley GL, Vandesompele J, Wittwer CT (2009) The MIQE guidelines: minimum information for publication of quantitative real-time PCR experiments. Clinical chemistry 55:611-622.

Dhingra A, Ramakrishnan H, Neinstein A, Fina ME, Xu Y, Li J, Chung DC, Lyubarsky A, Vardi N (2012) Gbeta3 is required for normal light ON responses and synaptic maintenance. The Journal of neuroscience : the official journal of the Society for Neuroscience 32:11343-11355.

Dryja TP, McGee TL, Berson EL, Fishman GA, Sandberg MA, Alexander KR, Derlacki DJ, Rajagopalan AS (2005) Night blindness and abnormal cone electroretinogram ON responses in patients with mutations in the GRM6 gene encoding mGluR6. Proceedings of the National Academy of Sciences of the United States of America 102:4884-4889.

Hartveit E (1997) Functional organization of cone bipolar cells in the rat retina. Journal of neurophysiology 77:1716-1730.

Koike C, Obara T, Uriu Y, Numata T, Sanuki R, Miyata K, Koyasu T, Ueno S, Funabiki K, Tani A, Ueda H, Kondo M, Mori Y, Tachibana M, Furukawa T (2010) TRPM1 is a component of the retinal ON bipolar cell transduction channel in the mGluR6

cascade. Proceedings of the National Academy of Sciences of the United States of America 107:332-337.

Livak KJ, Schmittgen TD (2001) Analysis of relative gene expression data using real-time quantitative PCR and the 2(-Delta Delta C(T)) Method. Methods 25:402-408.

Montiani-Ferreira F, Li T, Kiupel M, Howland H, Hocking P, Curtis R, Petersen-Jones S (2003) Clinical features of the retinopathy, globe enlarged (rge) chick phenotype. Vision research 43:2009-2018.

Montiani-Ferreira F, Shaw GC, Geller AM, Petersen-Jones SM (2007) Electroretinographic features of the retinopathy, globe enlarged (rge) chick phenotype. Molecular vision 13:553-565.

Morgans CW, Brown RL, Duvoisin RM (2010) TRPM1: the endpoint of the mGluR6 signal transduction cascade in retinal ON-bipolar cells. BioEssays : news and reviews in molecular, cellular and developmental biology 32:609-614.

Nikonov SS, Lyubarsky A, Fina ME, Nikonova ES, Sengupta A, Chinniah C, Ding XQ, Smith RG, Pugh EN, Jr., Vardi N, Dhingra A (2013) Cones respond to light in the absence of transducin beta subunit. The Journal of neuroscience : the official journal of the Society for Neuroscience 33:5182-5194.

Pardue MT, Peachey NS (2014) Mouse b-wave mutants. Documenta ophthalmologica Advances in ophthalmology 128:77-89.

Peachey NS, Ray TA, Florijn R, Rowe LB, Sjoerdsma T, Contreras-Alcantara S, Baba K, Tosini G, Pozdeyev N, Iuvone PM, Bojang P, Jr., Pearring JN, Simonsz HJ, van Genderen M, Birch DG, Traboulsi EI, Dorfman A, Lopez I, Ren H, Goldberg AF, Nishina PM, Lachapelle P, McCall MA, Koenekoop RK, Bergen AA, Kamermans M, Gregg RG (2012) GPR179 is required for depolarizing bipolar cell function and is mutated in autosomal-recessive complete congenital stationary night blindness. American journal of human genetics 90:331-339.

Petersen-Jones SM, Shaw, G.C., Montiani-Ferreira, F. (2007) Drug dissection of the rge chicken electroretinogram suggests that gnb3 plays a role in inner retinal function. Investigative ophthalmology & visual science 48:E-Abstract 1939.

Shekhar K, Lapan SW, Whitney IE, Tran NM, Macosko EZ, Kowalczyk M, Adiconis X, Levin JZ, Nemesh J, Goldman M, McCarroll SA, Cepko CL, Regev A, Sanes JR (2016) Comprehensive Classification of Retinal Bipolar Neurons by Single-Cell Transcriptomics. Cell 166:1308-1323 e1330.

Shen Y, Rampino MA, Carroll RC, Nawy S (2012) G-protein-mediated inhibition of the Trp channel TRPM1 requires the Gbetagamma dimer. Proceedings of the National Academy of Sciences of the United States of America 109:8752-8757.

Sieving PA, Murayama K, Naarendorp F (1994) Push-pull model of the primate photopic electroretinogram: a role for hyperpolarizing neurons in shaping the b-wave. Visual neuroscience 11:519-532.

Spurr AR (1969) A low-viscosity epoxy resin embedding medium for electron microscopy. Journal of ultrastructure research 26:31-43.

Tummala H, Ali M, Getty P, Hocking PM, Burt DW, Inglehearn CF, Lester DH (2006) Mutation in the guanine nucleotide-binding protein beta-3 causes retinal degeneration and embryonic mortality in chickens. Investigative ophthalmology & visual science 47:4714-4718.

Vincent A, Audo I, Tavares E, Maynes JT, Tumber A, Wright T, Li S, Michiels C, Consortium GNB, Condroyer C, MacDonald H, Verdet R, Sahel JA, Hamel CP, Zeitz C, Heon E (2016) Biallelic Mutations in GNB3 Cause a Unique Form of Autosomal-Recessive Congenital Stationary Night Blindness. American journal of human genetics 98:1011-1019.

Wachtmeister L (1998) Oscillatory potentials in the retina: what do they reveal. Progress in retinal and eye research 17:485-521.

Xu L, Ball SL, Alexander KR, Peachey NS (2003) Pharmacological analysis of the rat cone electroretinogram. Visual neuroscience 20:297-306.

Xu Y, Orlandi C, Cao Y, Yang S, Choi CI, Pagadala V, Birnbaumer L, Martemyanov KA, Vardi N (2016) The TRPM1 channel in ON-bipolar cells is gated by both the alpha and the betagamma subunits of the G-protein Go. Scientific reports 6:20940.

Zeitz C, Jacobson SG, Hamel CP, Bujakowska K, Neuille M, Orhan E, Zanlonghi X, Lancelot ME, Michiels C, Schwartz SB, Bocquet B, Congenital Stationary Night Blindness C, Antonio A, Audier C, Letexier M, Saraiva JP, Luu TD, Sennlaub F, Nguyen H, Poch O, Dollfus H, Lecompte O, Kohl S, Sahel JA, Bhattacharya SS, Audo I (2013) Whole-exome sequencing identifies LRIT3 mutations as a cause of autosomal-recessive complete congenital stationary night blindness. American journal of human genetics 92:67-75.

CHAPTER 4

DEVELOPING AN AAV-MEDIATED GENE THERAPY FOR ON BIPOLAR CELL GENETIC DISORDERS

4.1 Introduction

Recombinant adeno-associated viral vectors (AAV) have been shown to be effective in targeting photoreceptors and retinal pigment epithelium in animal models (Komaromy et al., 2010, Mowat et al., 2013, Boyd et al., 2016). Recently, a study showed a successful use of AAV gene therapy to treat a CSNB mouse model (Scalabrino et al., 2015). This was the first time that gene therapy targeting ON-BCs was capable of restoring the signaling pathway.

As described in chapter 1, bipolar cells (BCs) are second order neurons that convey signals from the photoreceptors to the ganglion cells before being transmitted to the brain. Rods connect to a single form of depolarizing (ON) BC while cones synapse with both ON and hyperpolarizing (OFF) forms of BC. Mutations in ON BC genes are a cause of congenital stationary night blindness (CSNB). The G protein beta subunit 3 (Gβ3) encoded by the gene *Gnb3*, has been recently shown to be important for ON BC signaling (Dhingra et al., 2012).

The purpose of this study was to test an AAV vector designed to target BCs in rats as the first step towards gene therapy in the *Gnb3*$^{-/-}$ rat model of CSNB.

4.2 Methods

4.2.1 Ethics Statement

All procedures were performed in accordance with the ARVO statement for the Use of Animals in Ophthalmic and Vision Research and approved by Michigan State University Institutional Animal Care and Use Committees.

4.2.2 Animals

The rats used in this study were maintained in a colony at Michigan State University as described in section 3.2.2 on Chapter 3.

4.2.3 Gene therapy

Recombinant AAV2 vectors AAV2/2 (Quad+T>V)-PCP2-L7-hGFP (AAV-GFP) and AAV2/2 (Quad+T>V)-PCP2-L7-mGNB3 (AAV-GNB3) were designed and manufactured at University of Florida College of Medicine (Gainesville, FL) using previously published methods (Scalabrino et al., 2015). The designed vector is a recombinant AAV2 genome packaged in an AAV2 capsid with quadruple replacement of tyrosine to phenylalanine residues, a promoter specific for ON BC (PCP2-L7) (Portales-Casamar et al., 2010, Lu et al., 2013) and the reporter gene (GFP) or gene of interest (GNB3). The strategy was to initially test reporter gene efficiency to show that the construct could target ON BC cells and then to use it to introduce GNB3 cDNA as treatment of *Gnb3*$^{-/-}$ rats. The study was

divided in: 1- Evaluation of intravitreal and subretinal injection efficiency with AAV-GFP at post-natal day 30 (P30); 2- Comparison of outcome when vector is injected at P2 and P30 using the AAV-GFP; and 3- Gene therapy aiming to rescue the *Gnb3*$^{-/-}$ rat phenotype.

4.2.4 Injection methods

For the intravitreal vs subretinal injection efficiency evaluation, eyes of P30 WildType rats were dilated 30 minutes prior the injection with 1 % topical tropicamide (Falcon Pharmaceuticals, Ltd., Fort Worth TX). Anesthesia was induced and maintained by isoflurane 2% (IsoFlo; Abbott Laboratories, North Chicago IL) in oxygen. Injections were performed under an ophthalmic operating microscope (Opmi6. Carl Zeiss Meditech Inc, Dublin, CA). A coverslip was placed on the cornea coupled with sterile methylcellulose to allow visualization of the posterior segment. Subretinal injections were performed as follows: a 30G needle was used to create a sclerotomy 1mm posterior to the limbus through which a blunt 34G needle on a Hamilton syringe was introduced. This was advanced to the retina to form a retinotomy and inject vector (5µl) into the subretinal space creating a temporary retinal detachment. Intravitreal injections (5µl) of AAV-GFP were perfomed using a beveled 34G needle on a Hamilton syringe (Fig.4.1). One eye of each P30 animal was given an intravitreal injection over the optic nerve head region. The other eye received a subretinal injection of the same construct; the blebs were made nasal to the optic disk. P2 animals were anesthetized on ice, and virus was delivered (1 µl) via trans-scleral intravitreal injection using a 34G beveled needle mounted on a Hamilton syringe. Vectors were delivered undiluted (3.05 x10^{13} vg/mL- AAV-GFP and

2.65 x10^{13} vg/Ml – AAV-GNB3) in all cases. For the P2/P30 comparison experiment, wildtype (WT) rats received the AAV-GFP by intravitreal injection in both eyes. For the *Gnb3* gene therapy portion, *Gnb3*$^{-/-}$rats received the AAV-GNB3 in one eye and the AAV-GFP in the contralateral eye as a control both intravitreally. The details of animals used are shown in Table 4.1.

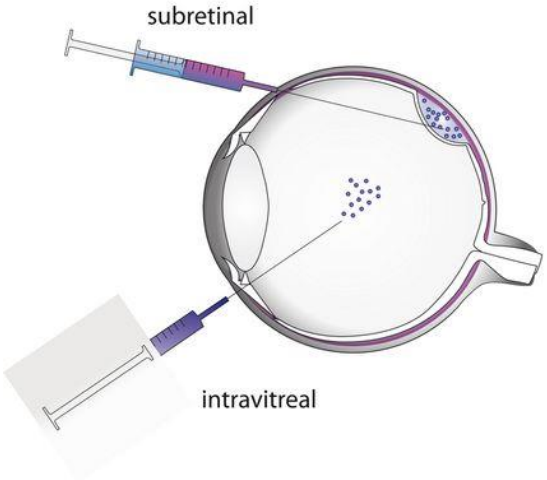

Figure 4.1. Diagram showing intraocular delivery methods. The subretinal injection is performed via a transvitreal approach through a sclerotomy and delivers the AAV between the photoreceptors and retinal pigmented epithelium (RPE), creating a “bleb”. Intravitreal injection is made through the sclera 1mm posterior to the limbus to deliver the AAV into the vitreous. Modified from: http://www.vision-research.eu/index.php?id=906.

4.2.5 *In vivo* imaging

Scanning laser ophthalmoscopy (cSLO) (Spectralis, Heidelberg Engeneering Inc., Franklin, MA) was performed to evaluate the GFP expression in the retina. This uses a 820nm laser for infrared fundus imaging and a “blue-peak” 488nm laser for fluorescence imaging (in this study to detect GFP expression).

Table 4.1. Number of rats used on AAV study

Rat #	Genotype	Gender	Vector and route of delivery		Age at injection
			OD	OS	
1	WT	F	AAV-GFP, SR	AAV-GFP, IVT	P30
2	WT	F	AAV-GFP, SR	AAV-GFP, IVT	P30
3	WT	M	AAV-GFP, SR	AAV-GFP, IVT	P30
4	WT	M	AAV-GFP, SR	AAV-GFP, IVT	P30
5	WT	M	AAV-GFP, SR	AAV-GFP, IVT	P30
6	WT	F	AAV-GFP, IVT	AAV-GFP, IVT	P2
7	WT	F	AAV-GFP, IVT	AAV-GFP, IVT	P2
8	WT	F	AAV-GFP, IVT	AAV-GFP, IVT	P2
9	WT	M	AAV-GFP, IVT	AAV-GFP, IVT	P2
10	WT	M	AAV-GFP, IVT	AAV-GFP, IVT	P2
11	WT	F	AAV-GFP, IVT	AAV-GFP, IVT	P30
12	WT	M	AAV-GFP, IVT	AAV-GFP, IVT	P30
13	WT	M	AAV-GFP, IVT	AAV-GFP, IVT	P30
14	WT	M	AAV-GFP, IVT	AAV-GFP, IVT	P30
15	WT	F	AAV-GFP, IVT	AAV-GFP, IVT	P30
16	*Gnb3* $^{-/-}$	F	AAV-GNB3, IVT	AAV-GFP, IVT	P2
17	*Gnb3* $^{-/-}$	F	AAV-GNB3, IVT	AAV-GFP, IVT	P2
18	*Gnb3* $^{-/-}$	F	AAV-GNB3, IVT	AAV-GFP, IVT	P2
19	*Gnb3* $^{-/-}$	F	AAV-GNB3, IVT	AAV-GFP, IVT	P2
20	*Gnb3* $^{-/-}$	F	AAV-GNB3, IVT	AAV-GFP, IVT	P2
21	*Gnb3* $^{-/-}$	M	AAV-GNB3, IVT	AAV-GFP, IVT	P2
22	*Gnb3* $^{-/-}$	M	AAV-GNB3, IVT	AAV-GFP, IVT	P2
23	*Gnb3* $^{-/-}$	M	AAV-GNB3, IVT	AAV-GFP, IVT	P2
24	*Gnb3* $^{-/-}$	M	AAV-GNB3, IVT	AAV-GFP, IVT	P2

Key: SR- Subretinal; IVT- Intravitreal

4.2.6 Electroretinography

ERG was performed at 45, 60 and 90 days after injection in the *Gnb3*$^{-/-}$ rats that received the *GNB3* construct. Prior to ERGs the animals were dark adapted for 12 hours. After dark adaptation using a dim red light, animals were anesthetized with isoflurane 2% (IsoFlo; Abbott Laboratories, North Chicago IL) in oxygen for induction and maintainance. Body temperature was maintained with a heating table. Pupils were dilated with 1 % topical tropicamide (Falcon Pharmaceuticals, Ltd., Fort Worth TX). Corneal electrodes (Mayo, Japan) were placed against the cornea coupled with 2.5% Hypromellose Ophthalmic demulcent solution (Akorn Pharmaceuticals, Lake Forest, IL). A clip reference electrode was placed on the tongue and as a ground a platinum subdermal needle electrode (Grass Technologies, Warwick RI) placed subcutaneously over the dorsum. ERGs were recorded with an Espion E^2 electrophysiology system with a ColorDome Ganzfeld (Diagnosys LLC, Lowell, MA, USA). A dark-adapted luminance-response series (-2.3 to 2.8 log cd.s/m^2), followed by light adaptation (10 minutes exposure to a 30 cd/m^2 white light), and a light-adapted series (−0.9 to 2.8 log cd.s/m^2) were recorded and transferred to a computer for storage and analysis. ERG a- and b-wave amplitudes and implicit times were measured in a standard fashion. Statistical comparisons for ERG measures were made using a Two-way ANOVA with significance set at $p< 0.05$.

4.2.7 Collection of retinal samples

Rats were euthanized following the AVMA guidelines for rodent euthanasia. Animals received 8% CO_2 in air until loss of consciousness followed by an intraperitoneal injection of pentobarbitone (100mg/kg – Fatal Plus, Vortech Pharmaceuticals, Dearborn MI) and creation of a pneumothorax. Following euthanasia, the globes were enucleated.

4.2.8 Immunohistochemistry (IHC)

The globes were placed in 4% buffered paraformaldehyde in phosphate buffer saline (PBS) for 10 minutes, and then the posterior segment was dissected (eyecup) and placed back in the same fixative for 10 minutes. Eyecups were then rinsed 3 times in PBS for 5 minutes, transferred to 30% buffered sucrose for 30 minutes, and then embedded in OCT medium (Tissue-Tek® O.C.T. Compound, Sakura Finetek USA Inc, Torrance CA) and frozen in liquid nitrogen. Samples were stored at -80^{o}C until used. Sagittal cryosections (14µm thick) were cut using a cryostat-microtome (Leica CM3050-S, Leica Microsystems, Buffalo Grove IL), placed on slides and frozen at -20^{o}C until use. Slides were defrosted at room temperature and sections were first hydrated in PBS for 10 minutes, then blocked with 10% normal horse serum and 0.5% Triton X-100 (Triton X-100, Sigma Aldrich, St. Louis, MO) in PBS for 2 hours, then finally incubated in primary antibody at 4^{o}C overnight. They were then washed 3 times in PBS with 0.1% Triton X-100 for 5 minutes and incubated for 1 ½ hours in secondary antibody (Table 4.2) conjugated with a fluorescent marker, then washed 3 times in PBS with 0.1% Triton X-100 for 5 minutes, counterstained with DAPI (4',6-diamidino-2-phenylindole; Invitrogen) for 5 minutes and cover slipped and imaged using a confocal microscope (Olympus

FluoView 1000 confocal, Center Valley, PA). Images from three retinal sections per eye were captured. Bipolar cells expressing GFP or GNB3 were counted. With the GFP/GNB3 signal masked and bipolar cells labeled with PCP2, a blinded observer counted and marked 100 BC bodies. The GFP signal was then unmasked and all marked cell bodies positive for GFP/GNB3 expression were counted. Number of marked BC bodies with transgene expression was recorded.

Table 4.2. Primary and secondary antibodies for Immunohistochemistry

Antibody	Host	Concentration	Source
Anti-Gβ3	Rabbit	1:400	Santa Cruz
Anti-PCP2 (Purkinje cell protein 2)	Mouse	1:500	BD Biosciences
Anti-GFP	Rabbit	1:1000	Thermo Fisher
AlexaFluor 594	Goat anti-mouse	1:500	Thermo Fisher
AlexaFluor 488	Goat anti-rabbit	1:500	Thermo Fisher

4.2.9 Quantification of mRNA by real-time PCR

Retinas were dissected, flash frozen in liquid nitrogen and stored at -80°C until use. They were homogenized in lysis buffer (Buffer RLT; RNeasy Protect Mini Kit; Qiagen, Inc., Hilden, Germany). RNA extraction was performed with a stabilization and purification kit (RNeasy Protect Mini Kit; Qiagen, Inc.), adding the DNase step to remove contaminating DNA (RNase-Free DNase set, Qiagen, Inc.). One microgram of DNase-treated RNA was reverse transcribed to make single-stranded cDNA (Transcriptor First Strand cDNA Synthesis Kit, Roche Molecular Systems, Inc., Basel, Switzerland) this was used as a template in real-time PCR (Prime-Time® Gene Expression Master Mix,

Integrated DNA Technologies (IDT), Coralville, IA; and 7500 Fast Real-Time PCR System, ThermoFischer Scientific Inc., Waltham, MA) to measure GFP, *GNB3* and β-actin transcripts. PrimeTime mixes containing primer pairs and probe (Integrated DNA Technologies) for each transcript are included in Table 4.3. Primer pairs for AAV-GNB3 were designed to flank the 3′ *Gnb3* gene and 5′ SV40 polyA and generate an amplicon of 127 bps. PrimeTime mixes were validated according to Bustin et al. (2009) guidelines. Results are the average of three technical replicates and were calculated using the ΔΔCq method with expression normalized to β-actin (actb).

Table 4.3. qRT-PCR primers/probe

Primer Name	Sequence 5’ to 3’
actb FWD	GGCATAGAGGTCTTTACGGATG
actb REV	TCACTATCGGCAATGAGCG
actb probe	56-FAM/TCCTGGGTA/ZEN/TGGAATCCTGTGGC/3IABkFQ/
AAV-GFP FWD	GGTTTGTCCAAACTCATCAAT
AAV-GFP REV	CAGTCTGCCCTGTCTAAAG
AAV-GFP probe	56-FAM/ACATGGTCC/ZEN/TGCTGGAGTTTGTGA/3IABkFQ/
AAV-GNB3 FWD	GTCACTGCTGACGGCATGGCT
AAV-GNB3 REV	TGTCCAAACTCATCAATGTATCTTATC
AAV-GNB3 probe	56-FAM/ACTCAGTTC/ZEN/CAGATTTTGAGGAAGCTGT/3IABkFQ/

Probes are double-quenched using a 5′ 6-FAM fluorophore, 3′ IBFQ quencher and inner ZEN quencher, all trademark Integrated DNA Technologies. Actb= beta actin.

4.3 Results

4.3.1 Evaluation of intravitreal and subretinal injection efficiency with AAV-GFP at P30

Five P30 WildType rats had a subretinal injection in one eye (right) and an intravitreal injection in the other eye (left) of an AAV-GFP and followed for 6 weeks. No ocular or systemic abnormality was noted during the study period. All of the intravitreally-injected eyes and 3 out of the 5 subretinally-injected eyes showed evidence of GFP expression. This appeared as punctate fluorescence on cSLO exam (Fig 4.2 A & B). Immunohistochemistry of the retinal sections showed the presence of INL transduced cells in both intravitreally-injected and subretinally-injected (sections through the bleb) eyes. The intravitreally-injected eyes had a higher number of INL transduced GFP cells compared to those with subretinal injections (Fig 4.2 C-E and Fig. 4.3). In subretinally-injected retinas the GFP expression was restricted to the site of injection (Fig. 4.2 E), while in intravitreally-injected GFP expressing cells were present across all sections examined. Fig. 4.2C shows GFP expression in the central retina and Fig. 4.2D shows GFP expression in peripheral retina of intravitreally-injected eyes.

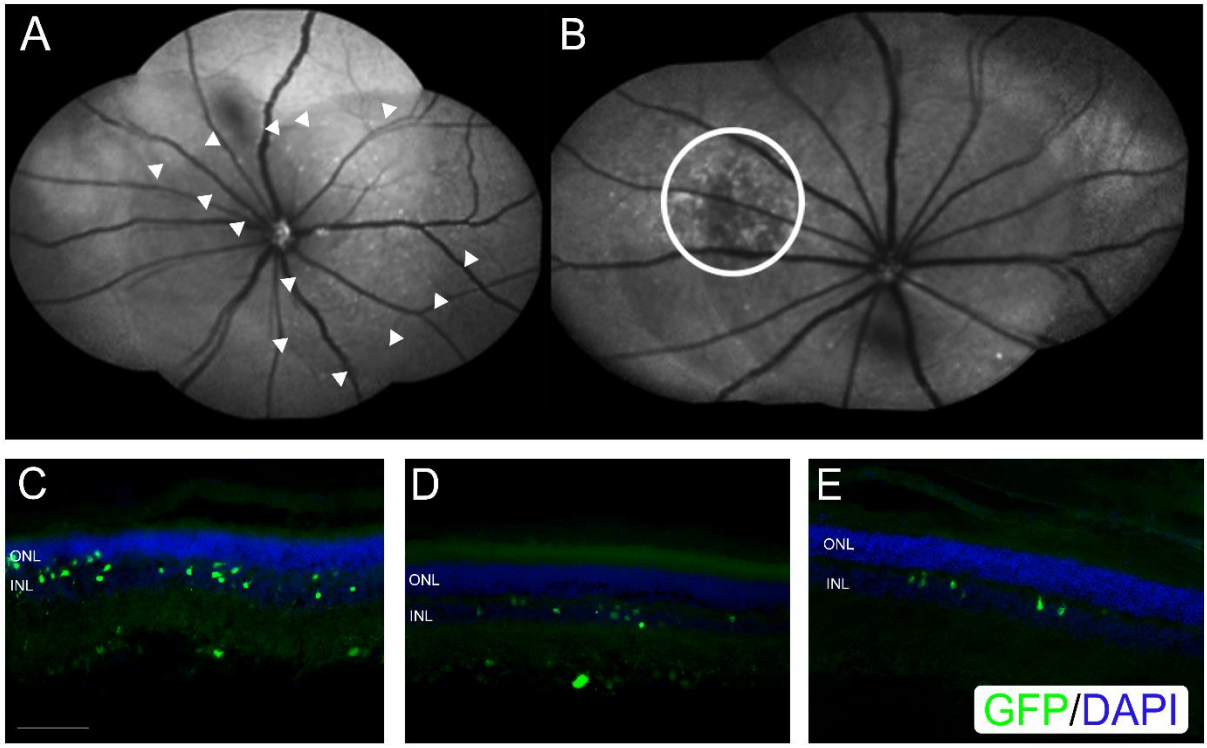

Figure 4.2. Expression of AAV2/2 (Quad+T>V)-PCP2-L7-hGFP construct in Wild (WT) rat retina 6 weeks after intravitreal or subretinal injections. A and **B**. Right and left eyes from a WT rat using Scanning laser ophthalmoscopy (cSLO). **A**. intravitreal injection. Arrows indicate points of fluorescence. **B**. subretinal injection. Circle indicates the site of injection (bleb) and the fluorescence. **C-E**. Immunohistochemistry using GFP antibody (green labeling) shows GFP expression in bipolar cells. **C**. central retina of intravitreal injection eye shown in A. **D**. lateral retina of intravitreal injection eye shown in A. **E**. cross section through the site of the subretinal injection of the eye shown in B. Blue labeling: DAPI. Calibration bar: 50µm.

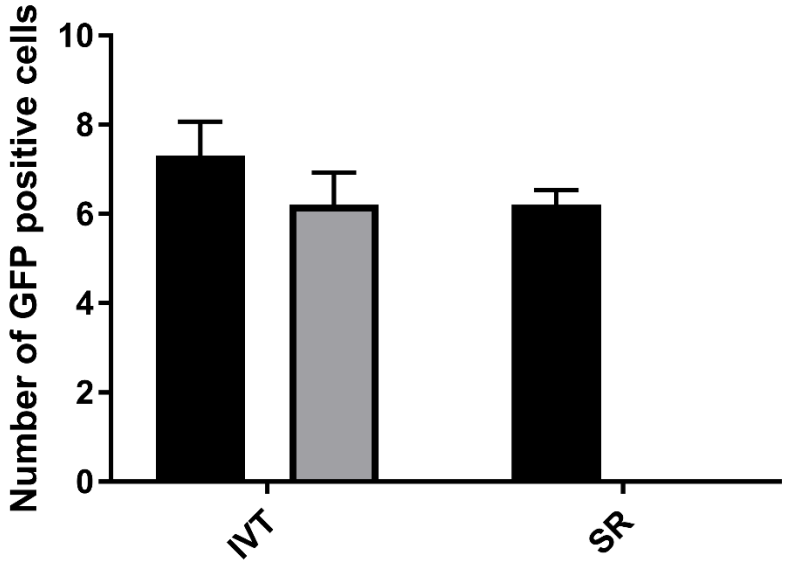

Figure 4.3. Number of GFP positive cells per 100 INL cells 6 weeks after intravitreal (IVT) and subretinal (SR) injection of AAV2/2 (Quad +T>V)-PCP2-L7-hGFP in wildtype (WT) rats P30. Black column represents central retina for IVT injected rats and retinal bleb for SR animals; grey/black column represents retina periphery in IVT injected rats.

4.3.2 Comparison of transgene expression in P2 and P30 rats

Previous gene therapy studies in *Nyx*^{nob} mice targeting bipolar cells had found that rescue was achieved when mice were injected at P2 but not at P30 (Scalabrino et al., 2015). We therefore investigated whether more efficient transduction of BCs in rats occurred when they were injected at an early age.

Five P2 and five P30 WT rats were intravitreally injected using AAV-GFP. All the rats that received the AAV-GFP at P2 had retinal fluorescence visible on cSLO imaging. Intravitreal injection at P2 is technically difficult due to the size of the eye which makes it difficult to visualize the injection site. At P30 animals are larger and easier to inject. Retinal scars could be seen on two eyes injected at P2, and one eye developed cataract after

injection at P2. However, in 7 out of 10 eyes, no adverse consequences were observed. IHC showed GFP expression in BCs of all animals injected at 2 days of age (Fig. 4.4 B-D). Four eyes of P30 rats showed points of GFP expression in the retina. IHC showed GFP expression in a moderate number of BCs in 6 out of the 10 subretinally-injected eyes (Fig. 4.4 E-G).

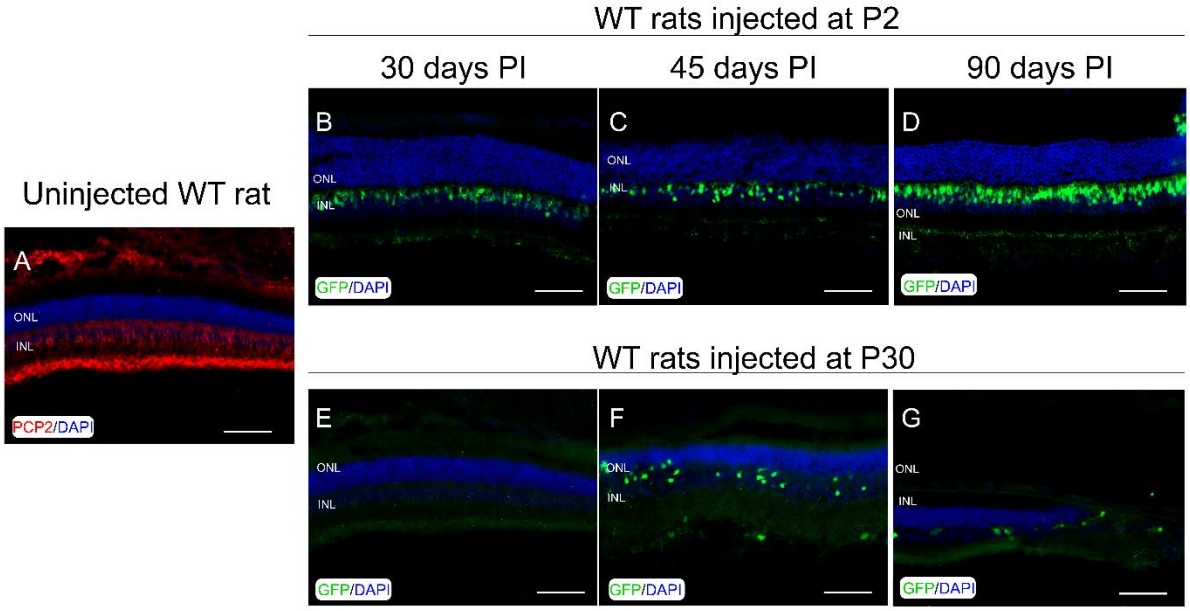

Figure 4.4. Retinal transduction following intravitreal injection of AV2/2 (Quad+T>V)-PCP2-L7-hGFP at P2 or P30. A. Control P90 WT rat retina labeled with Purkinje cell protein 2 (PCP), showing the ON-bipolar cell expression in the retina. **B-D.** P2 injected rats. **E-G**. P30 injected rats. **B and E**. Expression of GFP in WT rats euthanized after 30 days of injection. **C and F**. Expression of GFP in WT rats euthanized after 45 days of injection. **D and G.** Expression of GFP in WT rats euthanized after 90 days of injection. Calibration bar: 50µm.

Quantification of GFP- expressing BC showed that animals injected at P2 had a larger number of GFP-positive cells compared to those injected at P30 ($p<0.001$).

Moreover, rats euthanized at 45 and 90 days after injection showed a higher number of labeled cells in comparison to the rats euthanized after 30 days of injection ($p<0.001$) (Fig.4.5).

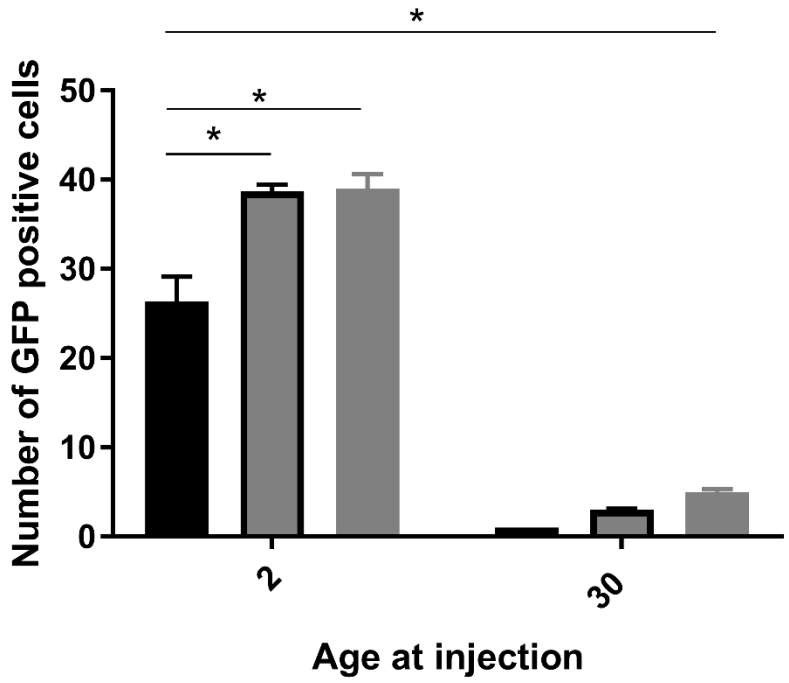

Figure 4.5. Number of GFP positive cells per 100 INL cells in WildType (WT) rats intravitreally injected with AAV2/2 (Quad +T>V)-PCP2-L7-hGFP at P2 or P30 days of age. Black column represents animals euthanized 30 days after injection, grey/black column represents 45 days after injection and grey column, 90 days after injection. * $p<0.001$.

4.3.3 Gene therapy aiming to rescue the *Gnb3*$^{-/-}$ rats phenotype

Nine P2 *Gnb3*$^{-/-}$ rats were intravitreally-injected with AAV-GNB3 in one eye and with AAV-GFP in the contralateral eye as control. Animals were euthanized 90 days after injection. All animals underwent ophthalmic examination every week during this time. Two

out of 9 animals showed bilateral cataract and 1 animal unilateral cataract after injection, no other complication was observed.

ERGs were performed at 45, 60 and 90 days after injection in all animals. A dark-adapted b-wave was not detected in any eyes (data not shown). Table 4.4 shows the mean light-adapted ERG b-wave of injected rats and *Gnb3*$^{-/-}$ uninjected rats. There were no significant difference between any treatment groups. Six of the AAV-GNB3 and AAV-GFP injected eyes were collected for IHC, and three for qRT-PCR. All AAV-GFP injected eyes had GFP positive INL cells on IHC (Fig. 4.6A) as previously seen before in WT rats. IHC with an anti-GNB3 antibody did not label any INL cells in AAV-GNB3 injected eyes (Fig. 4.6B). Note that this antibody labels rod outer segment (Fig. 4.6B&C) because it cross reacts with $G\beta_1$ (the Sigma anti-$G\beta_3$ antibody that was used in early parts of this study and was specific for $G\beta_3$ was no longer available when the gene therapy study was done).

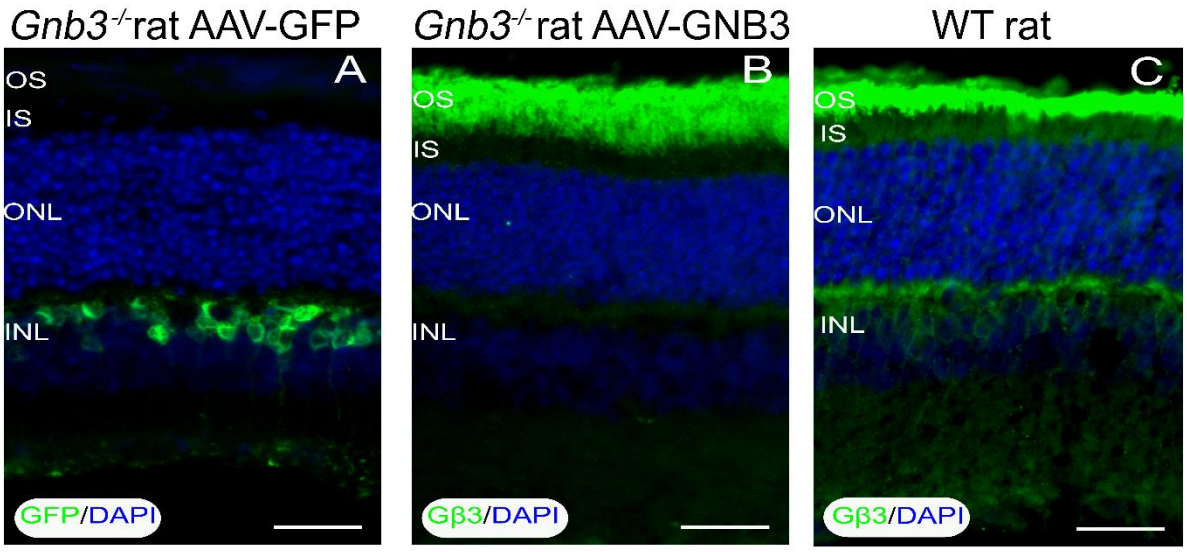

Figure 4.6. Gene Therapy treated *Gnb3*$^{-/-}$ rats injected at P2 with AAV2/2 (Quad+T>V)-PCP2-L7-GFP (A) and AAV2/2 (Quad+T>V)-PCP2-L7-mGNB3 (B) 90 days after injection. A. AAV-GFP eye showing GFP expression in ON bipolar cells **B**. AAV-GNB3 injected eye showing there is no $G\beta_3$ labeling of INL cells. Note that rod outer segments are labeled because the antibody cross recats with $G\beta_1$. **C.** WT eye labeled with $G\beta_3$ antibody showing $G\beta_1$ expression in rods. Calibration bar: 50µm. Blue staining: DAPI.

Table 4.4. Mean light-adapted b-wave amplitude (µV) with standard error in *Gnb3*$^{-/-}$ rats injected with AAV2/2 (Quad+T>V)-PCP2-L7-mGNB3 (AAV-GNB3) and AAV2/2 (Quad+T>V)-PCP2-L7-GFP (AAV-GFP) 90 days post-injection.

Luminance (cd.s/m^2)	AAV-GNB3	AAV-GFP	*Gnb3*$^{-/-}$
0.08	15.7+/-0.76	16.25+/-0.32	16.58+/-2.7
0.4	28.2+/-1.15	29.4+/-0.42	32.04+/-3.8
0.7	39.9+/-0.73	43.85+/-2	40.01+/-4.64
1.09	53.7+/-1.79	57.3+/-1.12	56.62+/-6.28
2	61.25+/-1.72	65.25+/-0.71	66.69+/-6.65

qRT-PCR analyses showed presence of the mRNA transcript in all retinas tested for AAV-GNB3 and AAV-GFP injected eyes relative to the β-actin mRNA transcript control (Fig. 4.7).

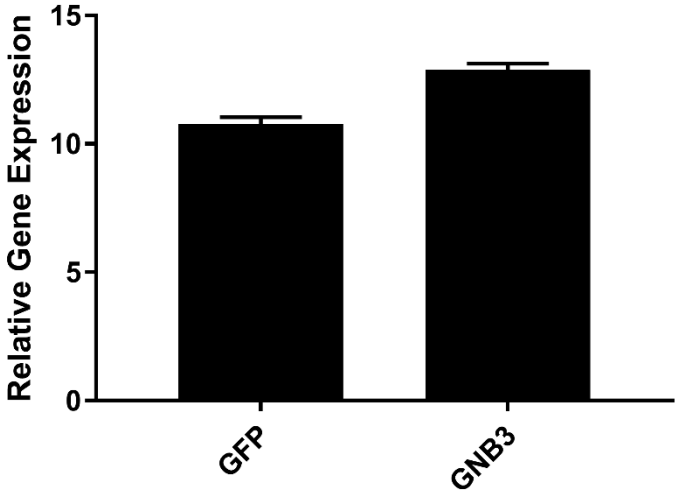

Figure 4.7. Relative gene expression of AAV-GNB3 and AAV-GFP injected in P2 *Gnb3*$^{-/-}$ rat eyes. Standard deviations were calculated from three replicate reactions performed for each sample. Expression normalized to β-actin.

4.4 Discussion

Disruption in ON BC function results in CSNB (Bech-Hansen et al., 2000, Dryja et al., 2005, Audo et al., 2009, Peachey et al., 2012, Zeitz et al., 2013). Recently, *GNB3* mutation was identified in humans resulting in ON BC dysfunction (Arno et al., 2016, Vincent et al., 2016). *GNB3* encodes the $G\beta_3$ protein which is part of the cone and ON BC signaling cascades.

Gene therapy studies can efficiently target photoreceptors (Boyd et al., 2016, Wassmer et al., 2017), retinal pigmented epithelium (RPE) (Komaromy et al., 2010, Mowat et al., 2013). More recently vectors to target ON BCs have been developed (Scalabrino et al., 2015). Scalabrino et al. (2015), achieved a partial rescue of the ERG b-wave of nyctalopin knockout mice after injection of an AAV2(quad Y-F+T-V) Ple155-YFP_NYX. We have conducted two preliminary studies to determine both optimum delivery route (intravitreal vs subretinal) and whether transduction was more efficient in P2 or P30 rats using a reporter gene before initiating therapeutic gene therapy studies to treat *Gnb3*$^{-/-}$ rats.

Two delivery routes are commonly used in gene therapy studies to target the retinal cells; intravitreal and subretinal. We found that the intravitreal delivery route resulted in transduction of a higher proportion of BCs than achieved by subretinal delivery. Furthermore subretinal delivery only transduced cells in the region of the bleb. Both early (P2) and late (P30) intravitreal injection of the AAV-GFP resulted in BC transduction. However the percentage of INL cells transduced was significantly higher in P2 injected eyes. BCs and Müller cells are the latest to reach full differentiation in the retina (Rapaport

et al., 2004), perhaps contributing to the higher efficiency when injections were performed in immature eyes.

Based on the reporter gene studies we delivered the AAV-GNB3 construct by intravitreal injection in *Gnb3*$^{-/-}$ rats at P2. As expected all the contralateral control eyes injected with AAV-GFP had GFP expression, as previously shown in wildtype eyes. However, we could not detect GNB3 expression in INL cells in any of the eyes injected and no functional rescue was observed by ERG. We could, however, show the presence of GNB3 mRNA in the retinas after injection. It is not clear whether the lack of $G\beta_3$ protein was due to a lack of translation of the mRNA or a rapid degradation of the protein. It is conceivable that even when treated at P2 there is already down regulation of the signaling subunits and that $G\beta_3$ requires their presence for stability and to avoid degradation. It is note that others have had similar difficulties in achieving expression of ON BC genes by AAV (Shannon Boye, personal communication). Further studies are required to investigate the lack of $G\beta_3$ in the transduced retinas.

Currently, many different approaches are available to enhance transgene expression from AAV gene therapy. Exosome–associated AAVs injected intravitreally showed improved transduction over non-exosome-associated AAVs probably associated with increased efficiency in penetrating physical barriers (Wassmer et al., 2017). The precise mechanism is not completely understood but the exosome-associated AAVs are likely to use the same intracellular pathway as plain AAVs. A study using human retinal explants showed an increase of mRNA levels in RPE and photoreceptors could be achieved by addition of Woodchuck Hepatitis Virus posttranscriptional regulatory element (WPRE) in the expression cassette (Patricio et al., 2017). Inclusion of a small intron and

other techniques such as codon optimization can also enhance transgene expression. Altering AAV capsid residues is an additional way to increase transduction efficiency. Capsid mutant vectors can have increased transgene expression and decreased immune response (Schultz and Chamberlain, 2008, Kay et al., 2013, Wassmer et al., 2017). We used a vector with a quadruple Y-V (tyrosine to phenylalanine) mutation, which has been shown to improve retinal penetration and transduction (Mowat et al., 2014, Bogner et al., 2015), and an ON BC specific promoter (PCP2-L7) in an attempt to optimize transduction of the target ON BCs. Scalabrino et al. (2016) using a similar construct but expressing nyctalopin were able to partially rescue the phenotype of nyctalopin knockout mice.

Recently a study using an mGluR6 promoter with enhancers showed efficient targeting of rod BCs (Lu et al., 2016). This promoter has not been directly compared with PCP2-L7 promoter. If more efficient, it could be used in future studies. A recent study comparing the novel AAV capsids variants AAV7m8, AAV8BP2, AAV7m8(Y444F) and Opto-mGluR6 showed that there was good transduction in healthy mouse retina but not in degenerated *rd1* mouse retina (van Wyk et al., 2017). Moreover, the results differed between mouse and human retina, suggesting that there may be species-specific differences (van Wyk et al., 2017). We also demonstrated that the AAV-GFP construct we used transduced bipolar cells in wildtype retinas but when used with a therapeutic vector (AAV-GNB3) in *Gnb3*$^{-/-}$ retinas detectable levels of the transgene product were not achieved.

Future studies are required to investigate the apparent lack of translation or rapid protein degradation of $G\beta_3$ of the AAV delivered GNB3 cDNA in *Gnb3*$^{-/-}$ rats. This will be important in developing a translated therapy for GNB3 mutant patients.

REFERENCES

REFERENCES

Arno G, Holder GE, Chakarova C, Kohl S, Pontikos N, Fiorentino A, Plagnol V, Cheetham ME, Hardcastle AJ, Webster AR, Michaelides M, Consortium UKIRD (2016) Recessive Retinopathy Consequent on Mutant G-Protein beta Subunit 3 (GNB3). JAMA ophthalmology 134:924-927.

Audo I, Kohl S, Leroy BP, Munier FL, Guillonneau X, Mohand-Said S, Bujakowska K, Nandrot EF, Lorenz B, Preising M, Kellner U, Renner AB, Bernd A, Antonio A, Moskova-Doumanova V, Lancelot ME, Poloschek CM, Drumare I, Defoort-Dhellemmes S, Wissinger B, Leveillard T, Hamel CP, Schorderet DF, De Baere E, Berger W, Jacobson SG, Zrenner E, Sahel JA, Bhattacharya SS, Zeitz C (2009) TRPM1 is mutated in patients with autosomal-recessive complete congenital stationary night blindness. American journal of human genetics 85:720-729.

Bech-Hansen NT, Naylor MJ, Maybaum TA, Sparkes RL, Koop B, Birch DG, Bergen AA, Prinsen CF, Polomeno RC, Gal A, Drack AV, Musarella MA, Jacobson SG, Young RS, Weleber RG (2000) Mutations in NYX, encoding the leucine-rich proteoglycan nyctalopin, cause X-linked complete congenital stationary night blindness. Nature genetics 26:319-323.

Bogner B, Boye SL, Min SH, Peterson JJ, Ruan Q, Zhang Z, Reitsamer HA, Hauswirth WW, Boye SE (2015) Capsid Mutated Adeno-Associated Virus Delivered to the Anterior Chamber Results in Efficient Transduction of Trabecular Meshwork in Mouse and Rat. PloS one 10:e0128759.

Boyd RF, Sledge DG, Boye SL, Boye SE, Hauswirth WW, Komaromy AM, Petersen-Jones SM, Bartoe JT (2016) Photoreceptor-targeted gene delivery using intravitreally administered AAV vectors in dogs. Gene therapy 23:400.

Dhingra A, Ramakrishnan H, Neinstein A, Fina ME, Xu Y, Li J, Chung DC, Lyubarsky A, Vardi N (2012) Gbeta3 is required for normal light ON responses and synaptic maintenance. The Journal of neuroscience : the official journal of the Society for Neuroscience 32:11343-11355.

Dryja TP, McGee TL, Berson EL, Fishman GA, Sandberg MA, Alexander KR, Derlacki DJ, Rajagopalan AS (2005) Night blindness and abnormal cone electroretinogram ON responses in patients with mutations in the GRM6 gene encoding mGluR6. Proceedings of the National Academy of Sciences of the United States of America 102:4884-4889.

Kay CN, Ryals RC, Aslanidi GV, Min SH, Ruan Q, Sun J, Dyka FM, Kasuga D, Ayala AE, Van Vliet K, Agbandje-McKenna M, Hauswirth WW, Boye SL, Boye SE

(2013) Targeting photoreceptors via intravitreal delivery using novel, capsid-mutated AAV vectors. PloS one 8:e62097.

Komaromy AM, Alexander JJ, Rowlan JS, Garcia MM, Chiodo VA, Kaya A, Tanaka JC, Acland GM, Hauswirth WW, Aguirre GD (2010) Gene therapy rescues cone function in congenital achromatopsia. Human molecular genetics 19:2581-2593.

Lu Q, Ganjawala TH, Ivanova E, Cheng JG, Troilo D, Pan ZH (2016) AAV-mediated transduction and targeting of retinal bipolar cells with improved mGluR6 promoters in rodents and primates. Gene therapy 23:680-689.

Lu Q, Ivanova E, Ganjawala TH, Pan ZH (2013) Cre-mediated recombination efficiency and transgene expression patterns of three retinal bipolar cell-expressing Cre transgenic mouse lines. Molecular vision 19:1310-1320.

Mowat FM, Breuwer AR, Bartoe JT, Annear MJ, Zhang Z, Smith AJ, Bainbridge JW, Petersen-Jones SM, Ali RR (2013) RPE65 gene therapy slows cone loss in Rpe65-deficient dogs. Gene therapy 20:545-555.

Mowat FM, Gornik KR, Dinculescu A, Boye SL, Hauswirth WW, Petersen-Jones SM, Bartoe JT (2014) Tyrosine capsid-mutant AAV vectors for gene delivery to the canine retina from a subretinal or intravitreal approach. Gene therapy 21:96-105.

Patricio MI, Barnard AR, Orlans HO, McClements ME, MacLaren RE (2017) Inclusion of the Woodchuck Hepatitis Virus Posttranscriptional Regulatory Element Enhances AAV2-Driven Transduction of Mouse and Human Retina. Molecular therapy Nucleic acids 6:198-208.

Peachey NS, Ray TA, Florijn R, Rowe LB, Sjoerdsma T, Contreras-Alcantara S, Baba K, Tosini G, Pozdeyev N, Iuvone PM, Bojang P, Jr., Pearring JN, Simonsz HJ, van Genderen M, Birch DG, Traboulsi EI, Dorfman A, Lopez I, Ren H, Goldberg AF, Nishina PM, Lachapelle P, McCall MA, Koenekoop RK, Bergen AA, Kamermans M, Gregg RG (2012) GPR179 is required for depolarizing bipolar cell function and is mutated in autosomal-recessive complete congenital stationary night blindness. American journal of human genetics 90:331-339.

Portales-Casamar E, Swanson DJ, Liu L, de Leeuw CN, Banks KG, Ho Sui SJ, Fulton DL, Ali J, Amirabbasi M, Arenillas DJ, Babyak N, Black SF, Bonaguro RJ, Brauer E, Candido TR, Castellarin M, Chen J, Chen Y, Cheng JC, Chopra V, Docking TR, Dreolini L, D'Souza CA, Flynn EK, Glenn R, Hatakka K, Hearty TG, Imanian B, Jiang S, Khorasan-zadeh S, Komljenovic I, Laprise S, Liao NY, Lim JS, Lithwick S, Liu F, Liu J, Lu M, McConechy M, McLeod AJ, Milisavljevic M, Mis J, O'Connor K, Palma B, Palmquist DL, Schmouth JF, Swanson MI, Tam B, Ticoll A, Turner JL, Varhol R, Vermeulen J, Watkins RF, Wilson G, Wong BK, Wong SH, Wong TY, Yang GS, Ypsilanti AR, Jones SJ, Holt RA, Goldowitz D, Wasserman WW, Simpson EM (2010) A regulatory toolbox of MiniPromoters to

drive selective expression in the brain. Proceedings of the National Academy of Sciences of the United States of America 107:16589-16594.

Rapaport DH, Wong LL, Wood ED, Yasumura D, LaVail MM (2004) Timing and topography of cell genesis in the rat retina. The Journal of comparative neurology 474:304-324.

Scalabrino ML, Boye SL, Fransen KM, Noel JM, Dyka FM, Min SH, Ruan Q, De Leeuw CN, Simpson EM, Gregg RG, McCall MA, Peachey NS, Boye SE (2015) Intravitreal delivery of a novel AAV vector targets ON bipolar cells and restores visual function in a mouse model of complete congenital stationary night blindness. Human molecular genetics 24:6229-6239.

Schultz BR, Chamberlain JS (2008) Recombinant adeno-associated virus transduction and integration. Molecular therapy : the journal of the American Society of Gene Therapy 16:1189-1199.

van Wyk M, Hulliger EC, Girod L, Ebneter A, Kleinlogel S (2017) Present Molecular Limitations of ON-Bipolar Cell Targeted Gene Therapy. Frontiers in neuroscience 11:161.

Vincent A, Audo I, Tavares E, Maynes JT, Tumber A, Wright T, Li S, Michiels C, Consortium GNB, Condroyer C, MacDonald H, Verdet R, Sahel JA, Hamel CP, Zeitz C, Heon E (2016) Biallelic Mutations in GNB3 Cause a Unique Form of Autosomal-Recessive Congenital Stationary Night Blindness. American journal of human genetics 98:1011-1019.

Wassmer SJ, Carvalho LS, Gyorgy B, Vandenberghe LH, Maguire CA (2017) Exosome-associated AAV2 vector mediates robust gene delivery into the murine retina upon intravitreal injection. Scientific reports 7:45329.

Zeitz C, Jacobson SG, Hamel CP, Bujakowska K, Neuille M, Orhan E, Zanlonghi X, Lancelot ME, Michiels C, Schwartz SB, Bocquet B, Congenital Stationary Night Blindness C, Antonio A, Audier C, Letexier M, Saraiva JP, Luu TD, Sennlaub F, Nguyen H, Poch O, Dollfus H, Lecompte O, Kohl S, Sahel JA, Bhattacharya SS, Audo I (2013) Whole-exome sequencing identifies LRIT3 mutations as a cause of autosomal-recessive complete congenital stationary night blindness. American journal of human genetics 92:67-75.

CHAPTER 5

CONCLUSIONS AND FUTURE DIRECTIONS

GNB3 mutations in different species lead to different phenotypes. Currently, there are four different species with different mutations in *GNB3*. This potentially expands the tools to study G-protein signaling as well as novel therapies for Gβ3-associated retinopathies.

In chapter 2, we created a cost-effective alternative facemask for use of inhalatory anesthesia in rodents and chicks for ophthalmic procedures. Generation of the *Gnb3*$^{-/-}$ rat allowed further characterization of the *Gnb3*$^{-/-}$ phenotype (Chapter 3). We confirmed that the strategy to knockout the gene was successful, by showing lack of Gβ3 by western blot and immunohistochemistry and of *Gnb3* mRNA by qRT-PCR. The *Gnb3*$^{-/-}$ rats had no retinal morphological changes detectable on plastic embedded sections. Future studies using electron microscopy will determine if there are changes in rod BC synapses, preliminary example is shown in Fig. 5.1. It would beneficial for future studies to re-generate this knockout rat on a pigmented background. Our animals were generated in a Dahl/salt sensitive albino rat background for hypertension studies. The Dalh/salt sensitive background require that the rats are fed a special low-salt diet to prevent development of hypertension. Previous studies have shown that albino rats have lower visual acuity than pigmented rats which could be linked to albinism (Creel et al., 1970, Prusky et al., 2002). Due to that, the generation of a *Gnb3*$^{-/-}$ rat in a pigmented and no salt sensitive background would be advantageous not just for husbandry (diet) but as well for vision testing studies. Additionally, studies to generate antibodies for ON BC cascade proteins in rats would be valuable for the characterization since we found that most commercially available antibodies did not work in rat retinal sections.

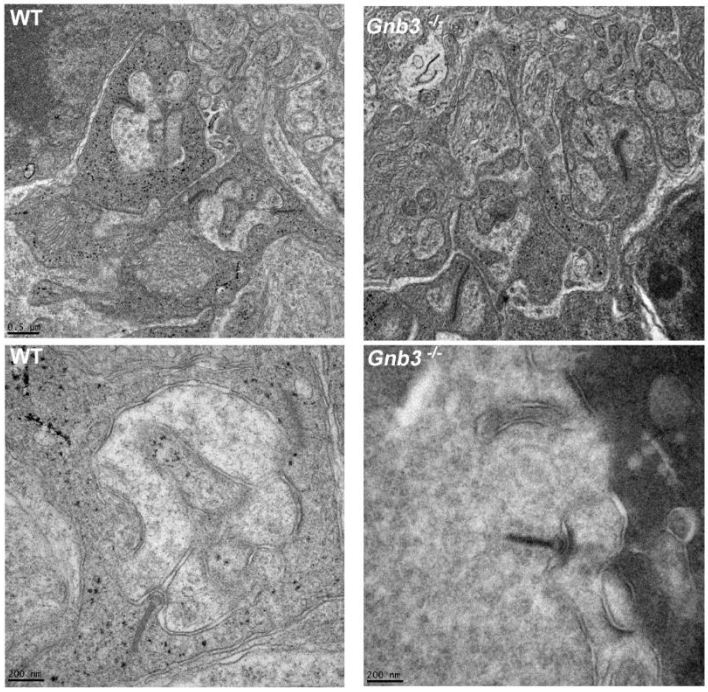

Figure 5.1. Ultra-thin retinal sections of 6 month old WildType and *Gnb3*$^{-/-}$ rat. Upper sections show outer plexiform layer synaptic triads are visible. Calibration bar: 0.5 µm. Lower sections at higher magnitude show rod synaptic ribbons. Calibration bar: 200nm.

Gnb3$^{-/-}$ rats showed a lack of rod BC function and modest decrease in the cone ON-BC function. To confirm the origin of the light-adapted b-wave in *Gnb3*$^{-/-}$ rats, intravitreal L-AP4 to block photoreceptor to ON BC connections was used. L-AP4 removed the b-wave in WT and *Gnb3*$^{-/-}$ rats confirming that in the Gnb3-/- rats the light adapted b-wave originated from ON-BC function. The ERG drug dissection was confirmed by single cell recording which showed a lack of rod BC response and a small cone BC response to light stimulus. Although, we have not performed cone single cell recordings, a-wave amplitude post L-AP4 suggest there may be reduced cone sensitivity. Single cell recording of OFF-BC in *Gnb3*$^{-/-}$ rats showed that those cells also had slower

and smaller responses than WT rats. Further studies are needed to establish wheter this is due to reduced cone responses leading to lower OFF BC stimulus or wheter there is a direct effect of the phenotype on OFF BC.

There are a lack of studies for molecular characterization of the different subtypes of BCs in rats. We hypothesize that rats may have different signaling cascades in different subtypes of ON-BCs than other species. Future studies addressing the subtypes of ON-BCs and the proteins that are involved in their signaling cascade would be valuable. Understanding these species differences will help in understanding the ON signaling pathway and the different phenotypes in $G\beta_3$-associated retinopathy.

A detailed characterization of the different GNB3 mutation phenotypes can be used as information for future gene therapy studies (Chapter 4). We made initial gene augmentation attempts to treat $G\beta_3$-associated retinopathy. The initial work with reporter genes showed transgene expression in BCs using an AAV vector. Our results suggest the intravitreal application of the viral vector at early ages provides the greatest transgene expression in ON-BCs. Contrary to our hypothesis, gene therapy using the GNB3 construct did not show functional rescue (dark-adapted ERG b-wave rescue), and although mRNA was detectable in all retinas analyzed by qRT-PCR. Future studies analyzing the apparent lack of *Gnb3* mRNA translation or the possible rapid degradation of the protein after translation are needed. Even though $G\beta_3$ is conserved between species an AAV made with a rat cDNA would be advantageous to treat *Gnb3*$^{-/-}$ rats. Novel AAV strategies could also be used to enhance transgene expression, such as exosome-associated AAVs, use of different promoters, codon optimization and enhancers.

REFERENCES

REFERENCES

Creel DJ, Dustman RE, Beck EC (1970) Differences in visually evoked responses in albino versus hooded rats. Experimental neurology 29:298-309.

Prusky GT, Harker KT, Douglas RM, Whishaw IQ (2002) Variation in visual acuity within pigmented, and between pigmented and albino rat strains. Behavioural brain research 136:339-348.